ANTIBIOTIC DISCOVERY TARGETING BACTERIAL

GROEL/GROES CHAPERONIN SYSTEMS

Trent A. Kunkle

Submitted to the faculty of the University Graduate School
in partial fulfillment of the requirements
for the degree
Master of Science
in the Department of Biochemistry and Molecular Biology
Indiana University

August 2018

Accepted by the Graduate Faculty of Indiana University, in partial fulfillment of the requirements for the degree of Master of Science.

Steven M Johnson, Ph.D., Chair

Millie M. Georgiadis, Ph.D.

Master's Thesis Committee

Quyen Q. Hoang, Ph.D.

DEDICATION

To my mother, Donna, and my father, Alex, for supporting me through everything.

ACKNOWLEDGEMENTS

Dr. Steven Johnson and Jose Victorino for compound synthesis; Dr. Sanofar Abdeen for research training and performing the GroEL/ES-dRho refolding assay and native Rho enzymatic activity counter-screen, the HSP60/10-dMDH refolding assay, and the *S. aureus* biofilm and gain-of-resistance assays; Dr. Anne-Marie Ray for performing the human cell cytotoxicity assays and training in cell culturing techniques.

Trent A. Kunkle

ANTIBIOTIC DISCOVERY TARGETING BACTERIAL GROEL/GROES CHAPERONIN SYSTEMS

The Centers for Disease Control (CDC) and World Health Organizations (WHO) have highlighted six species of highly drug-resistant bacteria, commonly termed the *ESKAPE* pathogens, that new antibacterials are urgently needed to treat). The *ESKAPE* pathogens account for over two-million infections and have healthcare costs upwards of $20 billion dollars annually. Over the past several decades, pharmaceutical companies have drastically reduced their research programs for developing new antibacterial agents. As well, bacteria are predisposed to rapidly generate resistance against these "me too" drugs, making this strategy a temporary stop-gap in our ability to fight these pathogens. This has left the burden to identify new antibiotics that function through fundamentally unique mechanisms of action to academia. Towards this goal, we are developing a unique antibacterial strategy that functions through targeting the bacterial GroEL chaperonin systems. GroEL is a molecular chaperone that helps fold proteins into their functional states. Being an essential protein, inhibiting GroEL activity leads to global aggregation and bacterial cell death.

We previously reported a high-throughput screening effort that identified 235 GroEL inhibitors. A subsequent study with a subset of these inhibitors identified several that kill bacteria. To follow-up, we have synthesized 43 analogs of a hit-to-lead molecule, compound **1,** containing systematic deletions of substituents and substructures to determine the essential parts of the scaffold for inhibiting GroEL and killing bacteria. Along with inhibiting GroEL, several compound **1** analogs exhibit >50-fold therapeutic windows between antibacterial efficacy and cytotoxicity to human liver and kidney cells in cell culture. Evaluation of two lead candidates (**1** and **11**) in a gain-of-resistance assay indicated that MRSA bacteria were not able to easily generate resistance to this compound class. Compound **1** also exhibited the ability to permeate through already

established *S. aureus* biofilms and maintain its bactericidal effects, whereas vancomycin could not. Having established initial structure-activity relationships for the compound **1** substituents and substructures in this study, future efforts will focus on optimizing the antibacterial effects of lead candidates and reducing their off-target toxicity to human cells.

Steven M Johnson, Ph.D., Chair

TABLE OF CONTENTS

LIST OF TABLES

LIST OF FIGURES

LIST OF ABBREVIATIONS

Ala - Alanine
ATP - Adenosine triphosphate (ADP = diphosphate)
CC_{50} - Cytotoxicity concentration for half-maximal signal in human cell viability assays
CDC - Centers for Disease Control
Da - Dalton (molecular weight)
DCC - *N*,*N*'-Dicyclohexylcarbodiimide
DCM - Dichloromethane
DMAP - 4-Dimethylaminopyridine
DMF - Dimethylformamide
EC_{50} - Effective concentration for half-maximal signal in bacterial proliferation assays
EDC - 1-Ethyl-3-(3-dimethylaminopropyl)carbodiimide
ESKAPE - ***E****nterococcus faecium,* ***S****taphylococcus aureus,* ***K****lebsiella pneumoniae,* ***A****cinetobacter baumanii,* ***P****seudomonas aeruginosa,* ***E****nterobacter* species
^{1}H-NMR - Proton nuclear magnetic resonance
HSP - Heat-shock protein
IC_{50} - Inhibitory concentration for half-maximal signal in biochemical assays
ITC - Isothermal titration calorimetry
Lac - Lactate
LPS - Lipopolysaccharide
MDH - Malate dehydrogenase
MOA - Mechanism of action
MRSA - Methicillin-resistant *S. aureus*
MS - Mass spectrometry
NAD^+ - Nicotinamide adenine dinucleotide (oxidized form)
NADH - Nicotinamide adenine dinucleotide (reduced form)
OD - Optical density
PBS - Phosphate buffered saline
RP-HPLC - Reverse-phase high-performance liquid chromatography
SDS PAGE - Sodium dodecyl sulfate polyacrylamide gel electrophoresis
SPR - Surface plasmon resonance
TEA - Triethylamine
Van - Vancomycin
WT - Wild-ty

INTRODUCTION

Bacterial infections and the introduction of antibiotics

Prior to the 19th century, infectious diseases accounted for nearly half of all deaths in the United States (Armstrong 1999). Upon introduction of organized health departments, and advancements to sanitation systems, the decline in infection-related deaths dropped by nearly half. An initiative then began to combat more aggressive cases of infectious disease, in particular, to identify harmful bacterial strains and antibiotics that could be administered to kill them in infected patients (**Table 1**). Thus began the golden era of antibiotic development from 1940-1960 (Davies 2010; Lewis 2013).

Table 1. Information on classes of antibiotics (adapted from Lewis, 2013).

Antibiotic Class	Example	Mechanism of Action	Target Bacteria
Sulfa drugs	Prontosil	Inhibition of dihydropteroate synthase	Gram-positives
β-lactams	Penicillin	Inhibition of cell wall biosynthesis	Broad-spectrum
Aminoglycosides	Streptomycin	Binding of 30S ribosomal subunit	Broad-spectrum
Chloramphenicol	Chloramphenicol	Binding of 50S ribosomal subunit	Broad-spectrum
Macrolides	Erythromycin	Binding of 50S ribosomal subunit	Broad-spectrum
Tetracyclines	Chlorotetracycline	Binding of 30S ribosomal subunit	Broad-spectrum
Rifamycins	Rifampicin	Binding of RNA polymerase β-subunit	Gram-positives
Glycopeptides	Vancomycin	Inhibition of cell wall biosynthesis	Gram-positives

Emergence of bacterial resistance to antibiotics

Most of the first antibiotics introduced were highly effective against all species of bacteria (broad-spectrum); however, some classes were not as potent, or were

ineffective, against Gram-negative species. The difference in antibacterial efficacy against Gram-positive and Gram-negative bacteria can be attributed to key differences in their cellular structure. This is highlighted by their classification as “Gram-negative” and “Gram-positive” bacteria, which comes from their ability to retain crystal violet staining, which is retained in the presence of peptidoglycan, a polypeptide-cross-linked layer making up most of the outer structure in Gram-positive bacteria (Navarre 1999). While Gram-negative bacteria do contain a peptidoglycan layer, its abundance is far less than that found in Gram-positive. Furthermore, Gram-negative bacteria have a lipopolysaccharide (LPS) outer membrane that is impermeable to this stain, as well as many antibiotics, making them ineffective (Salton1996). Glycopeptides, for example, cannot diffuse across the LPS and are too large to cross porin channels to penetrate into Gram-negative bacteria (Nakae 1986; Yarlagadda 2016). Inefficacy across different strains can also be attributed to efflux pumps, which actively export molecules from the intracellular milieu, preventing antibiotics from being able to effectively engage intracellular targets and kill bacteria (Nikaido 1996).

As research progressed, it became apparent that bacteria had additional intrinsic mechanisms to evade the effects of antibiotics. For instance, many bacteria can surround themselves in a highly impermeable matrix made up of proteins and polysaccharides, known as biofilm. While vancomycin is effective at treating planktonic (free-floating) *Staphylococcus aureus*, it is impermeable to biofilms; thus, *S. aureus* bacteria are able to hide out within these reservoirs until drugs are systemically cleared (Stewart 2001; Singh 2010). Biofilm formation has been associated with poor prognosis in diseases such as cystic fibrosis, and enhances persistence and spread of infection by adhering to tissues and medical devices (Costerton 1999; Musk Jr. 2006). Continued presence of these biofilms has been a hallmark to cases of chronic infection,

demonstrating increased resistance to treatments through time as they persist (Bjarnsholt 2013).

While innate mechanisms predispose some bacteria to being naturally resistant to various classes of antibiotics, a striking observation was noted just a few short years after introduction of the early antibiotics: bacterial strains were identified that were resistant to what were previously effective drug dosages. Scientists began to realize that antibiotic-specific resistance was stemming from two primary mechanisms. In the first mechanism, bacteria were accumulating mutations in their own genes to prevent drugs from binding to their targets. An example of this is resistance to quinolone antibiotics, where bacteria accumulate mutations in topoisomerases including GyrA, GyrB, ParA, and ParC (Eaves 2004). This process raises fitness in cultures exhibiting this genotype, thriving where wild-type (WT) strains do not.

In the second mechanism of resistance, it was found that bacteria can acquire new genes from other bacteria through a process called conjugal transfer (Llosa 2002). For example, strains of *S. aureus* have become resistant to vancomycin by acquiring the *vanA* operon from *Enterococcus faecalis* (Hobbs 1973; Gonzalez-Zorn 2003). In the acquisition of this operon, *S. aureus* can synthesize peptide intermediates that aren't susceptible to vancomycin. These peptide intermediates can then cross-link forming peptidoglycan, thus continuing growth. This acquired mechanism of resistance is outlined in **Figure 1,** demonstrating how vancomycin, a reserved antibiotic prescribed usually to combat highly resistant bacteria, can be rendered ineffective (Gonzalez-Zorn 2003; Blue Health Intelligence 2017). In **Table 2**, antibiotic classes from **Table 1** are listed, showing the year of introduction, first year of observed resistance, and a brief description of the mechanism of resistance. With many bacteria becoming resistant to first-line therapies, it became clear that new antibiotics would need to be developed to counter these resistance mechanisms.

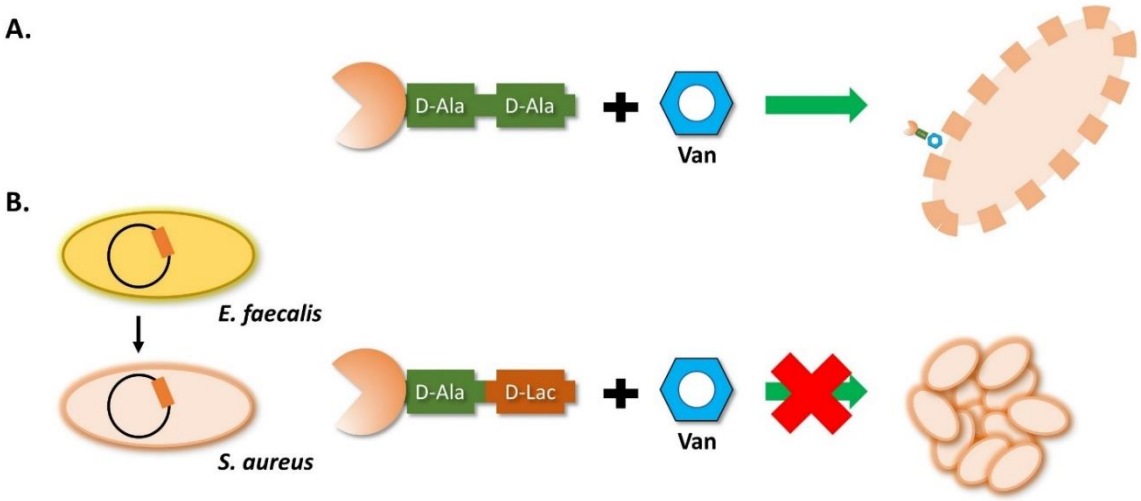

Figure 1. One potential mechanism whereby bacteria gain antibiotic resistance, with vancomycin as an example **A.** Canonical mechanism of action of vancomycin disrupting tripeptide cross-linking by binding to the D-Ala end residue, inhibiting formation of the peptidoglycan layer by peptide cross-linking and inducing cell death. **B.** Conjugal transfer of plasmid containing *vanA* operon to synthesize D-Lac tripeptide, which prevents vancomycin binding and thus permits peptidoglycan assembly and bacterial proliferation.

Table 2. Information on antibiotic resistance in bacteria (adapted from Giedraitiene 2011; Lewis 2013)

Antibiotic Class	Year Introduced	Resistance Observed	Mechanism of Resistance
Sulfa drugs	1936	1942	Mutation altering target binding site, reducing affinity
β-lactams	1938	1942	β-lactamase facilitated hydrolysis, inactivating MOA
Aminoglycosides	1946	1946	Drugs enzymatically modified, reducing their binding affinities
Chloramphenicol	1948	1950	Reduced binding from antibiotic acetylation
Macrolides	1951	1955	Methylated target binding site, reducing affinity
Tetracyclines	1952	1950	Newly produced proteins binding and altering conformation/active site
Rifamycin	1958	1962	Mutations altering target site/reducing affinity
Glycopeptides	1958	1962	Altered peptidoglycan cross-linking

Emergence of the *ESKAPE* pathogens and efforts to combat drug resistance

In 2013, the Centers for Disease Control (CDC) released a report highlighting the dangers posed by multi-drug resistant bacteria, in particular a group of six that have

been termed the ***ESKAPE*** pathogens: ***E****nterococcus faecium* (Gram-positive), ***S****taphylococcus aureus* (Gram-positive), ***K****lebsiella pneumoniae* (Gram-negative), ***A****cinetobacter baumanii* (Gram-negative), ***P****seudomonas aeruginosa* (Gram-negative), and the ***E****nterobacter* species (Gram-negative). The report estimated these bacteria infect over two-million people annually, leading to ~23,000 deaths, despite the expenditure of $20 billion for treating these patients. Of the *ESKAPE* pathogens, methicillin-resistant strains of *S. aureus* (MRSA) were found to be the deadliest, causing ~80,000 infections and ~11,000 deaths. These astonishing statistics for once easily treatable diseases demonstrate the urgency for developing effective therapeutics that may lower the mortality rate. The severity of the *ESKAPE* pathogens and necessity to develop new antibiotics to target them was further reaffirmed by a 2017 report by the World Health Organization (WHO).

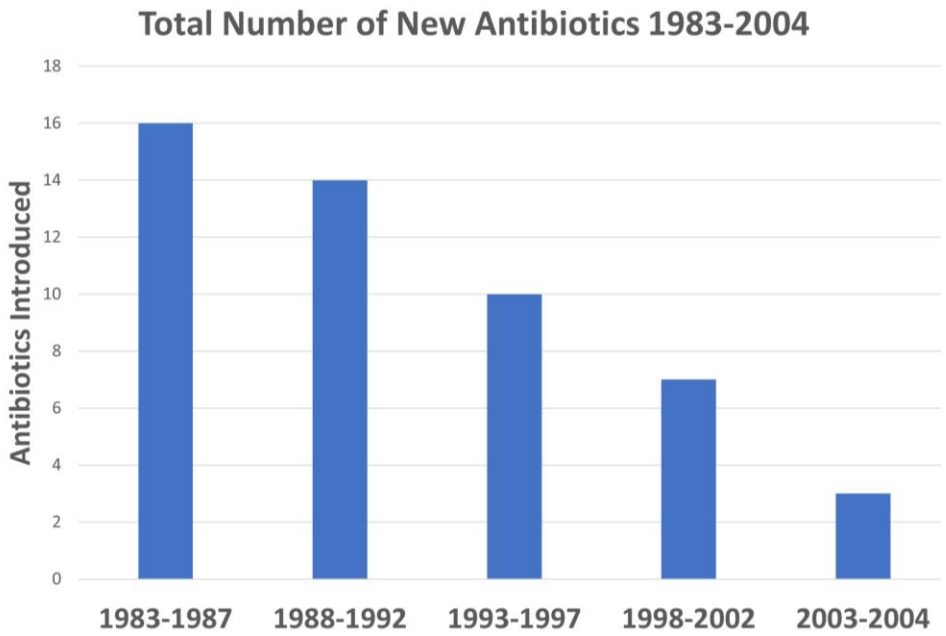

Figure 2. Number of new antibiotics introduced from 1983-2004 (adapted from Nathan 2004).

Unfortunately, the development of new antibiotics over the past four decades has continually declined (**Figure 2**, Boucher 2009). In the past 50 years, only two classes of synthetic antibiotics (fluoroquinolones and oxazolidinones) and three natural product-

derived antibiotics (daptomycin, quinupristin, and fidaxomicin) have been introduced (Lewis 2013). Some antibiotics were introduced as last resort treatments even though resistant strains had already emerged (Wright 2007). Tetracycline, for example, was introduced even after resistance was identified two years prior. Drugs such as this may continue to be prescribed as they can exhibit synergistic effects when co-administered with other antibiotics (Brown 1976). However, the continued push in developing different molecules targeting the same pathways allows pre-disposed bacteria to develop resistance quickly, as seen with the multi-drug resistant *ESKAPE* pathogens. Linezolid, for example, inhibits protein synthesis by binding to the 50S ribosomal subunit, just as erythromycin does. However, whereas it took bacteria over four years to generate resistance to erythromycin (introduced in 1951), it took only one year for them to develop resistance to linezolid (introduced in 2000) (Lewis 2013). This illustrates the problem of how bacteria can quickly develop resistance to drugs that function through a common mechanism, despite the drugs being structurally dissimilar. To circumvent pre-disposed resistance mechanisms, the need for new antibacterials that function through new mechanisms of action and against previously unexploited pathways is necessary.

A mechanistically unique antibacterial strategy: Targeting the bacterial GroEL chaperonin system to disrupt protein folding

While disrupting protein homeostasis has proven an effective antibacterial strategy in the context of inhibiting the assembly of ribosomal or transcriptional machinery (**Table 1**), perturbing protein folding pathways has gone largely unexplored. To facilitate newly synthesized polypeptides folding to their active/native structural conformations, cells have evolved a class of accessory proteins termed molecular chaperones (Hartl 2011). Molecular chaperones, also known as Heat Shock Proteins (HSPs), are divided into 5 general classes based on the molecular weights of their subunits: HSP100, HSP90, HSP70, HSP60 chaperonins, and Small HSPs (Kumar

2015). When molecular chaperone functions are compromised, non-native polypeptides misfold and aggregate, which is detrimental to cell viability (Stefani 2004; Maisonneuve 2008; Carmichael 2000; Bao 2002). Thus, targeting molecular chaperones with small molecule inhibitors should be an effective strategy for killing bacteria that is unique from the mechanisms of current antibiotics.

The development of molecular chaperone inhibitors for killing cells is not a new concept, as significant efforts have been made developing HSP70 and HSP90 inhibitors for treating various cancers. For example, gamitrinib, an HSP90 inhibitor, has shown to be effective in synergistic studies with doxorubicin to reduce malignant tumors (Park 2014; Whitesell 2005). While studies have primarily focused on targeting HSP70 and HSP90 for developing anti-cancer agents, some groups have started looking at exploiting these chaperones for antibiotic development (Piper 2012). For example, Chiappori *et al.* have recently explored molecules that selectively bind DnaK, the bacterial homolog of human HSP70, to disrupt protein folding and kill *A. baumanii* (Chiappori 2015).

While research is underway to target HSP70 and HSP90 chaperones as antibiotic strategies, targeting HSP60 chaperonin systems, called GroEL chaperonins in bacteria, has gone largely unexplored. GroEL functions to refold substrate polypeptides through a mechanism unique from other molecular chaperones. GroEL is a homo-tetradecameric protein that consists of two, seven-membered rings that stack back-to-back with each other (**Figure 3**). To facilitate the folding of substrate polypeptides, GroEL requires binding of ATP and a co-chaperone, called GroES. GroES binding to the GroEL apical domains encapsulates the unfolded polypeptide, where it can attempt to fold within the ring and sequestered from the outside environment. A schematic overview of this folding process is presented in **Figure 4**.

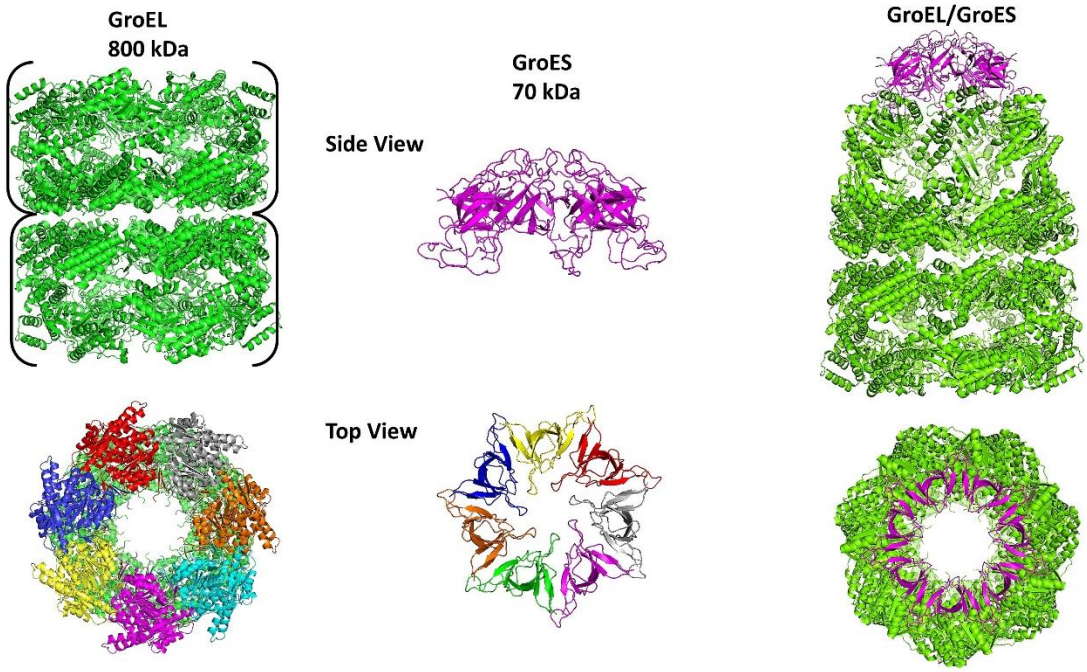

Figure 3. GroEL/GroES chaperonin structure. GroEL is as a homo-tetradecameric complex consisting of two, seven-subunit rings stacked back-to-back. To facilitate polypeptide folding, the 7-subunit GroES "lid" encapsulates one of the two rings (schematic of the polypeptide folding cycle is shown in **Figure 4**). Images are adapted from the 4V43 and 1SX4 crystal structures.

Figure 4. Schematic of the GroEL/ES folding cycle (Horwich 2007). **1.** Unfolded polypeptide binds to the GroEL apical domains, and ATP binds to the GroEL equatorial domains. **2.** GroES binds to the GroEL apical domains and releases the unfolded polypeptide into the GroEL *cis*-cavity where polypeptide folding occurs. **3.** ATP hydrolysis releases the negative cooperativity to the GroEL *trans*-ring. **4.** ATP, another unfolded polypeptide, and GroES bind to the GroEL *trans*-ring, signaling ejection of cargo from the initial *cis*-ring. The folding cycle continues in the new *cis*-ring.

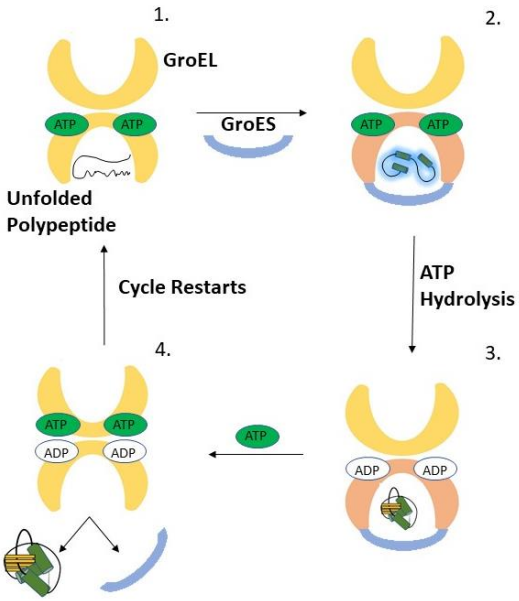

We hypothesize that blocking GroEL folding functions with small molecule inhibitors should be an effective strategy to kill bacteria as this chaperonin system is essential for bacterial viability under all conditions. Supporting this hypothesis, Chapman *et al.* previously used a temperature-

sensitive GroEL mutant to study the effects that loss of chaperonin function had on *Escherichia coli* (Chapman 2006). This mutant strain harbors the E461K mutation, which, at higher temperatures, disrupts the inter-ring allosteric signaling by ATP binding and hydrolysis, locking up the refolding cycle. Compared to *E. coli* containing WT-GroEL, bacteria engineered to express the E461K GroEL mutant ceased replicating 2 h after shifting to non-permissive temperatures, and were no longer viable after culturing for 12 h.

Because GroEL is conserved across bacteria (**Table 3**), blocking the chaperonin folding cycle should be an effective broad-spectrum antibacterial strategy. A caveat to this strategy is that human HSP60 is moderately conserved (48%) with the bacterial homologs, which raises the question of potential off-target effects against human cells. However, HSP60 is localized within the mitochondrial matrix of human cells, which is highly impermeable to penetration by small molecules. Thus, even if compounds can inhibit HSP60 *in-vitro*, they may never reach and inhibit it in the mitochondrial matrix, permitting selective targeting of bacteria over human cells (Cheng 1989).

Table 3. Conservation between GroEL (HSP60) and GroES (HSP10) chaperonins from the *ESKAPE* bacteria and humans. Values represent % identical amino acids compared to *E. coli* GroEL and GroES.

Species	GroEL (HSP60)	GroES (HSP10)
E. coli	100%	100%
E. faecium	57%	47%
S. aureus	57%	44%
K. pneumoniae	97%	94%
A. baumanii	76%	62%
P. aeruginosa	80%	60%
E. cloacae	96%	94%
H. sapiens	48%	35%

Previous studies identifying GroEL inhibitors for hit-to-lead development as antibacterial candidates

In a previous study, we performed high-throughput screening to identify inhibitors of the GroEL/ES folding cycle (Johnson 2014). A schematic of the general GroEL/ES-mediated folding assay protocol is outlined in **Figure 5**. Briefly, a denatured reporter enzyme (typically either β-arylsulfotransferase-IV {AST-IV}, malate dehydrogenase {MDH}, or rhodanese {Rho}) is mixed to create a binary complex with GroEL. Addition of GroES and ATP initiates the folding cycle, and the amount of enzymatic activity by the refolded reporter enzyme is monitored. Thus, this is a coupled assay with reporter enzymatic activity being proportional to the functioning of the GroEL/ES chaperonin system. Using this general assay protocol, 235 GroEL inhibitors were identified by screening against a library of 700,000 molecules (Johnson 2014).

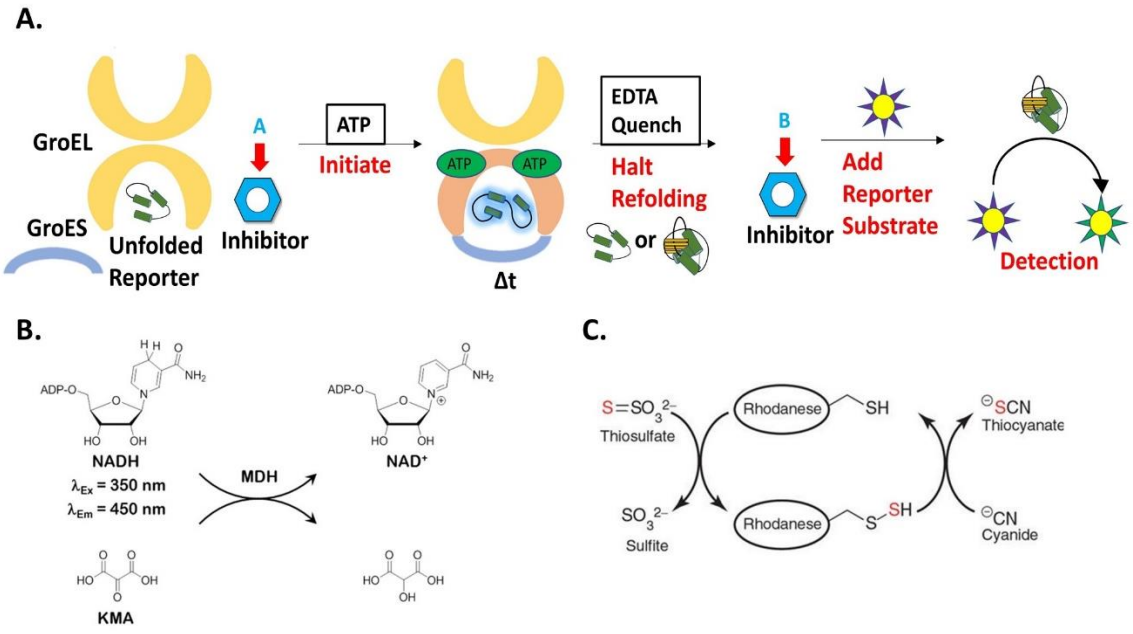

Figure 5. Schematic of the general GroEL/ES folding assays used for evaluating test compounds **A.** Compounds are added to a binary mixture of GroEL, GroES, and unfolded enzyme reporter. ATP is added to initiate the folding cycle, and after a short incubation time (15-60 min, depending on the particular enzyme to be folded), EDTA is added to quench the cycle. Inhibitors can be added at this point (B) rather than point A, to determine inhibition of native enzyme reporter activity. Reporter substrates are added

to determine the activity of the reporter enzyme and whether refolding was inhibited or not (Johnson 2014). **B.** Malate Dehydrogenase and **C.** Rhodanese enzyme reporter reactions.

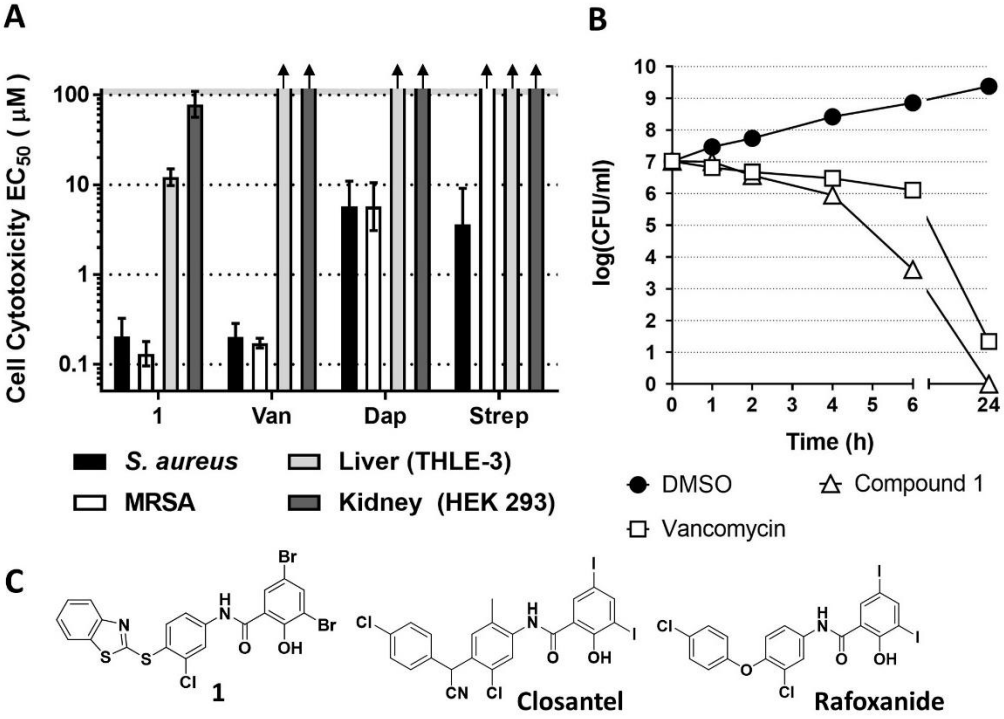

Figure 6. Summary of results from a previous study identifying hit-to-lead antibacterial candidates **A.** Compound **1** exhibits antibacterial effects against *S. aureus* comparable to vancomycin (Van), daptomycin (Dap), and streptomycin (Strep), but does show moderate to low cytotoxicity to human liver and kidney cells. Arrows indicate EC_{50} values have exceeded the maximum concentrations tested (100 μM). **B.** Compound **1** exhibits bactericidal effects against *S. aureus* comparable to vancomycin. Figure panels have been adapted from Abdeen *et al*., 2016. **C.** Compound **1** structure: *N*-(4-(Benzo[*d*]thiazol-2-ylthio)-3-chlorophenyl)-3,5-dibromo-2-hydroxybenzamide. The structurally-related compounds, closantel and rafoxanide, are anthelmintic (anti-parasitic) therapeutics used in veterinary medicine.

A follow-up study further evaluated 22 GroEL inhibitors for their antibacterial effects against the *ESKAPE* pathogens (Abdeen 2016). In that study, compound **1** (**Figure 6C**) emerged as a hit-to-lead candidate for further antibacterial development. While this compound showed moderate efficacy against *A. baumannii*, it was largely ineffective against the other Gram-negative bacteria tested. This was attributed to a combination of the presence of the impermeable LPS membrane of Gram-negative bacteria as well as drug efflux. Compound **1** exhibited the greatest efficacy against the Gram-positive bacterium, *S. aureus*, with bactericidal efficacy similar to vancomycin

(**Figure 6B**). While compound **1** exhibits low to moderate cytotoxicity against human liver (THLE3) and kidney (HEK 293) cell lines, it still has a >50-fold therapeutic window for killing *S. aureus* bacteria. Intriguingly, two anthelminthic drugs used to treat parasitic infections in livestock, closantel and rafoxanide (**Figure 6C**), bear striking resemblances to the compound **1** scaffold (Stromberg 1984). Due to these drugs current use in the field of veterinary medicine, this suggests that compound **1** may be an excellent scaffold to take forward for further pharmacological optimization as an antibiotic candidate.

Current study to develop preliminary SAR for the compound 1 scaffold

While compound **1** itself is a promising GroEL inhibitor to take forward as an antibacterial candidate, there is room for further optimization before proceeding into proof of principle antibacterial efficacy models in animals (e.g. mice systemically infected with *S. aureus*). As a first step in our optimization strategy, though, rather than adding various substituents and substructures to the scaffold as is often done in drug development, we chose an opposite approach where we systematically remove the various substituents and substructures (**R^1-R^5** – **Figure 7**) to evaluate each of their contributions to inhibitor potency and selectivity. Thus, we synthesized a library of 43 analogs that contain all the different ± combinations of the **R^1-R^5** groups. We then tested them in a series of assays to obtain three primary objectives: 1) determine which groups are crucial to inhibit GroEL/ES and HSP60/10 folding function *in vitro*; 2) identify groups that expand the therapeutic window further between antibacterial efficacy and human cell cytotoxicity; and 3) determine if this series of molecules are quick to generate resistance in bacteria, and if they are effective against bacteria in biofilms. Results from these assays would then allow us to identify the smallest effective inhibitor that maintains potency against bacteria while reducing cytotoxicity to human cells. Knowing this information would then allow us to build upon this base scaffold in a more rational approach to improve the pharmacological properties of this antibacterial series.

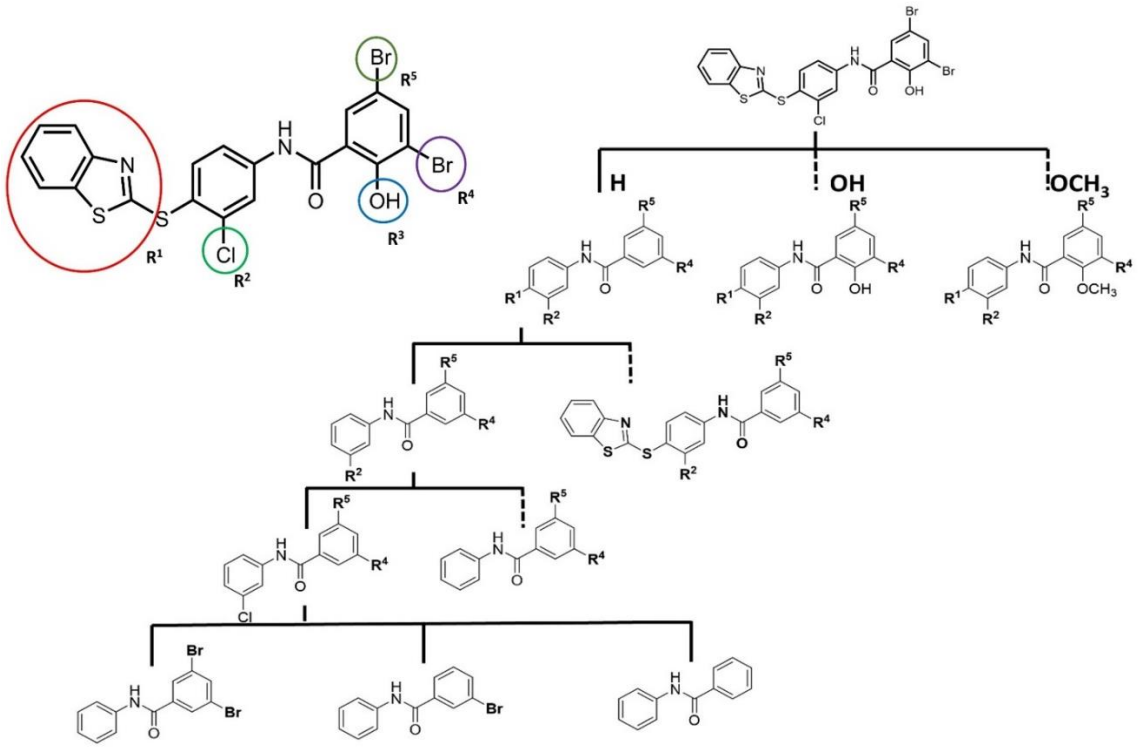

Figure 7. Systematic removal process of compound **1** to synthesize 43 analogs**.** Substituents and substructures (**R**^{1}-**R**^{5}) of the parent compound **1** scaffold were systematically removed in various combinations, as represented by the dendrogram that follows one series of analogs as groups are removed (additional arms/series have been removed for clarity). Each tier branches and differentiates from the previous tiered molecules, which ultimately generates a library of 43 different analogs.

RESULTS AND DISCUSSION

Identifying the efficacies of compound 1 analogs for inhibiting the GroEL/ES-mediated folding cycle

As a first step in this study, we synthesized analogs **1**-**44** as per the general pathways outlined in **Scheme 1**. Detailed synthetic protocols and compound characterizations (e.g. ^{1}H-NMR, MS, and RP-HPLC) are presented in the Experimental section. We also purchased the two highly related anthelmintic drugs used in veterinary medicine, closantel and rafoxanide, to determine whether they are also able to inhibit the GroEL/ES chaperonin system. While their mode of action is reported to involve uncoupling of the proton gradient of oxidative phosphorylation, and thus ATP production in the mitochondria of parasites, it is possible that these compounds function through other mechanisms of action as well (Martin 1997). Thus, this study is an initial step to identify whether or not targeting GroEL/ES (HSP60/10) chaperonin systems may also contribute to their anthelmintic properties.

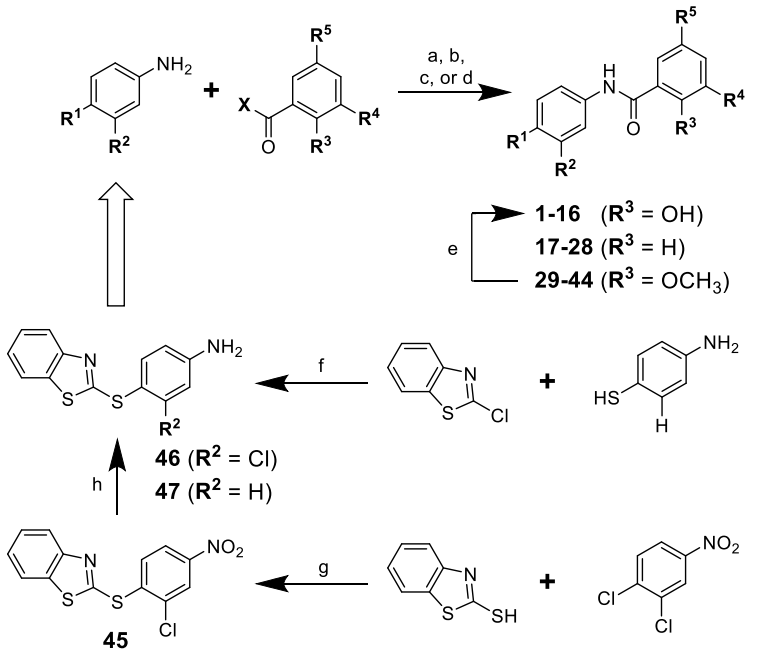

Scheme 1. General procedures to synthesize the compound **1** analog library where the **R^1** to **R^5** substituents and substructures have been systematically removed. Reagents and conditions: a) **X** = Cl: pyridine, CH_2Cl_2; b) **X** = OH: $SOCl_2$, 60°C, then concentrate

and add arylamine, pyridine, and CH_2Cl_2; c) **X** = OH: DCC, DMAP, CH_2Cl_2, then add arylamine and pyridine; d) **X** = OH: EDC, HOBt•H_2O, TEA, CH_2Cl_2; e) BBr_3, DCM; f) K_2CO_3, EtOH; g) K_2CO_3, DMF, R.T to 80°C) Tin powder, HCl/AcOH.

Upon successful generation of the analog library, we next employed a series of well-established biochemical assays to evaluate compound inhibitory effects against the GroEL/ES chaperonin system. As in previous studies (Abdeen 2016; Johnson 2014), chaperonin-mediated folding assays were performed using malate dehydrogenase (MDH) and rhodanese (Rho) as the unfolded reporter enzymes. Inhibition results for testing of compounds in these assays are shown below in **Table 4**.

Table 4. IC_{50} results for compounds tested in the GroEL/ES-mediated dMDH and dRho folding assays, and the native MDH and Rho reporter counter-screens. Log-transformed results with standard deviations are found in **Table 7** in the Appendix.

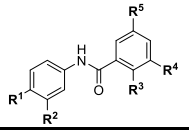

Compound Substituents & Substructures					Compound # / Name	Biochemical Assay IC_{50} (μM)			
						Native Rho Reporter	Native MDH Reporter	GroEL/ES-dRho Refolding	GroEL/ES-dMDH Refolding
R^1	R^2	R^3	R^4	R^5	Closantel	>100	4.9	1.5	2.1
					Rafoxanide	>100	13	2.2	2.8
	Cl	OH	Br	Br	**1**	>100	8.8	1.5	1.8
	Cl	OH	Br	H	**2**	>100	>63	3.8	9.5
	Cl	OH	H	Br	**3**	>100	>63	11	37
	Cl	OH	H	H	**4**	>100	>63	63	42
	H	OH	Br	Br	**5**	>100	8.4	1.3	2.7
	H	OH	Br	H	**6**	>100	>63	14	33
	H	OH	H	Br	**7**	>100	>63	30	38
	H	OH	H	H	**8**	>100	>63	87	40
H	Cl	OH	Br	Br	**9**	>100	27	47	24
H	Cl	OH	Br	H	**10**	>100	>63	>100	>100
H	Cl	OH	H	Br	**11**	>100	>63	>100	>100
H	Cl	OH	H	H	**12**	>100	>63	>100	>100
H	H	OH	Br	Br	**13**	>100	51	>100	61
H	H	OH	Br	H	**14**	>100	>63	>100	>100
H	H	OH	H	Br	**15**	>100	>63	>100	>100
H	H	OH	H	H	**16**	>100	>63	>100	>100
	Cl	H	Br	Br	**17**	>100	>63	>100	>100
	Cl	H	Br (H)	H (Br)	**18**	>100	>63	>100	>100
	Cl	H	H	H	**19**	>100	>63	>100	>100
	H	H	Br	Br	**20**	>100	>63	>100	>100
	H	H	Br (H)	H (Br)	**21**	>100	>63	>100	>100
	H	H	H	H	**22**	>100	>63	>100	>100
H	Cl	H	Br	Br	**23**	>100	>63	>100	>100
H	Cl	H	Br (H)	H (Br)	**24**	>100	>63	>100	>100
H	Cl	H	H	H	**25**	>100	>63	>100	>100
H	H	H	Br	Br	**26**	>100	>63	>100	>100
H	H	H	Br (H)	H (Br)	**27**	>100	>63	>100	>100
H	H	H	H	H	**28**	>100	>63	>100	>100
	Cl	OCH_3	Br	Br	**29**	>100	>63	>100	>100
	Cl	OCH_3	Br	H	**30**	>100	>63	>100	>100
	Cl	OCH_3	H	Br	**31**	>100	>63	>100	>100
	Cl	OCH_3	H	H	**32**	>100	>63	>100	>100
	H	OCH_3	Br	Br	**33**	>100	>63	>100	>100
	H	OCH_3	Br	H	**34**	>100	>63	>100	>100
	H	OCH_3	H	Br	**35**	>100	>63	>100	>100
	H	OCH_3	H	H	**36**	>100	>63	>100	>100
H	Cl	OCH_3	Br	Br	**37**	>100	>63	>100	>100
H	Cl	OCH_3	Br	H	**38**	>100	>63	>100	>100
H	Cl	OCH_3	H	Br	**39**	>100	>63	>100	>100
H	Cl	OCH_3	H	H	**40**	>100	>63	>100	>100
H	H	OCH_3	Br	Br	**41**	>100	>63	>100	>100
H	H	OCH_3	Br	H	**42**	>100	>63	>100	>100
H	H	OCH_3	H	Br	**43**	>100	>63	>100	>100
H	H	OCH_3	H	H	**44**	>100	>63	>100	>100

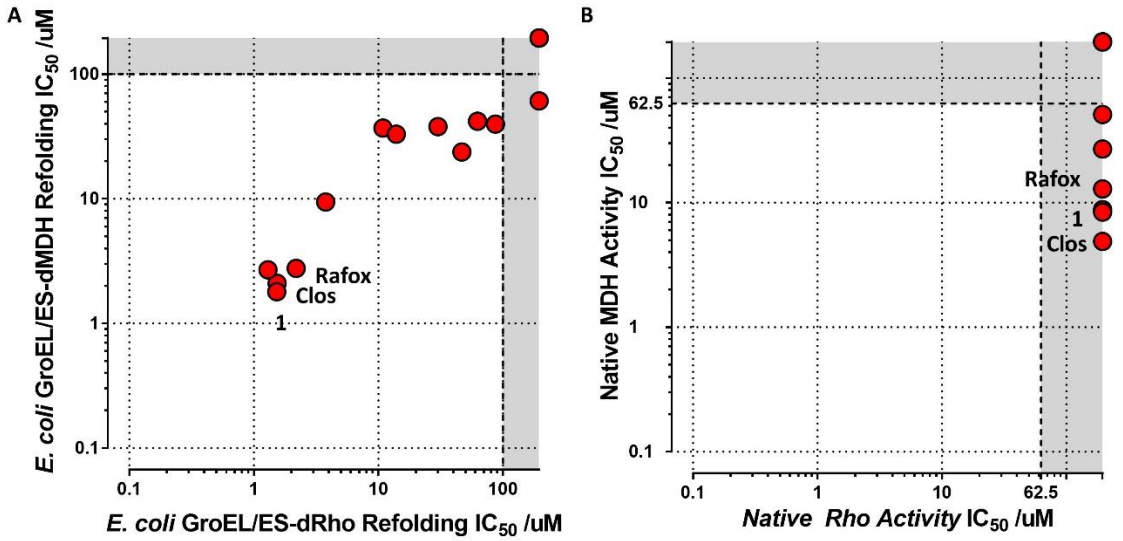

Figure 8 A. Correlation plot of IC_{50} values for compounds tested in the GroEL/ES-dMDH and dRho refolding assays. **B.** Correlation plot of IC_{50} values for compounds tested in the native MDH and native Rho reporter enzymatic counter-screens. Results plotted in the grey zones represent IC_{50} values higher than the maximum concentrations listed.

As visualized in the correlation plot in **Figure 8A**, compounds were nearly equipotent at inhibiting in both of the GroEL/ES-mediated folding assays. As we do not know where the binding sites are for this series of inhibitors, precise structure-function interpretation of the results remains elusive. In general, though, the **R^1** benzothiazole coupled with the **R^3** hydroxyl are required for compounds to inhibit GroEL/ES-mediated folding of the denatured enzymes. Halogenation at the **R^2** position (Cl) and **R^4/R^5** positions (Br) increases inhibitor potency, likely through increased hydrophobic interactions within the binding cavities. However, the bromines would also serve to lower the pK_a of the hydroxyl on the salicylate ring, which could further enhance polar interactions. Perhaps not surprisingly, we found that closantel and rafoxanide were, indeed, potent GroEL/ES inhibitors, suggesting that targeting chaperonin systems could be contributing to their anthelmintic efficacies. We next evaluated compounds for their ability to inhibit native MDH and Rho to identify false-positives that simply inhibit the enzymatic reporter reactions of the coupled folding assays. Schematics of these assays are outlined in **Figure 5**, with detailed experimental protocols presented in the

Experimental section. While some compounds were found to inhibit native MDH (e.g. **1**, **5**, closantel, and rafoxanide), none of the analogs were found to inhibit native rhodanese enzymatic activity (**Table 4** and **Figure 8B**). These results support that inhibitors are inhibiting the chaperonin-mediated folding cycle, although it appears that selectivity issues may be a liability that future studies would need to address.

Determining antibacterial efficacy against the *ESKAPE* pathogens

We next evaluated compounds for antibacterial efficacy against the *ESKAPE* pathogens in liquid media culture as we previously reported (Abdeen 2016), with one primary modification – media was supplemented with 12.5 mg/L of Mg^{2+} and 25 mg/L Ca^{2+}. This was done to more accurately mimic the concentrations of free Mg^{2+} and Ca^{2+} *in vivo*, since chelating to divalent cations can alter the antibacterial efficacies of some compounds, which is the case for daptomycin. Inhibition results for testing of compounds in these bacterial proliferation assays are shown below in **Table 5**.

In general, this series of analogs is ineffective against the Gram-negative bacteria (*K. pneumonia, A. baumannii, P. aeruginosa, E. cloacae*), likely owing to drug efflux and/or impermeability to the lipopolysaccharide (LPS) outer membranes of Gram-negative bacteria. However, with regards to *A. baumannii*, notable exceptions are compounds **2** and **6**, which exhibit EC_{50} values of 2.9 and 12 μM, respectively. This suggests that these drug efflux and LPS impermeability issues may not be insurmountable with further inhibitor optimization. As previously observed with compound **1**, several analogs retained antibacterial efficacy against the Gram-positive bacteria, *E. faecium* and *S. aureus*. Strikingly, inhibitors were much more effective at killing *S. aureus* than *E. faecium*, which has also been noted for other antibiotics. For example, quinupristin/dalfopristin is bactericidal against *S. aureus,* but bacteriostatic against *E. faecium* (Hancock 2005). For our inhibitor series, the presence of the hydroxyl at the $\mathbf{R^3}$ position appears to be integral for potent inhibition of *S. aureus* bacteria. With

the exception of compound **16**, hydroxylation at the $\mathbf{R^3}$ position affords potent inhibitors of *S. aureus* proliferation almost regardless of substituents and substructures at the other positions. However, it is noted that incorporation of the benzothiazole substructure at the $\mathbf{R^1}$ position are the most potent inhibitors, with EC_{50} values in the nanomolar range, which may support on-target effects since these analogs are able to inhibit GroEL/ES-mediated folding functions. Importantly, these analogs are all equipotent against the MRSA strain that we evaluated against.

When we compare the EC_{50} results of this series of compounds against *E. faecium* and *S. aureus* bacteria with the IC_{50} values obtained in the GroEL/ES-dMDH refolding assay (**Figure 9**), an interesting observation is noted. With respect to *E. faecium,* there is an indication of on-target effects against GroEL/ES driving antibacterial activity. However, with MRSA, although a trend is evident between antibacterial efficacy and GroEL/ES inhibition, several compounds that are not GroEL/ES inhbitors still remain effective against bacteria (e.g. **10**-**15**). While this could indicate potential off-target effects, it could also be a result of *S. aureus* GroEL/ES functioning differently than the *E. coli* GroEL/ES chaperonin system, which we use as a surrogate in these studies. Further studies are warranted to determine how *E. faecium* and *S. aureus* GroEL/ES function compared to *E. coli* GroEL/ES, and to identify the specific mechanisms of action of these inhibitors in both *E. faecium* and *S. aureus* bacteria.

Table 5. Log(EC_{50}) results for compounds tested in the bacterial proliferation assays. Log-transformed results with standard deviations are found in **Table 8** in the Appendix.

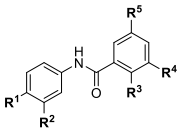

Compound Substituents & Substructures					Compound # / Name	Bacterial Proliferation EC_{50} /μM						
							S. aureus					
R^1	R^2	R^3	R^4	R^5		*E. faecium*	*Sensitive*	*Resistant*	*K. pneumoniae*	*A. baumanii*	*P. aeruginosa*	*E. cloacae*
					Closantel	1.2	0.47	0.42	>100	>100	>100	>100
					Rafoxanide	1.0	0.32	0.30	>100	31	>100	40
	Cl	OH	Br	Br	**1**	0.52	0.36	0.46	>100	66	>100	>100
	Cl	OH	Br	H	**2**	24	0.45	0.55	>100	2.9	>100	>100
	Cl	OH	H	Br	**3**	15	0.12	0.11	>100	>100	>100	>100
	Cl	OH	H	H	**4**	64	0.31	0.42	>100	>100	>100	>100
	H	OH	Br	Br	**5**	0.88	0.44	0.49	>100	>100	>100	>100
	H	OH	Br	H	**6**	8.3	0.76	0.93	>100	11.5	>100	>100
	H	OH	H	Br	**7**	19	0.12	0.13	>100	>100	>100	>100
	H	OH	H	H	**8**	67	0.20	0.34	>100	>100	>100	>100
H	Cl	OH	Br	Br	**9**	15	0.66	1.0	95	46	>100	78
H	Cl	OH	Br	H	**10**	>100	1.3	1.4	>100	>100	>100	>100
H	Cl	OH	H	Br	**11**	>100	0.46	0.46	>100	>100	>100	>100
H	Cl	OH	H	H	**12**	>100	3.1	4.1	>100	>100	>100	>100
H	H	OH	Br	Br	**13**	>100	1.2	1.7	>100	>100	>100	>100
H	H	OH	Br	H	**14**	>100	6.4	8.8	>100	>100	>100	>100
H	H	OH	H	Br	**15**	>100	2.8	4.0	78	>100	>100	>100
H	H	OH	H	H	**16**	>100	28	47	>100	>100	>100	>100
	Cl	H	Br	Br	**17**	>100	>100	>100	>100	>100	>100	>100
	Cl	H	Br (H)	H (Br)	**18**	>100	>100	>100	>100	>100	>100	>100
	Cl	H	H	H	**19**	>100	43	>100	>100	>100	>100	>100
	H	H	Br	Br	**20**	>100	>100	>100	>100	>100	>100	>100
	H	H	Br (H)	H (Br)	**21**	>100	>100	>100	>100	>100	>100	>100
	H	H	H	H	**22**	>100	>100	>100	>100	>100	>100	>100
H	Cl	H	Br	Br	**23**	>100	14	12	>100	>100	>100	>100
H	Cl	H	Br (H)	H (Br)	**24**	>100	47	68	>100	>100	>100	>100
H	Cl	H	H	H	**25**	>100	>100	>100	>100	>100	>100	>100
H	H	H	Br	Br	**26**	>100	>100	>100	>100	>100	>100	>100
H	H	H	Br (H)	H (Br)	**27**	>100	>100	>100	>100	>100	>100	>100
H	H	H	H	H	**28**	>100	>100	>100	>100	>100	>100	>100
	Cl	OCH_3	Br	Br	**29**	>100	>100	>100	>100	>100	>100	>100
	Cl	OCH_3	Br	H	**30**	>100	>100	>100	>100	>100	>100	>100
	Cl	OCH_3	H	Br	**31**	>100	>100	>100	>100	>100	>100	>100
	Cl	OCH_3	H	H	**32**	>100	>100	>100	>100	>100	>100	>100
	H	OCH_3	Br	Br	**33**	>100	>100	>100	>100	>100	>100	>100
	H	OCH_3	Br	H	**34**	>100	>100	>100	>100	>100	>100	>100
	H	OCH_3	H	Br	**35**	>100	>100	>100	>100	>100	>100	>100
	H	OCH_3	H	H	**36**	>100	>100	>100	>100	>100	>100	>100
H	Cl	OCH_3	Br	Br	**37**	>100	46	>100	>100	>100	>100	>100
H	Cl	OCH_3	Br	H	**38**	>100	>100	>100	>100	>100	>100	>100
H	Cl	OCH_3	H	Br	**39**	>100	>100	>100	>100	>100	>100	>100
H	Cl	OCH_3	H	H	**40**	>100	>100	>100	>100	>100	>100	>100
H	H	OCH_3	Br	Br	**41**	>100	>100	>100	>100	>100	>100	>100
H	H	OCH_3	Br	H	**42**	>100	>100	>100	>100	>100	>100	>100
H	H	OCH_3	H	Br	**43**	>100	>100	>100	>100	>100	>100	>100
H	H	OCH_3	H	H	**44**	>100	>100	>100	>100	>100	>100	>100
					Ampicillin	9.5	0.11	>100	>100	>100	>100	>100
					Minocycline	0.13	0.15	1.2	2	0.1	26	4.4
					Rifampicin	6.0	<0.05	0.14	11	1.3	7.8	8.8
					Chloramphenicol	6.4	3.3	2.7	2.9	>100	37	2.8
					Kanamycin	>100	1.1	>100	>100	>100	>100	>100
					Streptomycin	>100	17	>100	52	>100	>100	>100
					Vancomycin	1.2	0.5	0.35	>100	>100	>100	>100
					Daptomycin	11	0.53	0.095	>100	>100	>100	>100

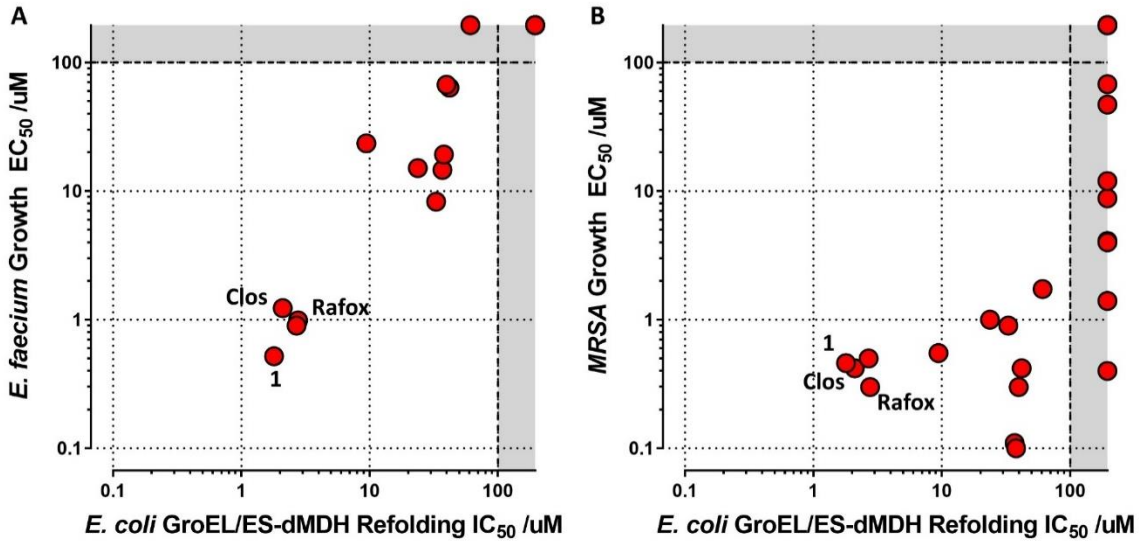

Figure 9. Correlation plot comparing GroEL/ES-dMDH folding and bacterial inhibition results. **A.** *E. faecium* proliferation EC_{50} vs GroEL/ES-dMDH refolding IC_{50} results. **B.** MRSA proliferation EC_{50} vs GroEL/ES-dMDH refolding IC_{50} results.

GroEL inhibitors can also target human HSP60 *in vitro*, yet display moderate to low cytotoxicity to human cells.

Knowing which compounds were effective GroEL inhibitors with antibacterial properties, we next evaluated whether they would inhibit human HSP60 and exhibit cytotoxicity to two cell lines that we typically employ for general cytotoxicity testing *in vitro*: THLE3 liver cells and HEK 293 kidney cells. These assays were performed as previously reported, with detailed protocols presented in the Experimental section. Briefly, the HSP60/10-dMDH folding assay was conducted analogous to the GroEL/ES-dMDH folding assay so IC_{50} results could be directly compared. The human cell cytotoxicity assays used Alamar blue cell viability reagents to measure the viability of liver and kidney cells that had been incubated with test compounds over a 72 h time period. Inhibition and cytotoxicity results for these assays are presented in **Table 6**.

Table 6. IC_{50} and CC_{50} results for compounds tested in the human HSP60/10-dMDH folding assay and the THLE3 and HEK 293 cytotoxicity assays. Log-transformed results with standard deviations are found in **Table 9** in the Appendix.

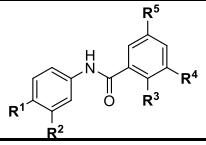

Compound Substituents & Substructures					Compound # / Name	Biochemical Assay IC_{50} (µM)	Cell Viability CC_{50} (µM)	
						HSP60/10-dMDH Refolding	THLE3 (Liver)	HEK 293 (Kidney)
R^1	R^2	R^3	R^4	R^5				
					Closantel	1.5	42	65
					Rafoxanide	1.6	23	>100
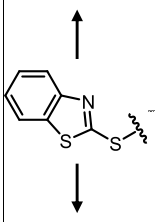	Cl	OH	Br	Br	**1**	3.9	15	86
	Cl	OH	Br	H	**2**	5.4	18	63
	Cl	OH	H	Br	**3**	>100	13	36
	Cl	OH	H	H	**4**	>100	29	58
	H	OH	Br	Br	**5**	3.3	19	61
	H	OH	Br	H	**6**	28	38	73
	H	OH	H	Br	**7**	>100	9.9	17
	H	OH	H	H	**8**	>100	27	63
H	Cl	OH	Br	Br	**9**	28	9.5	12
H	Cl	OH	Br	H	**10**	>100	17	15
H	Cl	OH	H	Br	**11**	>100	2.8	2.8
H	Cl	OH	H	H	**12**	>100	14	12
H	H	OH	Br	Br	**13**	61	27	25
H	H	OH	Br	H	**14**	>100	59	58
H	H	OH	H	Br	**15**	>100	16	15
H	H	OH	H	H	**16**	>100	71	81
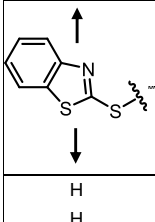	Cl	H	Br	Br	**17**	>100	>100	>100
	Cl	H	Br (H)	H (Br)	**18**	>100	88	>100
	Cl	H	H	H	**19**	>100	82	90
	H	H	Br	Br	**20**	>100	>100	>100
	H	H	Br (H)	H (Br)	**21**	>100	82	74
	H	H	H	H	**22**	>100	>100	>100
H	Cl	H	Br	Br	**23**	>100	45	53
H	Cl	H	Br (H)	H (Br)	**24**	>100	50	51
H	Cl	H	H	H	**25**	>100	>100	>100
H	H	H	Br	Br	**26**	>100	>100	>100
H	H	H	Br (H)	H (Br)	**27**	>100	>100	>100
H	H	H	H	H	**28**	>100	>100	>100
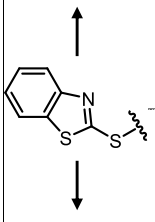	Cl	OCH_3	Br	Br	**29**	>100	>100	>100
	Cl	OCH_3	Br	H	**30**	>100	>100	>100
	Cl	OCH_3	H	Br	**31**	>100	>100	>100
	Cl	OCH_3	H	H	**32**	>100	>100	>100
	H	OCH_3	Br	Br	**33**	>100	>100	>100
	H	OCH_3	Br	H	**34**	>100	>100	>100
	H	OCH_3	H	Br	**35**	>100	>100	>100
	H	OCH_3	H	H	**36**	>100	>100	>100
H	Cl	OCH_3	Br	Br	**37**	>100	>100	>100
H	Cl	OCH_3	Br	H	**38**	>100	>100	>100
H	Cl	OCH_3	H	Br	**39**	>100	94	>100
H	Cl	OCH_3	H	H	**40**	>100	>100	>100
H	H	OCH_3	Br	Br	**41**	>100	>100	>100
H	H	OCH_3	Br	H	**42**	>100	>100	>100
H	H	OCH_3	H	Br	**43**	>100	>100	>100
H	H	OCH_3	H	H	**44**	>100	>100	>100

While some analogs selectively inhibit *E. coli* GroEL over human HSP60 (e.g. **3**, **4**, **7**, and **8**), IC_{50} values between the GroEL/ES-dMDH and HSP60/10-dMDH folding assays were nearly the same for many of the more potent analogs (**Figure 10A**); however, comparison of these results is convoluted by the fact that some of these analogs also inhibit native MDH, and thus could be false positives in the HSP60/10-dMDH folding assay owing to simply inhibiting the MDH reporter reaction. While HSP60 inhibition could potentially be teased out by employing dRho as the denatured reporter enzyme as we do in the case of the GroEL/ES-dRho folding assay, in our experience, the equivalent HSP60/10-dRho folding assay does not provide reliable results, potentially owing to the lower stability of human HSP60 compared to *E. coli* GroEL. Of note when comparing the biochemical and cell-based results is that there does not appear to be a noticeable trend between HSP60/10-dMDH folding assay IC_{50} values liver and kidney cytotoxicity assay CC_{50} values (**Figure 10B**). Interestingly, compounds that bear the $\mathbf{R^1}$ benzothiazole and $\mathbf{R^3}$ hydroxyl substructures (**1**-**8**) are generally less cytotoxic against the HEK 293 cells than their counterparts without the $\mathbf{R^1}$ benzothiazole (**9**-**16**), and also less cytotoxic to the THLE3 liver cells. Since inclusion of these two substructures generally afforded potent chaperonin inhibitors, the differences between these results may suggest that compound cytotoxicities are predominantly a result of off-target effects and not from targeting HSP60 itself. This would not be surprising since some analogs are also able to inhibit native MDH (e.g. **1**, **5**, **9**, **13**, closantel, and rafoxanide). When comparing EC_{50} values of compounds inhibiting the proliferation of susceptible and methicillin-resistant *S. aureus* with CC_{50} values of cytotoxicity against the human liver and kidney cells (**Figure 11**), we note that many analogs exhibit >50-fold therapeutic windows. Considering we have only been looking at the effects that removing substituents and substructures have on the potency and selectivity of this series of analogs (i.e. somewhat of a de-optimization process), these are exciting initial

results to move forward from in future med-chem efforts where we begin to append and optimize the various substituents and substructures of this scaffold.

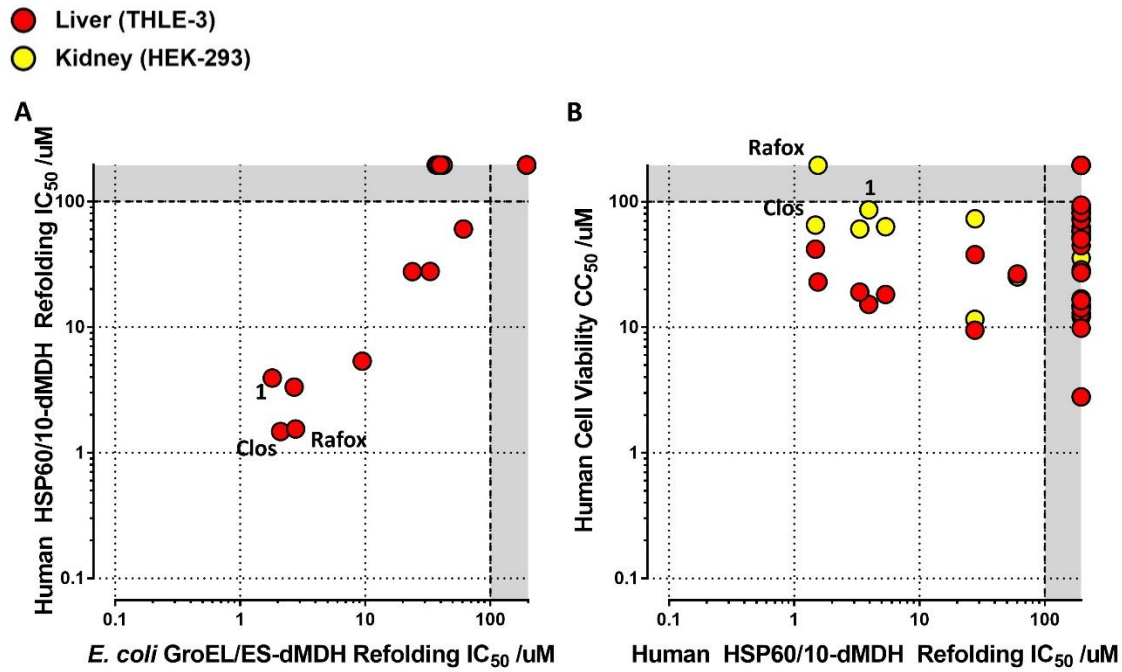

Figure 10. Correlation plots comparing human HSP60/10-dMDH folding inhibition results with GroEL/ES-dMDH folding inhibition and human cell cytotoxicity results (**A**) and human cell cytotoxicity (**B**) results.

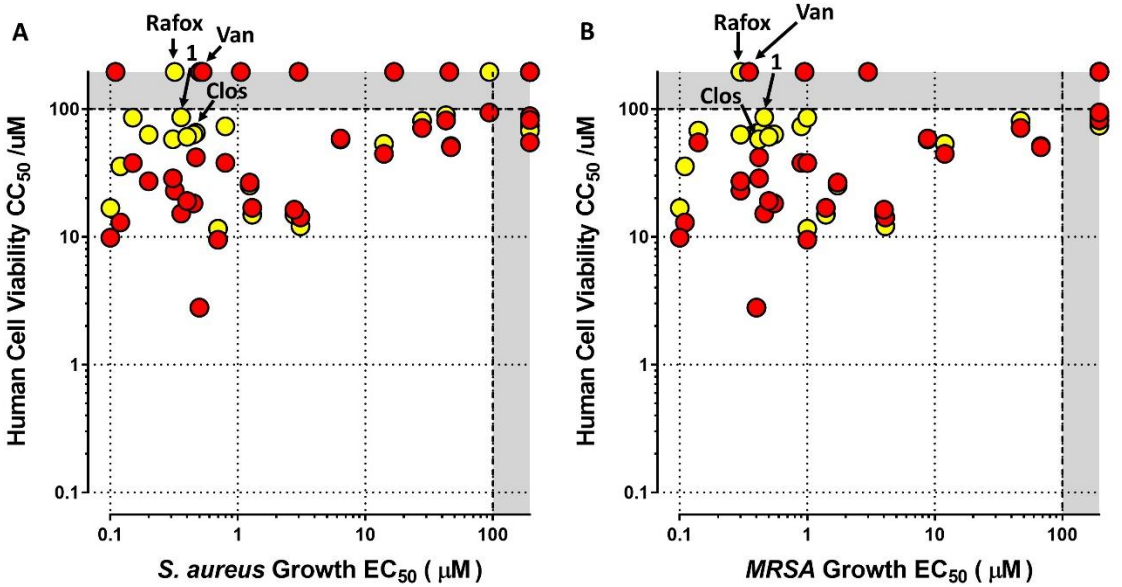

Figure 11. Correlation plots comparing human cell cytotoxicity results with susceptible S. aureus (**A**) and MRSA (**B**) proliferation inhibition results.

MRSA cannot easily generate resistance to lead analogs

After identifying which compounds were able to selectively inhibit the GroEL chaperonin system and kill bacteria, we next evaluated whether bacteria would be able to quickly develop resistance to lead candidate inhibitors. This was a concern we encountered with another series of GroEL inhibitors we have been studying, represented by the bis-sulfonamido compound **28R** shown in **Figure 12B** (unpublished results). For this experiment, we adapted a liquid culture resistance assay from the previously established procedures of Kim *et al.* (Kim 2014), and used our MRSA strain as the test bacteria. An outline of the general protocol is presented in **Figure 12A**, with detailed procedures presented in the Experimental section. Briefly, test compounds were incubated in dilution series with MRSA for 24 h and an EC_{50} was determined. The first well where bacterial growth was >50% was then sub-cultured for another 24 h with test compound again in dilution series. Serial passage in this manner was conducted for a total of 12 days, each day determining a new EC_{50} value for the test compound. Test compounds that MRSA can rapidly generate resistance to will exhibit increases in their EC_{50} over each successive passage, which was found to be the case for **28R**. We evaluated two of our lead GroEL inhibitors, **1** and **11**, along with vancomycin as a control as we have found this strain cannot easily generate resistance to this antibiotic. Over the 12-day course of this experiment, compounds **1** and **11** exhibited exemplary antibiotic efficacy that this MRSA strain was not able to easily generate resistance to. We also found that compounds **1** and **11** maintained efficacy against the resistant strain generated by **28R** in this experiments (results not shown).

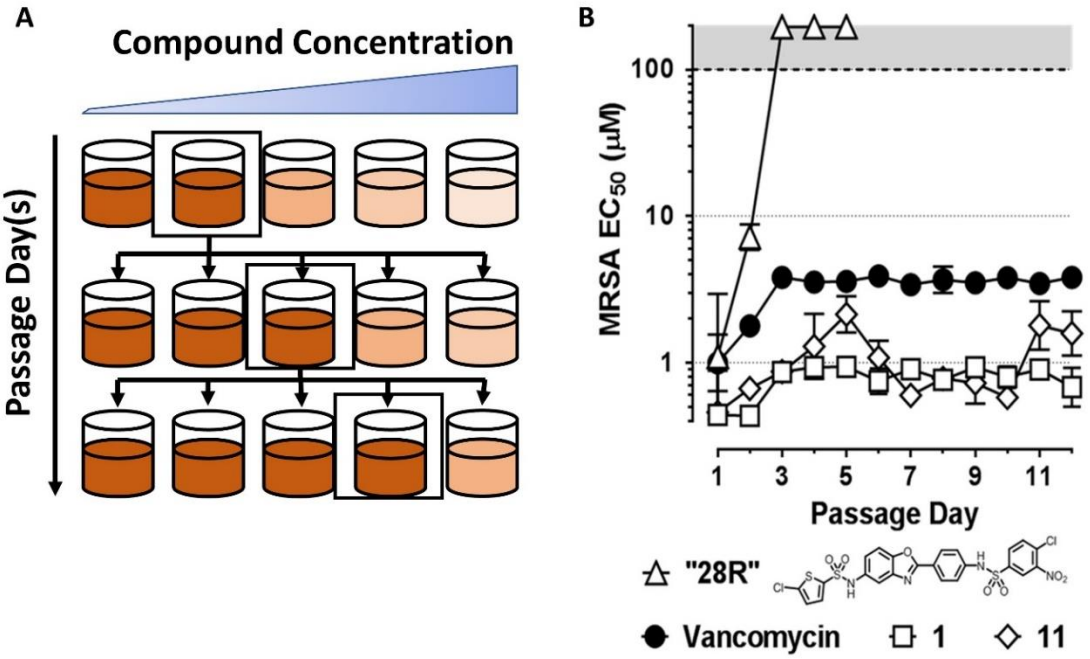

Figure 12. MRSA Gain-of-resistance assay protocol overview and results. **A.** General protocol of the MRSA gain-of-resistance assay. Each level of wells represents a new "passage" of inoculated sample from the previous day. Wells with a black box around represent the sample that exhibits viability at the highest compound concentration, which will be used to inoculate for the next passage. EC_{50} values were calculated in each day of passage (adapted from Kim *et al.,* 2014) **B.** Methicillin-resistant *S. aureus* (MRSA) gain-of-resistance assay with a compound from another series (**28R**), the parent scaffold (**1**), analog **11**, and vancomycin. Each passage day is representative of the EC_{50} values recorded prior in the two-fold dilution series of each compound. The final EC_{50} values were recorded at day 12.

Compound 1 is bactericidal to *S. aureus* within established biofilms

While we found that *S. aureus* is not able to easily generate resistance to compounds **1** and **11**, what remained to be seen was whether this series of inhibitors would be effective at preventing bacteria from establishing biofilms and be able to kill bacteria within established biofilms. Establishing biofilms is another effective mechanism by which *S. aureus* can evade the effects of many current antibiotics, including vancomycin. To gauge the efficacy of lead inhibitor **1** at preventing *S. aureus* from forming biofilms in the first place, we employed an assay similar to the liquid culture

assay we used to determine inhibition of bacterial proliferation, with a few modifications (detailed procedures presented in the Experimental section). Briefly, compound **1** was incubated with *S. aureus* bacteria in media supplemented with 0.5% glucose (to support biofilm formation) for 24 h at 37°C. After 24 h, the supernatant was gently washed from the wells, and the biofilm that had formed on the well surface was stained with crystal-violet and quantified by UV-Vis spectroscopy. We found that both compound **1** and vancomycin were able to prevent *S. aureus* from forming biofilms with EC_{50} values nearly equipotent to antibacterial EC_{50}s we determined against planktonic bacterial growth (**Figure 13**). This is probably not surprising as compound **1** and vancomycin are bactericidal against *S. aureus*, and thus dead bacteria are not able to form biofilms. Next, we evaluated whether or not compound **1** would be bactericidal to *S. aureus* that were within already established biofilms. In this assay, we first grew *S. aureus* bacteria for 24 h in the absence of test compounds so that they could establish biofilms in the wells. After 24 h, the cultures were removed, the wells were washed gently, and fresh media was added along with compound **1** and vancomycin. The cultures were incubated in the presence of test compounds for another 24 h, then the wells were gently washed again to remove compound and any planktonic bacteria that had emerged. Fresh media was then added and the cultures were incubated for another 24 h to allow any viable bacteria remaining in the biofilms to emerge and grow planktonically again. While there is about a 7-fold shift in EC_{50} values for compound **1** killing planktonic bacteria (EC_{50} = 0.36 μM) vs. biofilm bacteria (EC_{50} = 2.4 μM), this is still a very exciting result considering vancomycin was completely ineffective against biofilm bacteria, and especially since this inhibitor has not yet been optimized from the initial GroEL inhibitor hit. Thus, this scaffold shows considerable promise to take forward for further development as an antibacterial candidate.

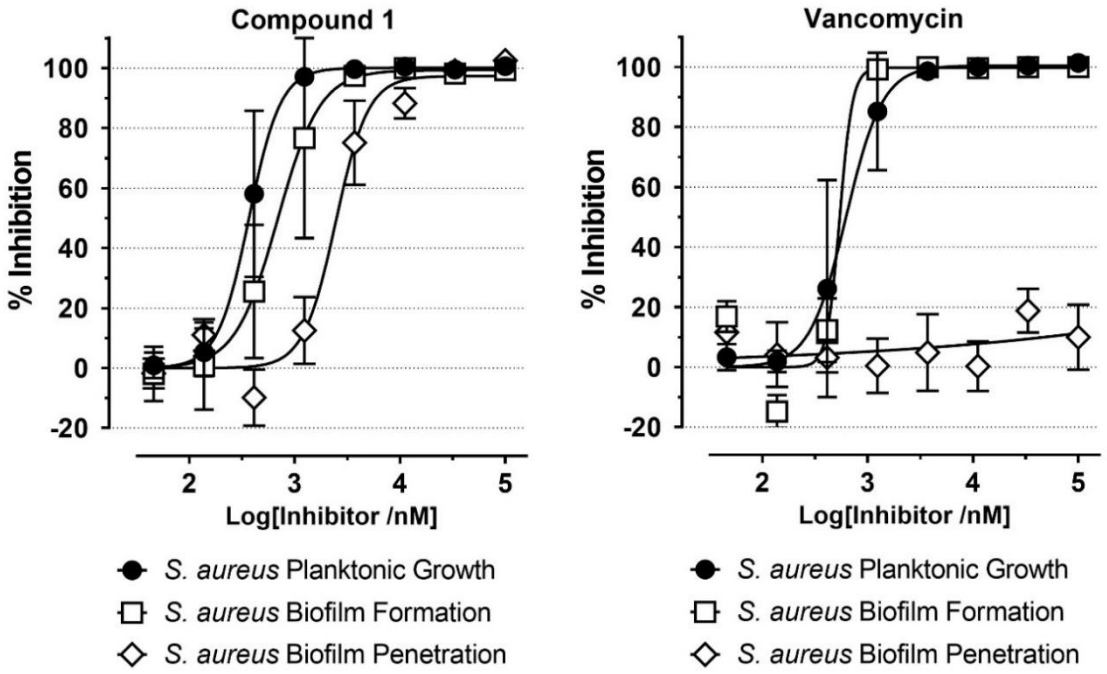

Figure 13. Biofilm and growth assay results. Percent inhibition plot showing results from biofilm prevention of formation, biofilm penetration, and planktonic growth with the parent scaffold (Compound **1**) and vancomycin.

CONCLUSIONS AND FUTURE DIRECTIONS

In this study, we developed a series of analogs of the previously identified hit GroEL inhibitor, compound **1**, and systematically evaluated the contributions that the $\mathbf{R^1}$ to $\mathbf{R^5}$ substituents and substructures make to being able to selectively inhibit the GroEL/ES chaperonin system and kill bacteria. Potent inhibitors (<10 μM) primarily resembled the parent scaffold (**1**), where a maximum of only one substituent, being bromine at $\mathbf{R^5}$ or chlorine at $\mathbf{R^2}$ or could be removed. It was found that these inhibitors correlate closely to disruption of growth in primarily Gram-positive species in the *ESKAPE* pathogens, a correlation not seen in human chaperonin (HSP60/10) inhibition vs HEK 293/THLE3 human cell toxicity. Structurally mapping this therapeutic window identifies the $\mathbf{R^3}$ hydroxyl group facilitating antibacterial efficacy and $\mathbf{R^1}$ benzothiazole buffering HEK 293/THLE3 toxicity, summarized in **Figure 14**. Additionally, compound **1** and vancomycin both did not encounter resistance through an 11-day passage in MRSA, maintaining efficacy ≤4 μM. However, it was found *S. aureus* biofilms are susceptible to compound **1** penetration, where vancomycin is not. This result validates the series as a strong antimicrobial hit that can penetrate biofilms, an innate resistance mechanism associated with chronic infection.

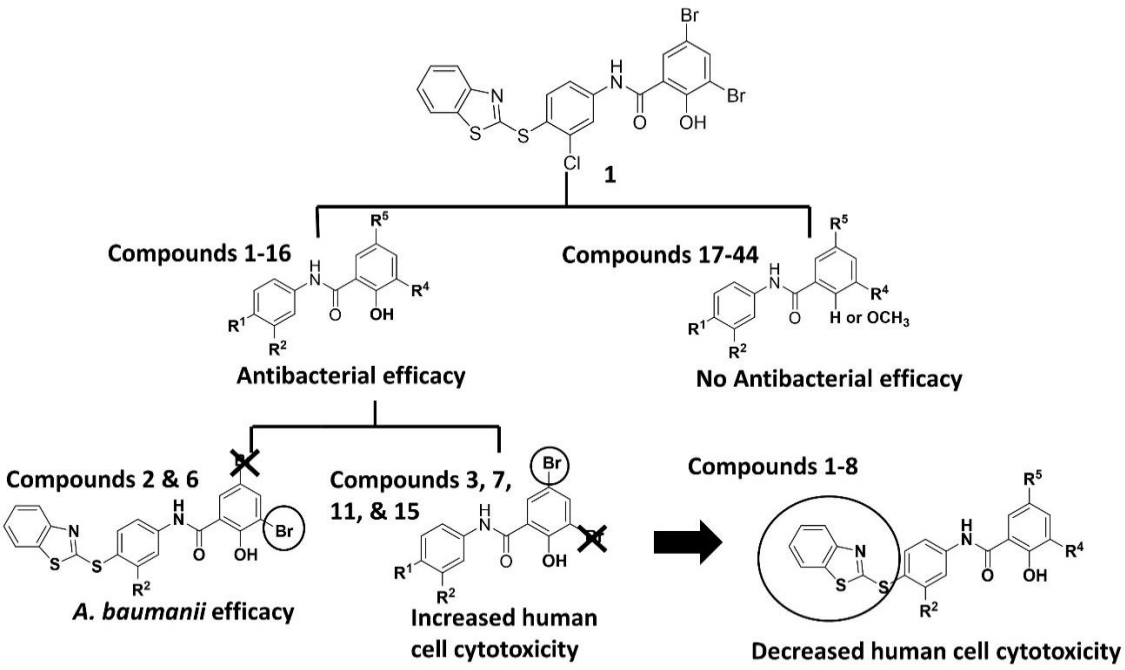

Figure 14. SAR breakdown of compound 1 scaffold. Antibacterial efficacy and human cell toxicity breakdown of substituents on the compound **1** scaffold. When groups are not represented by "**R"** it signifies an importance of the drawn group to the labeled phenotype. Broken down into 3 tiers, tier 1 (top) shows the parent compound **1.** Tier 2 shows the split between effective antibacterial analogs with a hydroxyl-OH at **R^3.** Tier 3 shows the split between **R^4** and **R^5** positioned bromine to both reduce human cell toxicity and enhance *A. baumanii* efficacy (which also requires benzothiazole as drawn). Tier 3 also includes an arrow highlighting the importance of benzothiazole to buffer human cell toxicity in antibacterial analogs.

In deriving a minimal scaffold that removes unneeded groups from compound **1**, compounds **2** and **5** are the best inhibitors that omit any substituents. Moving forward in the goal of synthesizing an antibiotic, optimization by adding various chemical groups to this scaffold will work to retain antibacterial efficacy and minimize any off-target toxicities. Future studies will also center around expression and purification of chaperonin proteins from *ESKAPE* pathogens to determine if inhibition correlates to efficacy better than utilized *E. coli* GroEL/ES. Additionally, the detailed mechanism of action these inhibitors have on the chaperonin system has yet to be fully elucidated. Future experiments centered around binding studies such as isothermal titration calorimetry (ITC), X-ray crystallography, and surface plasmon resonance (SPR) will

have to be utilized to elucidate a detailed MOA. Mouse studies with optimized analogs in the future will also provide insight into ADME properties for these molecules, as well as efficacy within infected animals.

EXPERIMENTAL

Compound Synthesis and Characterization

Unless otherwise stated, all chemicals were purchased from commercial suppliers and used without further purification. Reaction progress was monitored by thin-layer chromatography on silica gel 60 F254 coated glass plates (EM Sciences). Flash chromatography was performed using a Biotage Isolera One flash chromatography system and eluting through Biotage KP-Sil Zip or Snap silica gel columns for normal-phase separations (hexanes:EtOAc gradients) or Snap KP-C18-HS columns for reverse-phase separations (H_2O:MeOH gradients). Reverse-phase high-performance liquid chromatography (RP-HPLC) was performed using a Waters 1525 binary pump, 2489 tunable UV/Vis detector (254 and 280 nm detection), and 2707 autosampler. For preparatory HPLC purification, samples were chromatographically separated using a Waters XSelect CSH C18 OBD prep column (part number 186005422, 130 Å pore size, 5 μm particle size, 19x150 mm), eluting with a H_2O:CH_3CN gradient solvent system. Linear gradients were run from either 100:0, 80:20, or 60:40 A:B to 0:100 A:B (A = 95:5 H_2O:CH_3CN, 0.05% TFA; B = 5:95 H_2O:CH_3CN, 0.05% TFA. Products from normal-phase separations were concentrated directly, and reverse-phase separations were concentrated, diluted with H_2O, frozen, and lyophilized. For primary compound purity analyses (HPLC-1), samples were chromatographically separated using a Waters XSelect CSH C18 column (part number 186005282, 130 Å pore size, 5 μm particle size, 3.0x150 mm), eluting with the above H_2O:CH_3CN gradient solvent systems. For secondary purity analyses (HPLC-2) of final test compounds, samples were chromatographically separated using a Waters XBridge C18 column (either part number 186003027, 130 Å pore size, 3.5 μm particle size, 3.0x100 mm, or part number 186003132, 130 Å pore size, 5.0 μm particle size, 3.0x100 mm), eluting with a

H_2O:MeOH gradient solvent system. Linear gradients were run from either 100:0, 80:20, 60:40, or 20:80 A:B to 0:100 A:B (A = 95:5 H_2O:MeOH, 0.05% TFA; B = 5:95 H_2O:MeOH, 0.05% TFA). Test compounds were found to be >95% in purity from both RP-HPLC analyses. Mass spectrometry data were collected using either an Agilent analytical LC-MS at the IU Chemical Genomics Core Facility (CGCF), or a Thermo-Finnigan LTQ LC-MS in-lab. ^{1}H-NMR spectra were recorded on a Bruker 300 MHz spectrometer at the CGCF. Chemical shifts are reported in parts per million and calibrated to the d_6-DMSO solvent peaks at 2.50 ppm.

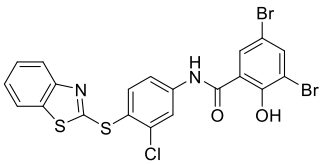

1: *N*-(4-(Benzo[*d*]thiazol-2-ylthio)-3-chlorophenyl)-3,5-dibromo-2- hydroxybenzamide. To a stirring mixture of **29** (51.0 mg, 0.0872 mmol) in anhydrous DCM (5 mL) was added BBr_3 (0.26 mL of 1 M in DCM, 0.26 mmol). The reaction was allowed to stir at R.T. (under Ar) for 18 h and then quenched with MeOH. Flash chromatographic purification (hexanes:EtOAc gradient) afforded **1** as an off-white solid (34.4 mg, 69% yield). ^{1}H-NMR (300 MHz, d_6-DMSO) δ 11.14 (br s, 1H), 8.19 (dd, *J* = 6.2, 2.2 Hz, 2H), 7.94-8.05 (m, 3H), 7.82-7.89 (m, 2H), 7.47 (td, *J* = 7.7, 1.3 Hz, 1H), 7.33-7.40 (m, 1H); MS (ESI) $C_{20}H_{10}Br_2ClN_2O_2S_2$ $[M-H]^-$ *m/z* expected = 566.8, observed = 566.6; HPLC-1 = 99%; HPLC-2 = 98%.

.....

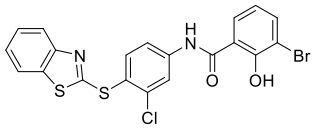

2: *N*-(4-(Benzo[*d*]thiazol-2-ylthio)-3-chlorophenyl)-3-bromo-2-hydroxybenzamide. To a stirring mixture of **30** (70.4 mg, 0.139 mmol) in anhydrous DCM (5 mL) was added BBr_3 (0.42 mL of 1 M in DCM, 0.42 mmol). The reaction was allowed to stir at R.T. (under Ar) for 18 h and then quenched with MeOH. Flash chromatographic purification (hexanes:EtOAc gradient) afforded **2** as an off-white solid (53.0 mg, 77% yield). ^{1}H-NMR (300 MHz, d_6-DMSO) δ 12.19 (br s, 1H), 10.93 (s, 1H), 8.22 (d, *J* = 2.1 Hz, 1H), 7.94-8.03 (m, 3H), 7.81-7.90 (m,

3H), 7.47 (t, *J* = 7.6 Hz, 1H), 7.33-7.40 (m, 1H), 6.99 (t, *J* = 7.9 Hz, 1H); MS (ESI) $C_{20}H_{11}BrClN_2O_2S_2$ $[M-H]^-$ *m/z* expected = 488.9, observed = 488.7; HPLC-1 = 99%; HPLC-2 = 99%.

.....

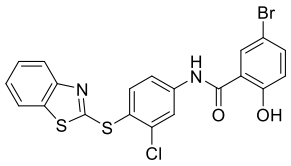

3: *N*-(4-(Benzo[*d*]thiazol-2-ylthio)-3-chlorophenyl)-5-bromo-2-hydroxybenzamide. To a stirring mixture of **31** (69.0 mg, 0.136 mmol) in anhydrous DCM (5 mL) was added BBr_3 (0.41 mL of 1 M in DCM, 0.41 mmol). The reaction was allowed to stir at R.T. (under Ar) for 18 h and then quenched with MeOH. Flash chromatographic purification (hexanes:EtOAc gradient) afforded **3** as an off-white solid (57.4 mg, 86% yield). ^{1}H-NMR (300 MHz, d_6-DMSO) δ 11.47 (br s, 1H), 10.74 (s, 1H), 8.25 (d, *J* = 2.2 Hz, 1H), 7.93-8.01 (m, 3H), 7.82-7.89 (m, 2H), 7.60 (dd, *J* = 8.8, 2.6 Hz, 1H), 7.47 (t, *J* = 7.1 Hz, 1H), 7.31-7.39 (m, 1H), 6.99 (d, *J* = 8.8 Hz, 1H); MS (ESI) $C_{20}H_{11}BrClN_2O_2S_2$ $[M-H]^-$ *m/z* expected = 488.9, observed = 488.7; HPLC-1 = 99%; HPLC-2 = 98%.

.....

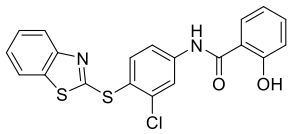

4: *N*-(4-(Benzo[*d*]thiazol-2-ylthio)-3-chlorophenyl)-2-hydroxybenzamide. To a stirring mixture **32** (151 mg, 0.353 mmol) in anhydrous DCM (5 mL) was added BBr_3 (1.06 mL of 1 M in DCM, 1.06 mmol). The reaction was allowed to stir at R.T. (under Ar) for 18 h and then quenched with MeOH. Flash chromatographic purification (hexanes:EtOAc gradient), followed by preparatory RP-HPLC purification, afforded **4** as an off-white solid (100 mg, 69% yield). ^{1}H-NMR (300 MHz, d_6-DMSO) δ 11.35 (s, 1H), 10.71 (s, 1H), 8.28 (d, *J* = 2.1 Hz, 1H), 7.93-8.00 (m, 2H), 7.83-7.90 (m, 3H), 7.72-7.50 (m, 2H), 7.32-7.38 (m, 1H), 6.95-7.05 (m, 2H); MS (ESI) $C_{20}H_{12}ClN_2O_2S_2$ $[M-H]^-$ *m/z* expected = 411.0, observed = 410.9; HPLC-1 = 99%; HPLC-2 = >99%.

.....

5: *N*-(4-(Benzo[*d*]thiazol-2-ylthio)phenyl)-3,5-dibromo-2-hydroxybenzamide. To a stirring mixture **33** (123 mg, 0.223 mmol) in anhydrous DCM (5 mL) was added BBr_3 (0.67 mL of 1 M in DCM, 0.67 mmol). The reaction was allowed to stir at R.T. (under Ar) for 18 h and then quenched with MeOH. Flash chromatographic purification (hexanes:EtOAc gradient), followed by preparatory RP-HPLC purification, afforded **5** as a white solid (72.9 mg, 61% yield). ^{1}H-NMR (300 MHz, d_6-DMSO) δ 12.25-13.00 (br s, 1H), 10.94 (s, 1H), 8.25 (d, *J* = 2.3 Hz, 1H), 8.04 (d, J = 2.2 Hz, 1H), 7.88-7.96 (m, 3H), 7.80-7.87 (m, 3H), 7.42-7.48 (m, 1H), 7.30-7.37 (m, 1H); MS (ESI) $C_{20}H_{11}Br_2N_2O_2S_2$ $[M-H]^-$ *m/z* expected = 532.9, observed = 532.7; HPLC-1 = 97%; HPLC-2 = >99%.

.....

6: *N*-(4-(Benzo[*d*]thiazol-2-ylthio)phenyl)-3-bromo-2-hydroxybenzamide. To a stirring mixture **34** (108 mg, 0.228 mmol) in anhydrous DCM (5 mL) was added BBr_3 (0.68 mL of 1 M in DCM, 0.68 mmol). The reaction was allowed to stir at R.T. (under Ar) for 18 h and then quenched with MeOH. Flash chromatographic purification (hexanes:EtOAc gradient), followed by preparatory RP-HPLC purification, afforded **6** as a tan solid (55.5 mg, 53% yield). ^{1}H-NMR (300 MHz, d_6-DMSO) δ 12.40-12.65 (br s, 1H), 10.96 (s, 1H), 8.05 (dd, *J* = 8.0, 1.4 Hz, 1H), 7.90-7.98 (m, 3H), 7.79-7.88 (m, 4H), 7.45 (td, *J* = 7.7, 1.3 Hz, 1H), 7.30-7.37 (m, 1H), 6.96 (t, *J* = 7.9 Hz, 1H); MS (ESI) $C_{20}H_{12}BrN_2O_2S_2$ $[M-H]^-$ *m/z* expected = 455.0, observed = 454.8; HPLC-1 = >99%; HPLC-2 = >99%.

.....

7: *N*-(4-(Benzo[*d*]thiazol-2-ylthio)phenyl)-5-bromo-2-hydroxybenzamide. To a stirring mixture **35** (90.6 mg, 0.192 mmol) in anhydrous DCM (5 mL) was added BBr_3 (0.58 mL of 1 M in DCM, 0.58 mmol).

The reaction was allowed to stir at R.T. (under Ar) for 18 h and then quenched with MeOH. Flash chromatographic purification (hexanes:EtOAc gradient), followed by preparatory RP-HPLC purification, afforded **7** as a white solid (24.8 mg, 28% yield). ^{1}H-NMR (300 MHz, d_6-DMSO) δ 11.56-11.66 (br s, 1H), 10.65 (s, 1H), 8.00 (d, J = 2.5 Hz, 1H), 7.90-7.98 (m, 3H), 7.78-7.87 (m, 3H), 7.59 (dd, J = 8.8, 2.5 Hz, 1H), 7.41-7.48(m, 1H), 7.30-7.37 (m, 1H), 6.99 (d, J = 8.8 Hz, 1H); MS (ESI) $C_{20}H_{12}BrN_2O_2S_2$ $[M-H]^-$ *m/z* expected = 455.0, observed = 454.8; HPLC-1 = 99%; HPLC-2 = >99%.

.....

8: *N*-(4-(Benzo[*d*]thiazol-2-ylthio)phenyl)-2-hydroxybenzamide. To a stirring mixture **36** (150 mg, 0.382 mmol) in anhydrous DCM (5 mL) was added BBr_3 (1.15 mL of 1 M in DCM, 1.15 mmol). The reaction was allowed to stir at R.T. (under Ar) for 18 h and then quenched with MeOH. Flash chromatographic purification (hexanes:EtOAc gradient), followed by preparatory RP-HPLC purification, afforded **8** as a white solid (97.3 mg, 67% yield). ^{1}H-NMR (300 MHz, d_6-DMSO) δ 11.47-11.60 (br s, 1H), 10.64 (s, 1H), 7.90-7.98 (m, 4H), 7.78-7.87 (m, 3H), 7.41-7.49 (m, 2H), 7.29-7.36 (m, 1H), 6.95-7.04 (m, 2H); MS (ESI) $C_{20}H_{13}N_2O_2S_2$ $[M-H]^-$ *m/z* expected = 377.0, observed = 376.9; HPLC-1 = >99%; HPLC-2 = >99%.

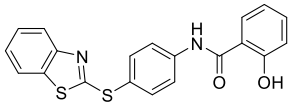

.....

9: 3,5-Dibromo-*N*-(3-chlorophenyl)-2-hydroxybenzamide. To a stirring mixture **37** (200 mg, 0.476 mmol) in anhydrous DCM (5 mL) was added BBr_3 (1.45 mL of 1 M in DCM, 1.45 mmol). The reaction was allowed to stir at R.T. (under Ar) for 3 days and then quenched with MeOH. The product was extracted into EtOAc and the organics were rinsed with brine, dried over Na_2SO_4, filtered, and concentrated. Flash chromatographic purification (hexanes:EtOAc gradient) afforded **9** as a tan solid (128 mg, 66% yield). ^{1}H-NMR (300 MHz, d_6-DMSO) δ

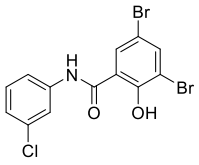

12.35-12.80 (br s, 1H), 10.74 (s, 1H), 8.24 (d, *J* = 2.2 Hz, 1H), 8.03 (d, *J* = 2.2 Hz, 1H), 7.85 (t, *J* = 1.9 Hz, 1H), 7.60-7.67 (m, 1H), 7.43 (t, *J* = 8.1 Hz, 1H), 7.23-7.29 (m, 1H); MS (ESI) $C_{13}H_7Br_2ClNO_2$ $[M-H]^-$ *m/z* expected = 401.9, observed = 401.7; HPLC-1 = 97%; HPLC-2 = 97%.

.....

10: 3-Bromo-*N*-(3-chlorophenyl)-2-hydroxybenzamide. To a stirring mixture **38** (155 mg, 0.455 mmol) in anhydrous DCM (5 mL) was added BBr_3 (1.35 mL of 1 M in DCM, 1.35 mmol). The reaction was allowed to stir at R.T. (under Ar) for 18 h and then quenched with MeOH. Reverse-phase flash chromatographic purification (H_2O:MeOH gradient) afforded **10** as a tan solid (138 mg, 93% yield). ^{1}H-NMR (300 MHz, *d*$_6$-DMSO) δ 12.60 (br s, 1H), 10.69 (s, 1H), 8.02 (dd, *J* = 8.0, 1.5 Hz, 1H), 7.87 (t, *J* = 2.0 Hz, 1H), 7.82 (dd, *J* = 7.9, 1.4 Hz, 1H), 7.65 (ddd, *J* = 8.2, 2.0, 0.9 Hz, 1H), 7.43 (t, *J* = 8.1 Hz, 1H), 7.25 (ddd, *J* = 8.0, 2.1, 0.9 Hz, 1H), 6.96 (t, *J* = 7.9 Hz, 1H); MS (ESI) $C_{13}H_{10}BrClNO_2$ $[MH]^+$ *m/z* expected = 327.96, observed = 328.10; HPLC-1 = >99%; HPLC-2 = >99%.

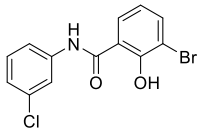

.....

11: 5-Bromo-*N*-(3-chlorophenyl)-2-hydroxybenzamide. To a stirring mixture **39** (205 mg, 0.602 mmol) in anhydrous DCM (5 mL) was added BBr_3 (1.80 mL of 1 M in DCM, 1.80 mmol). The reaction was allowed to stir at R.T. (under Ar) for 18 h and then quenched with MeOH. Reverse-phase flash chromatographic purification (H_2O:MeOH gradient) afforded **11** as a white solid (113 mg, 58% yield). ^{1}H-NMR (300 MHz, *d*$_6$-DMSO) δ 11.65 (br s, 1H), 10.50 (s, 1H), 8.00 (d, *J* = 2.5 Hz, 1H), 7.91 (t, *J* = 2.0 Hz, 1H), 7.55-7.64 (m, 2H), 7.40 (t, *J* = 8.1 Hz, 1H), 7.20 (ddd, *J* = 8.0, 2.0, 0.9 Hz, 1H), 6.97 (d, *J* = 8.8 Hz, 1H); MS (ESI) $C_{13}H_{10}BrClNO_2$ $[MH]^+$ *m/z* expected = 327.96, observed = 328.10; HPLC-1 = >99%; HPLC-2 = >99%.

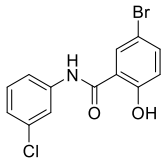

.....

12: *N*-(3-Chlorophenyl)-2-hydroxybenzamide. To a stirring mixture **40** (142 mg, 0.543 mmol) in anhydrous DCM (5 mL) was added BBr_3 (1.65 mL of 1 M in DCM, 1.65 mmol). The reaction was allowed to stir at R.T. (under Ar) for 18 h and then quenched with MeOH. Reverse-phase flash chromatographic purification (H_2O:MeOH gradient) afforded **12** as an off-white solid (142 mg, 70% yield). ^{1}H-NMR (300 MHz, d_6-DMSO) δ 11.55 (br s, 1H), 10.48 (s, 1H), 7.87-7.96 (m, 2H), 7.62 (ddd, *J* = 8.2, 2.0, 1.0 Hz, 1H), 7.36-7.48 (m, 2H), 7.19 (ddd, *J* = 8.0, 2.0, 0.9 Hz, 1H), 6.93-7.03 (m, 2H); MS (ESI) $C_{13}H_{11}ClNO_2$ $[MH]^+$ *m/z* expected = 248.05, observed = 248.11; HPLC-1 = >99%; HPLC-2 = >99%.

.....

13: 3,5-Dibromo-2-hydroxy-*N*-phenylbenzamide. To a stirring mixture **41** (149 mg, 0.386 mmol) in anhydrous DCM (5 mL) was added BBr_3 (1.15 mL of 1 M in DCM, 1.15 mmol). The reaction was allowed to stir at R.T. (under Ar) for 3 days and then quenched with MeOH. The product was extracted into EtOAc and the organics were rinsed with brine, dried over Na_2SO_4, filtered, and concentrated. Flash chromatographic purification (hexanes:EtOAc gradient) afforded **13** as a tan solid (128 mg, 66% yield). ^{1}H-NMR (300 MHz, d_6-DMSO) δ 12.90-13.10 (br s, 1H), 10.65 (s, 1H), 8.31 (d, *J* = 2.3 Hz, 1H), 8.03 (d, *J* = 2.2 Hz, 1H), 7.64-7.71 (m, 2H), 7.38-7.45 (m, 2H), 7.17-7.24 (m, 1H); MS (ESI) $C_{13}H_8Br_2NO_2$ $[M-H]^-$ *m/z* expected = 367.9, observed = 367.7; HPLC-1 = 98%; HPLC-2 = >99%.

.....

14: 3-Bromo-2-hydroxy-*N*-phenylbenzamide. To a stirring mixture **42** (186 mg, 0.608 mmol) in anhydrous DCM (5 mL) was added BBr_3 (1.80 mL of 1 M in DCM, 1.80 mmol). The reaction was allowed to stir at R.T. (under Ar) for 18 h and then quenched with MeOH. Reverse-phase flash chromatographic purification (H_2O:MeOH gradient) afforded **14** as a white solid (162 mg, 91% yield). ^{1}H-

NMR (300 MHz, d_6-DMSO) δ 13.01 (s, 1H), 10.59 (s, 1H), 8.08 (dd, *J* = 8.1, 1.4 Hz, 1H), 7.81 (dd, *J* = 7.9, 1.4 Hz, 1H), 7.65-7.73 (m, 2H), 7.35-7.45 (m, 2H), 7.14-7.24 (m, 1H), 6.95 (t, *J* = 7.9 Hz, 1H); MS (ESI) $C_{13}H_{11}BrNO_2$ $[MH]^+$ *m/z* expected = 292.0, observed = 292.1; HPLC-1 = >99%; HPLC-2 = >99%.

.....

15: 5-Bromo-2-hydroxy-*N*-phenylbenzamide. To a stirring mixture **43** (138 mg, 0.451 mmol) in anhydrous DCM (5 mL) was added BBr_3 (1.35 mL of 1 M in DCM, 1.35 mmol). The reaction was allowed to stir at R.T. (under Ar) for 18 h and then quenched with MeOH. Reverse-phase flash chromatographic purification (H_2O:MeOH gradient) afforded **15** as a white solid (63.3 mg, 48% yield). ^{1}H-NMR (300 MHz, d_6-DMSO) δ 11.89 (br s, 1H), 10.41 (s, 1H), 8.07 (d, *J* = 2.5 Hz, 1H), 7.66-7.74 (m, 2H), 7.58 (dd, *J* = 8.8, 2.5 Hz, 1H), 7.38 (t, *J* = 7.9 Hz, 2H), 7.09-7.19 (m, 1H), 6.96 (d, *J* = 8.8 Hz, 1H); MS (ESI) $C_{13}H_{11}BrNO_2$ $[MH]^+$ *m/z* expected = 292.0, observed = 292.1; HPLC-1 = >99%; HPLC-2 = >99%.

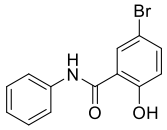

.....

16: 2-Hydroxy-*N*-phenylbenzamide. To a stirring mixture **44** (153 mg, 0.673 mmol) in anhydrous DCM (5 mL) was added BBr_3 (2.00 mL of 1 M in DCM, 2.00 mmol). The reaction was allowed to stir at R.T. (under Ar) for 18 h and then quenched with MeOH. Reverse-phase flash chromatographic purification (H_2O:MeOH gradient) afforded **16** as an off-white solid (95.5 mg, 67% yield). ^{1}H-NMR (300 MHz, d_6-DMSO) δ 11.81 (br s, 1H), 10.39 (s, 1H), 7.96 (dd, *J* = 7.8, 1.6 Hz, 1H), 7.67-7.74 (m, 2H), 7.34-7.46 (m, 3H), 7.10-7.17 (m, 1H), 6.93-7.01 (m, 2H); MS (ESI) $C_{13}H_{12}NO_2$ $[MH]^+$ *m/z* expected = 214.1, observed = 214.2; HPLC-1 = >99%; HPLC-2 = >99%.

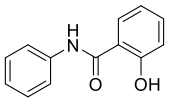

.....

17: *N*-(4-(Benzo[*d*]thiazol-2-ylthio)-3-chlorophenyl)-3,5-dibromobenzamide. 3,5-Dibromobenzoic acid (175 mg, 0.624 mmol) was stirred in anhydrous DCM (5 mL) with DCC (128 mg, 0.619 mmol) and DMAP (6.5 mg, 0.053 mmol) at R.T. for 1 h (under Ar). Compound **46** (150 mg, 0.514 mmol) was then added and the reaction was stirred for an additional 18 h. Flash chromatgraphic purification (hexanes:EtOAc gradient), followed by preparatory RP-HPLC purification, afforded **17** as a white solid (101 mg, 35% yield). ^{1}H-NMR (300 MHz, d_6-DMSO) δ 10.83 (br s, 1H), 8.24 (d, J = 2.1 Hz, 1H), 8.13-8.18 (m, 3H), 7.83-8.01 (m, 4H), 7.47 (td, J = 7.7, 1.3 Hz, 1H), 7.32-7.38 (m, 1H); MS (ESI) $C_{20}H_{10}Br_2ClN_2OS_2$ [M-H]$^-$ *m/z* expected = 550.8, observed = 550.6; HPLC-1 = 98%; HPLC-2 = 98%.

.....

18: *N*-(4-(Benzo[*d*]thiazol-2-ylthio)-3-chlorophenyl)-3-bromobenzamide. 3-Bromobenzoyl chloride (81.0 μL, 0.613 mmol), pyridine (61.0 μL, 0.748 mmol), and compound **46** (151 mg, 0.515 mmol) were stirred in anhydrous DCM (5 mL) at R.T. for 18 h (under Ar). Flash chromatographic purification (hexanes:EtOAc gradient) afforded **18** as a pale-yellow solid (226 mg, 92% yield). ^{1}H-NMR (300 MHz, d_6-DMSO) δ 10.79 (s, 1H), 8.28 (d, J = 2.0 Hz, 1H), 8.18 (t, J = 1.8 Hz, 1H), 7.90-8.00 (m, 4H), 7.83-7.88 (m, 2H), 7.54 (t, J = 7.9 Hz, 1H), 7.43-7.59 (m, 1H), 7.32-7.38 (m, 1H); MS (ESI) $C_{20}H_{11}BrClN_2OS_2$ [M-H]$^-$ *m/z* expected = 472.9, observed = 472.7; HPLC-1 = 98%; HPLC-2 = 98%.

.....

19: *N*-(4-(Benzo[*d*]thiazol-2-ylthio)-3-chlorophenyl)benzamide. Benzoyl chloride (71.0 μL, 0.616 mmol), pyridine (61.0 μL, 0.748 mmol), and compound **46** (153

mg, 0.522 mmol) were stirred in anhydrous DCM (5 mL) at R.T. for 18 h (under Ar). Flash chromatographic purification (hexanes:EtOAc gradient) afforded **19** as a pale-yellow solid (188 mg, 91% yield). ^{1}H-NMR (300 MHz, d_6-DMSO) δ 10.72 (s, 1H), 8.31 (d, J = 1.6 Hz, 1H), 7.92-8.03 (m, 5H), 7.86 (d, J = 7.6 Hz, 1H), 7.54-7.67 (m, 3H), 7.43-7.50 (m, 1H), 7.32-7.38 (m, 1H); MS (ESI) $C_{20}H_{12}ClN_2OS_2$ $[M-H]^-$ *m/z* expected = 395.0, observed = 394.9; HPLC-1 = 99%; HPLC-2 = 99%.

.....

20: *N*-(4-(Benzo[*d*]thiazol-2-ylthio)phenyl)-3,5-dibromobenzamide. 3,5-Dibromobenzoic acid (120 mg, 0.428 mmol), compound **47** (85.8 mg, 0.332 mmol), EDC (88.9 mg, 0.464 mmol), HOBt•H_2O (82.5 mg, 0.539 mmol), and TEA (69.5 μL, 0.499 mmol) were stirred in anhydrous DCM (5 mL) at R.T. for 18 h (under Ar). Flash chromatographic purification (hexanes:EtOAc gradient) afforded **20** as an off-white solid (27.2 mg, 16% yield). ^{1}H-NMR (300 MHz, d_6-DMSO) δ 10.73 (s, 1H), 8.17 (d, J = 2.0 Hz, 2H), 8.13-8.15 (m, 1H), 7.91-8.02 (m, 3H), 7.80-7.87 (m, 3H), 7.42-7.48 (m, 1H), 7.30-7.37 (m, 1H); MS (ESI) $C_{20}H_{11}Br_2N_2OS_2$ $[M-H]^-$ *m/z* expected = 516.9, observed = 516.7; HPLC-1 = >99%; HPLC-2 = >99%.

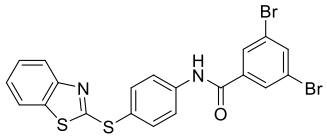

.....

21: *N*-(4-(Benzo[*d*]thiazol-2-ylthio)phenyl)-3-bromobenzamide. 3-Bromobenzoyl chloride (65.0 μL, 0.492 mmol), pyridine (40.0 μL, 0.491 mmol), and compound **47** (116 mg, 0.449 mmol) were stirred in anhydrous DCM (5 mL) at R.T. for 18 h (under Ar). Flash chromatographic purification (hexanes:EtOAc gradient) afforded **21** as a white solid (191 mg, 96% yield). ^{1}H-NMR (300 MHz, d_6-DMSO) δ 10.68 (s, 1H), 8.17 (d, J = 1.7 Hz, 1H), 7.96-8.03 (m, 3H), 7.91-7.95 (m, 1H), 7.79-7.86 (m, 4H), 7.50-7.57 (m, 1H), 7.45 (td, J = 7.7, 1.3 Hz,

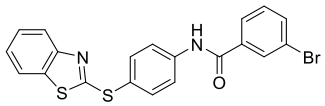

1H), 7.30-7.37 (m, 1H); MS (ESI) $C_{20}H_{12}BrN_2OS_2$ $[M-H]^-$ *m/z* expected = 439.0, observed = 438.8; HPLC-1 = 99%; HPLC-2 = >99%.

.....

22: *N*-(4-(Benzo[*d*]thiazol-2-ylthio)phenyl)benzamide.

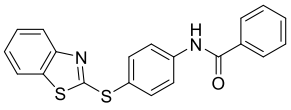

Benzoyl chloride (57.0 μL, 0.495 mmol), pyridine (44.0 μL, 0.540 mmol), and compound **47** (117 mg, 0.451 mmol) were stirred in anhydrous DCM (5 mL) at R.T. for 18 h (under Ar). Flash chromatographic purification (hexanes:EtOAc gradient) afforded **22** as a white solid (159 mg, 97% yield). ^{1}H-NMR (300 MHz, d_6-DMSO) δ 10.60 (s, 1H), 7.96-8.04 (m, 4H), 7.90-7.95 (m, 1H), 7.77-7.86 (m, 3H), 7.73-7.66 (m, 3H), 7.45 (td, *J* = 7.7, 1.2 Hz, 1H), 7.30-7.37 (m, 1H); MS (ESI) $C_{20}H_{13}N_2OS_2$ $[M-H]^-$ *m/z* expected = 361.1, observed = 361.0; HPLC-1 = >99%; HPLC-2 = 97%.

.....

23: 3,5-Dibromo-*N*-(3-chlorophenyl)benzamide. 3,5-Dibromobenzoic acid (299 mg, 1.07 mmol) was stirred in $SOCl_2$ (5 mL) at 60°C for 1 h, then was concentrated. Anhydrous DCM (5 mL), 3-chloroaniline (94.0 μL, 0.892 mmol), and pyridine (87.0 μL, 1.07 mmol) were added and the reaction was stirred at R.T. for 18 h (under Ar). Flash chromatographic purification (hexanes:EtOAc gradient) afforded **23** as an off-white solid (150 mg, 43% yield). ^{1}H-NMR (300 MHz, d_6-DMSO) δ 10.55 (s, 1H), 8.13 (d, *J* = 1.8 Hz, 2H), 8.02 (d, *J* = 1.9 Hz, 1H), 7.92 (t, *J* = 2.0 Hz, 1H), 7.65-7.71 (m, 1H), 7.40 (t, *J* = 8.1 Hz, 1H), 7.19 (ddd, *J* = 8.0, 2.1, 0.9 Hz, 1H); MS (ESI) $C_{13}H_9Br_2ClNO$ $[MH]^+$ *m/z* expected = 389.9, observed = 390.0; HPLC-1 = 97%; HPLC-2 = 97%.

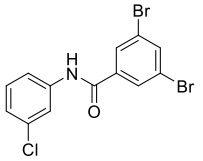

.....

24: 3-Bromo-*N*-(3-chlorophenyl)benzamide. 3-Bromobenzoyl chloride (0.23 mL, 1.7 mmol), pyridine (0.14 mL, 1.7 mmol), and 3-

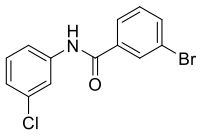

chloroaniline (0.15 mL, 1.4 mmol) were stirred in anhydrous DCM (5 mL) at R.T. for 18 h (under Ar). Flash chromatographic purification (hexanes:EtOAc gradient) afforded **24** as an off-white solid (338 mg, 77% yield). ^{1}H-NMR (300 MHz, d_6-DMSO) δ 10.50 (s, 1H), 8.14 (t, *J* = 1.8 Hz, 1H), 7.92-7.98 (m, 2H), 7.78-7.84 (m, 1H), 7.70 (ddd, *J* = 8.2, 2.0, 0.9 Hz, 1H), 7.51 (t, *J* = 8.1 Hz, 1H), 7.39 (t, *J* = 8.1 Hz, 1H), 7.18 (ddd, *J* = 8.0, 2.0, 0.9 Hz, 1H); MS (ESI) $C_{13}H_{10}BrClNO$ $[MH]^+$ *m/z* expected = 312.0, observed = 312.0; HPLC-1 = >99%; HPLC-2 = >99%.

.....

25: *N*-(3-Chlorophenyl)benzamide. Benzoyl chloride (0.26 mL, 1.7 mmol), pyridine (0.19 mL, 2.3 mmol), and 3-chloroaniline (0.20 mL, 2.3 mmol) were stirred in anhydrous DCM (5 mL) at R.T. for 18 h (under Ar).

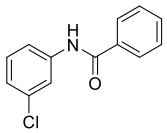

Flash chromatographic purification (hexanes:EtOAc gradient) afforded **25** as an off-white solid (414 mg, 94% yield). ^{1}H-NMR (300 MHz, d_6-DMSO) δ 10.42 (s, 1H), 7.93-7.99 (m, 3H), 7.71 (ddd, *J* = 8.2, 1.9, 0.9 Hz, 1H), 7.51-7.64 (m, 3H), 7.39 (t, *J* = 8.1 Hz, 1H), 7.16 (ddd, *J* = 8.0, 2.1, 0.9 Hz, 1H); MS (ESI) $C_{13}H_{11}ClNO$ $[MH]^+$ *m/z* expected = 232.1, observed = 232.0; HPLC-1 = >99%; HPLC-2 = >99%.

.....

26: 3,5-Dibromo-*N*-phenylbenzamide. 3,5-Dibromobenzoic acid (312 mg, 1.11 mmol) was stirred in $SOCl_2$ (5 mL) at 60°C for 1 h, then was concentrated. Anhydrous DCM (5 mL), aniline (85.0 μL, 0.931 mmol), and pyridine (90.0 μL, 1.10 mmol) were added and the reaction was stirred at R.T. for 18 h (under Ar).

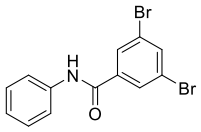

Flash chromatographic purification (hexanes:EtOAc gradient) afforded **26** as a white solid (224 mg, 68% yield). ^{1}H-NMR (300 MHz, d_6-DMSO) δ 10.42 (s, 1H), 8.14 (d, *J* = 1.7 Hz, 2H), 8.07-8.11 (m, 1H), 7.72-7.78 (m, 2H), 7.33-7.41 (m, 2H), 7.09-7.16 (m,

1H); MS (ESI) $C_{13}H_{10}Br_2NO$ $[MH]^+$ *m/z* expected = 355.9, observed = 356.0; HPLC-1 = >99%; HPLC-2 = >99%.

.....

27: 3-Bromo-*N*-phenylbenzamide. 3-Bromobenzoyl chloride (0.17 mL, 1.3 mmol), pyridine (0.11 mL, 1.3 mmol), and aniline (0.10 mL, 1.1 mmol) were stirred in anhydrous DCM (5 mL) at R.T. for 18 h (under Ar). Flash chromatographic purification (hexanes:EtOAc gradient) afforded **27** as a white solid (289 mg, 95% yield). ^{1}H-NMR (300 MHz, d_6-DMSO) δ 10.35 (s, 1H), 8.14 (t, *J* = 1.8 Hz, 1H), 7.95 (dt, *J* = 7.8, 1.3 Hz, 1H), 7.73-7.83 (m, 3H), 7.50 (t, *J* = 7.9 Hz, 1H), 7.32-7.39 (m, 2H), 7.08-7.16 (m, 1H); MS (ESI) $C_{13}H_{11}BrNO$ $[MH]^+$ *m/z* expected = 276.0, observed = 276.1; HPLC-1 = 98%; HPLC-2 = 98%.

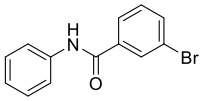

.....

28: *N*-Phenylbenzamide. Benzoyl chloride (0.30 mL, 2.6 mmol), pyridine (0.22 mL, 2.7mmol), and aniline (0.20 mL, 2.2 mmol) were stirred in anhydrous DCM (5 mL) at R.T. for 18 h (under Ar). Flash chromatographic purification (hexanes:EtOAc gradient) afforded **28** as a white solid (367 mg, 85% yield). ^{1}H-NMR (300 MHz, d_6-DMSO) δ 10.26 (s, 1H), 7.93-7.98 (m, 2H), 7.75-7.81 (m, 2H), 7.49-7.63 (m, 3H), 7.32-7.39 (m, 2H), 7.06-7.13 (m, 1H); MS (ESI) $C_{13}H_{12}NO$ $[MH]^+$ *m/z* expected = 198.1, observed = 198.0; HPLC-1 = >99%; HPLC-2 = >99%.

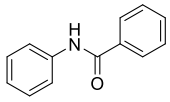

.....

29: *N*-(4-(Benzo[*d*]thiazol-2-ylthio)-3-chlorophenyl)-3,5-dibromo-2-methoxybenzamide. Compound **48** (225 mg, 0.726 mmol) was stirred in $SOCl_2$ (2 mL) at 60°C for 1 h, then was concentrated. Anhydrous DCM (5 mL), compound **46** (148 mg, 0.505 mmol), and pyridine (62.0 μL, 0.760 mol) were added and the reaction was stirred at R.T. for 18 h (under Ar). Flash chromatographic purification (hexanes:EtOAc gradient) afforded **29** as

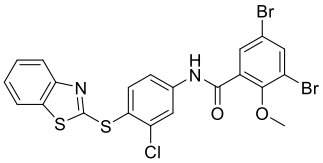

a yellow solid (58.6 mg, 20% yield). ^{1}H-NMR (300 MHz, d_6-DMSO) δ 11.00 (s, 1H), 8.21 (d, *J* = 2.1 Hz, 1H), 8.10 (d, *J* = 2.3 Hz, 1H), 7.97 (t, *J* = 8.3 Hz, 2H), 7.82-7.87 (m, 2H), 7.78 (dd, *J* = 8.6, 2.2 Hz, 1H), 7.47 (td, *J* = 7.7, 1.3 Hz, 1H), 7.32-7.38 (m, 1H), 3.84 (s, 3H); MS (ESI) $C_{21}H_{12}Br_2ClN_2O_2S_2$ $[M-H]^-$ *m/z* expected = 580.8, observed = 580.7; HPLC-1 = >99%; HPLC-2 = >99%.

.....

30: *N*-(4-(Benzo[*d*]thiazol-2-ylthio)-3-chlorophenyl)-3-bromo-2-methoxybenzamide. 3-Bromo-2-methoxybenzoic acid (171 mg, 0.741 mmol) was stirred in $SOCl_2$ (2 mL) at 60°C for 1 h, then was concentrated. Anhydrous DCM (5 mL), compound **46** (170 mg, 0.581 mmol), and pyridine (60.5 μL, 0.742 mol) were added and the reaction was stirred at R.T. for 18 h (under Ar). Flash chromatographic purification (hexanes:EtOAc gradient) afforded **30** as a yellow solid (48.6 mg, 17% yield). ^{1}H-NMR (300 MHz, d_6-DMSO) δ 10.94 (s, 1H), 8.24 (d, *J* = 2.1 Hz, 1H), 7.93-8.00 (m, 2H), 7.79-7.87 (m, 3H), 7.61 (dd, *J* = 7.6, 1.6 Hz, 1H), 7.47 (td, *J* = 7.7, 1.3 Hz, 1H), 7.32-7.39 (m, 1H), 7.24 (t, *J* = 7.8 Hz, 1H), 3.84 (s, 3H); MS (ESI) $C_{21}H_{13}BrClN_2O_2S_2$ $[M-H]^-$ *m/z* expected = 502.9, observed = 502.7; HPLC-1 = 98%; HPLC-2 = 98%.

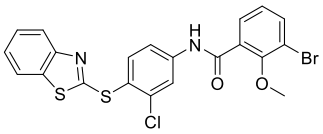

.....

31: *N*-(4-(Benzo[*d*]thiazol-2-ylthio)-3-chlorophenyl)-5-bromo-2-methoxybenzamide. Compound **49** (1.13 g, 4.88 mmol) was stirred in $SOCl_2$ (3 mL) at 60°C for 1 h, then was concentrated. Anhydrous DCM (10 mL), compound **46** (1.18 g, 4.04 mmol), and pyridine (0.49 mL, 6.0 mmol) were added and the reaction was stirred at R.T. for 18 h (under Ar). The reaction was then diluted into hexanes and the precipitate was filtered, rinsed with 1 M HCl and water, and dried. Flash chromatographic purification (hexanes:EtOAc gradient) afforded **31** as a yellow solid (1.80 g, 88% yield). ^{1}H-NMR (300 MHz, d_6-

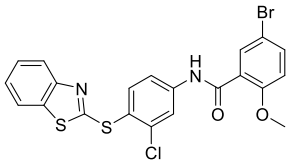

DMSO) δ 10.70 (s, 1H), 8.22 (d, *J* = 2.0 Hz, 1H), 7.93-7.99 (m, 2H), 7.80-7.87 (m, 2H), 7.67-7.76 (m, 2H), 7.47 (td, *J* = 7.7, 1.3 Hz, 1H), 7.32-7.38 (m, 1H), 7.19 (d, *J* = 8.8 Hz, 1H), 3.89 (s, 3H); MS (ESI) $C_{21}H_{13}BrClN_2O_2S_2$ $[M-H]^-$ *m/z* expected = 502.9, observed = 502.7; HPLC-1 = 98%; HPLC-2 = 98%.

.....

32: *N*-(4-(Benzo[*d*]thiazol-2-ylthio)-3-chlorophenyl)-2-methoxybenzamide. 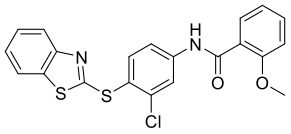

2-Methoxybenzoic acid (151 mg, 0.990 mmol) was stirred in $SOCl_2$ (1 mL) at 60°C for 1 h, then was concentrated. Anhydrous DCM (5 mL), compound **46** (192 mg, 0.654 mmol), and pyridine (80.0 μL, 0.981 mmol) were added and the reaction was stirred at R.T. for 18 h (under Ar). Flash chromatographic purification (hexanes:EtOAc gradient), followed by preparatory RP-HPLC purification, afforded **32** as an off-white solid (87.3 mg, 31% yield). ^{1}H-NMR (300 MHz, d_6-DMSO) δ 10.62 (s, 1H), 8.26 (d, *J* = 2.0 Hz, 1H), 7.91-7.98 (m, 2H), 7.82-7.90 (m, 2H), 7.63 (dd, *J* = 7.5, 1.7 Hz, 1H), 7.51-7.57 (m, 1H), 7.43-7.49 (m, 1H), 7.31-7.38 (m, 1H), 7.21 (d, *J* = 8.3 Hz, 1H), 7.05-7.14 (m, 1H), 3.89 (s, 3H); MS (ESI) $C_{21}H_{14}ClN_2O_2S_2$ $[MH]^+$ *m/z* expected = 427.0, observed = 427.0; HPLC-1 = 99%; HPLC-2 = 97%.

.....

33: *N*-(4-(Benzo[*d*]thiazol-2-ylthio)phenyl)-3,5-dibromo-2-methoxybenzamide. 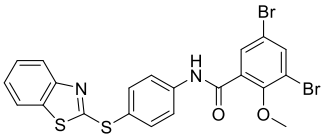

Compound **48** (172 mg, 0.555 mmol) was stirred in anhydrous DCM (5 mL) with DCC (120 mg, 0.579 mmol) and DMAP (9.0 mg, 0.074 mmol) at R.T. for 1 h (under Ar). Compound **47** (121 mg, 0.469 mmol) was then added and the reaction was stirred for an additional 18 h. Flash chromatgraphic purification (hexanes:EtOAc gradient) afforded **33** as a white solid (221 mg, 86% yield). ^{1}H-NMR (300 MHz, d_6-DMSO) δ 10.85 (s, 1H), 8.08 (d, *J* = 2.3 Hz, 1H), 7.89-7.96 (m, 3H), 7.79-7.86 (m, 4H), 7.45 (td, *J* = 7.7, 1.3 Hz, 1H), 7.30-7.37 (m, 1H), 3.84 (s, 3H);

MS (ESI) $C_{21}H_{13}Br_2N_2O_2S_2$ [M-H]$^-$ *m/z* expected = 546.9, observed = 456.7; HPLC-1 = 97%; HPLC-2 = 97%.

.....

34: *N*-(4-(Benzo[*d*]thiazol-2-ylthio)phenyl)-3-bromo-2-methoxybenzamide. 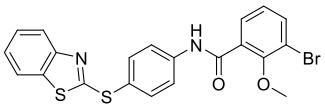

3-Bromo-2-methoxybenzoic acid (160 mg, 0.692 mmol) was stirred in anhydrous DCM (5 mL) with DCC (150 mg, 0.727 mmol) and DMAP (10.0 mg, 0.0819 mmol) at R.T. for 1 h (under Ar). Compound **47** (150 mg, 0.580 mmol) was then added and the reaction was stirred for an additional 18 h. Flash chromatgraphic purification (hexanes:EtOAc gradient) afforded **34** as a white solid (184 mg, 67% yield). ^{1}H-NMR (300 MHz, d_6-DMSO) δ 10.78 (s, 1H), 7.91-7.97 (m, 3H), 7.78-7.86 (m, 4H), 7.59 (dd, *J* = 7.6, 1.5 Hz, 1H), 7.45 (td, *J* = 7.7, 1.2 Hz, 1H), 7.30-7.37 (m, 1H), 7.19-7.26 (m, 1H), 3.84 (s, 3H); MS (ESI) $C_{21}H_{14}BrN_2O_2S_2$ [M-H]$^-$ *m/z* expected = 469.0, observed = 468.8; HPLC-1 = >99%; HPLC-2 = >99%.

.....

35: *N*-(4-(Benzo[*d*]thiazol-2-ylthio)phenyl)-5-bromo-2-methoxybenzamide. 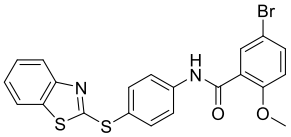

Compound **49** (154 mg, 0.667 mmol) was stirred in $SOCl_2$ (1 mL) at 60°C for 1 h, then was concentrated. Anhydrous DCM (5 mL), compound **47** (117 g, 0.453 mmol), and pyridine (55.0 μL, 0.674 mmol) were added and the reaction was stirred at R.T. for 18 h (under Ar). Flash chromatographic purification (hexanes:EtOAc gradient) afforded **35** as an off-white solid (199 mg, 93% yield). ^{1}H-NMR (300 MHz, d_6-DMSO) δ 10.56 (s, 1H), 7.90-7.97 (m, 3H), 7.77-7.86 (m, 3H), 7.66-7.74 (m, 2H), 7.42-7.48 (m, 1H), 7.30-7.37 (m, 1H), 7.18 (d, *J* = 8.8 Hz, 1H), 3.89 (s, 3H); MS (ESI) $C_{21}H_{14}BrN_2O_2S_2$ [M-H]$^-$ *m/z* expected = 469.0, observed = 468.8; HPLC-1 = >99%; HPLC-2 = >99%.

.....

36: *N*-(4-(Benzo[*d*]thiazol-2-ylthio)phenyl)-2-methoxybenzamide. 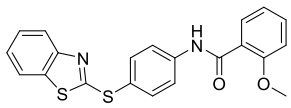 2-Methoxybenzoic acid (150 mg, 0.988 mmol) was stirred in $SOCl_2$ (1 mL) at 60°C for 1 h, then was concentrated. Anhydrous DCM (5 mL), compound **47** (170 mg, 0.657 mmol), and pyridine (81.0 μL, 0.993 mmol) were added and the reaction was stirred at R.T. for 18 h (under Ar). Flash chromatographic purification (hexanes:EtOAc gradient), followed by preparatory RP-HPLC purification, afforded **36** as a white solid (81.3 mg, 32% yield). ^{1}H-NMR (300 MHz, d_6-DMSO) δ 10.48 (s, 1H), 7.90-7.99 (m, 3H), 7.76-7.86 (m, 3H), 7.62 (dd, *J* = 7.5, 1.6 Hz, 1H), 7.49-7.57 (m, 1H), 7.42-7.49(m, 1H), 7.29-7.37 (m, 1H), 7.20 (d, *J* = 8.3 Hz, 1H), 7.08 (t, *J* = 7.4 Hz, 1H), 3.91 (s, 3H); MS (ESI) $C_{21}H_{15}N_2O_2S_2$ $[M-H]^-$ *m/z* expected = 391.1, observed = 390.9; HPLC-1 = >99%; HPLC-2 = >99%.

.....

37: 3,5-Dibromo-*N*-(3-chlorophenyl)-2-methoxybenzamide. 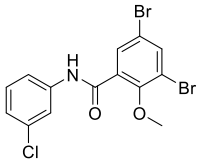 Compound **48** (259 mg, 0.835 mmol) was stirred in $SOCl_2$ (2 mL) at 60°C for 1 h, then was concentrated. Anhydrous DCM (5 mL), 3-chloroaniline (73.0 μL, 0.694 mmol), and pyridine (74.0 μL, 0.907 mol) were added and the reaction was stirred at R.T. for 18 h (under Ar). Flash chromatographic purification (hexanes:EtOAc gradient) afforded **37** as an off-white solid (280 mg, 80% yield). ^{1}H-NMR (300 MHz, d_6-DMSO) δ 10.68 (s, 1H), 8.06 (d, *J* = 2.4 Hz, 1H), 7.90 (t, *J* = 2.0 Hz, 1H), 7.77 (d, *J* = 2.4 Hz, 1H), 7.57 (d, *J* = 8.2 Hz, 1H), 7.39 (t, *J* = 8.1 Hz, 1H), 7.16-7.22 (m, 1H), 3.81 (s, 3H); MS (ESI) $C_{14}H_9Br_2ClNO_2$ $[M-H]^-$ *m/z* expected = 415.9, observed = 415.7; HPLC-1 = 99%; HPLC-2 = 97%.

.....

38: 3,5-Dibromo-*N*-(3-chlorophenyl)-2-methoxybenzamide. 3-Bromo-2-methoxybenzoic acid (382 mg, 1.65 mmol) was stirred in $SOCl_2$ (3 mL) at 60°C for 1 h, then was concentrated. Anhydrous DCM (5 mL), 3-chloroaniline (0.15 mL, 1.4 mmol), and pyridine (0.13 mL, 1.6 mmol) were added and the reaction was stirred at R.T. for 18 h (under Ar). Flash chromatographic purification (hexanes:EtOAc gradient) afforded **38** as a white solid (303 mg, 63% yield). ^{1}H-NMR (300 MHz, d_6-DMSO) δ 10.60 (s, 1H), 7.91-7.95 (m, 1H), 7.80 (dd, *J* = 8.0, 1.6 Hz, 1H), 7.57-7.62 (m, 1H), 7.55 (dd, *J* = 7.6, 1.6 Hz, 1H), 7.38 (t, *J* = 8.1 Hz, 1H), 7.15-7.23 (m, 2H), 3.81 (s, 3H); MS (ESI) $C_{14}H_{12}BrClNO_2$ $[MH]^+$ *m/z* expected = 342.0, observed = 342.1; HPLC-1 = >99%; HPLC-2 = >99%.

.....

39: 5-Bromo-*N*-(3-chlorophenyl)-2-methoxybenzamide. Compound **49** (327 mg, 1.42 mmol) was stirred in $SOCl_2$ (3 mL) at 60°C for 1 h, then was concentrated. Anhydrous DCM (5 mL), 3-chloroaniline (0.12 mL, 1.1 mmol), and pyridine (0.12 mL, 1.5 mmol) were added and the reaction was stirred at R.T. for 18 h (under Ar). Flash chromatographic purification (hexanes:EtOAc gradient) afforded **39** as an off-white solid (345 mg, 89% yield). ^{1}H-NMR (300 MHz, d_6-DMSO) δ 10.37 (s, 1H), 7.91 (t, *J* = 2.0 Hz, 1H), 7.65-7.72 (m, 2H), 7.57-7.63 (m, 1H), 7.37 (t, *J* = 8.1 Hz, 1H), 7.13-7.19 (m, 2H), 3.87 (s, 3H(; MS (ESI) $C_{14}H_{12}BrClNO_2$ $[MH]^+$ *m/z* expected = 342.0, observed = 342.1; HPLC-1 = >99%; HPLC-2 = >99%.

.....

40: *N*-(3-Chlorophenyl)-2-methoxybenzamide. 2-Methoxybenzoic acid (189 mg, 1.24 mmol) was stirred in $SOCl_2$ (2 mL) at 60°C for 1 h, then was concentrated. Anhydrous DCM (5 mL), 3-chloroaniline (0.11 mL, 1.0 mmol), and pyridine (0.10 mL, 1.2 mmol) were added and the reaction was stirred at R.T. for 18 h

(under Ar). Flash chromatographic purification (hexanes:EtOAc gradient), followed by preparatory RP-HPLC purification, afforded **40** as a white solid (81.3 mg, 32% yield). ^{1}H-NMR (300 MHz, d_6-DMSO) δ 10.30 (s, 1H), 7.95 (t, *J* = 2.0 Hz, 1H), 7.58-7.66 (m, 2H), 7.47-7.55 (m, 1H), 7.36 (t, *J* = 8.1 Hz, 1H), 7.12-7.21 (m, 2H), 7.07 (td, *J* = 7.5, 0.9 Hz, 1H), 3.89 (s, 3H); MS (ESI) $C_{14}H_{13}ClNO_2$ $[MH]^+$ *m/z* expected = 262.1, observed = 262.1; HPLC-1 = >99%; HPLC-2 = >99%.

.....

41: 3,5-Dibromo-2-methoxy-*N*-phenylbenzamide. Compound **48**

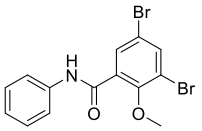

(274 mg, 0.885 mmol) was stirred in $SOCl_2$ (2 mL) at 60°C for 1 h, then was concentrated. Anhydrous DCM (5 mL), aniline (69.0 μL, 0.756 mmol), and pyridine (58.0 μL, 0.0.711 mol) were added and the reaction was stirred at R.T. for 18 h (under Ar). Flash chromatographic purification (hexanes:EtOAc gradient) afforded **41** as an off-white solid (258 mg, 80% yield). ^{1}H-NMR (300 MHz, d_6-DMSO) δ 10.49 (s, 1H), 8.04 (d, *J* = 2.3 Hz, 1H), 7.75 (d, *J* = 2.4 Hz, 1H), 7.67-7.73 (m, 2H), 7.36 (t, *J* = 7.9 Hz, 2H), 7.08-7.16 (m, 1H), 3.81 (s, 3H); MS (ESI) $C_{14}H_{10}Br_2NO_2$ $[M-H]^-$ *m/z* expected = 381.9, observed = 381.7; HPLC-1 = >99%; HPLC-2 = >99%.

.....

42: 3-Bromo-2-methoxy-*N*-phenylbenzamide. 3-Bromo-2-

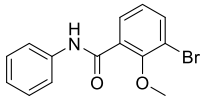

methoxybenzoic acid (356 mg, 1.54 mmol) was stirred in $SOCl_2$ (3 mL) at 60°C for 1 h, then was concentrated. Anhydrous DCM (5 mL), aniline (0.12 mL, 1.3 mmol), and pyridine (0.13 mL, 1.6 mmol) were added and the reaction was stirred at R.T. for 18 h (under Ar). Flash chromatographic purification (hexanes:EtOAc gradient) afforded **42** as a white solid (315 mg, 79% yield). ^{1}H-NMR (300 MHz, d_6-DMSO) δ 10.40 (s, 1H), 7.78 (dd, *J* = 8.0, 1.6 Hz, 1H), 7.69-7.75 (m, 2H), 7.54 (dd, *J* = 7.6, 1.6 Hz, 1H), 7.32-7.38 (m, 2H), 7.19 (t, *J* = 7.8 Hz, 1H), 7.07-7.14 (m, 1H), 3.82 (s, 3H); MS (ESI)

$C_{14}H_{13}BrNO_2$ $[MH]^+$ *m/z* expected = 306.0, observed = 306.1; HPLC-1 = >99%; HPLC-2 = >99%.

.....

43: 5-Bromo-2-methoxy-*N*-phenylbenzamide. Compound **49** (302 mg, 1.31 mmol) was stirred in $SOCl_2$ (3 mL) at 60°C for 1 h, then was concentrated. Anhydrous DCM (5 mL), aniline (0.10 mL, 1.1 mmol), and pyridine (0.11 mL, 1.3 mmol) were added and the reaction was stirred at R.T. for 18 h (under Ar). Flash chromatographic purification (hexanes:EtOAc gradient) afforded **43** as a white solid (250 mg, 74% yield). ^{1}H-NMR (300 MHz, d_6-DMSO) δ 10.20 (s, 1H), 7.63-7.73 (m, 4H), 7.31-7.37 (m, 2H), 7.15 (d, *J* = 8.8 Hz, 1H), 7.06-7.13 (m, 1H), 3.87 (s, 3H); MS (ESI) $C_{14}H_{13}BrNO_2$ $[MH]^+$ *m/z* expected = 306.0, observed = 306.1; HPLC-1 = >99%; HPLC-2 = >99%.

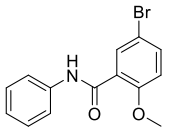

.....

44: 2-Methoxy-*N*-phenylbenzamide. 2-Methoxybenzoic acid (178 mg, 1.17 mmol) was stirred in $SOCl_2$ (2 mL) at 60°C for 1 h, then was concentrated. Anhydrous DCM (5 mL), aniline (0.10 mL, 1.1 mmol), and pyridine (0.10 mL, 1.2 mmol) were added and the reaction was stirred at R.T. for 18 h (under Ar). Flash chromatographic purification (hexanes:EtOAc gradient) afforded **44** as a white solid (235 mg, 94% yield). ^{1}H-NMR (300 MHz, d_6-DMSO) δ 10.12 (s, 1H), 7.71-7.77 (m, 2H), 7.62 (dd, *J* = 7.5, 1.8 Hz, 1H), 7.46-7.54 (m, 1H), 7.30-7.37 (m, 2H), 7.18 (d, *J* = 8.1 Hz, 1H), 7.04-7.12 (m, 2H), 3.89 (s, 3H); MS (ESI) $C_{14}H_{14}NO_2$ $[MH]^+$ *m/z* expected = 228.1, observed = 228.1; HPLC-1 = >99%; HPLC-2 = >99%.

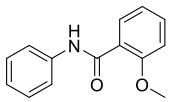

.....

46: 4-(Benzo[*d*]thiazol-2-ylthio)-3-chloroaniline. Tin powder (5.64 g, 47.5 mmol) was added slowly to a stirring mixture of **45** in a 1:10 mixture of HCl:AcOH (15 mL). The reaction was allowed to stir at R.T. for 2 days, then diluted

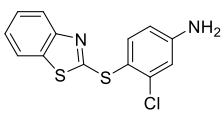

with EtOAc and H_2O, neutralized with $NaHCO_3$, and filtered. The filtrate was extracted with EtOAc and the organics dried over Na_2SO_4, filtered, and concentrated. The crude product was then chromatographed over silica (hexanes:EtOAc gradient) and concentrated. The residue was diluted in a 4:1 mixture of hexanes:DCM and the precipitate was filtered and dried to afford **46** as a yellow powder (3.73 g, 81% yield). ^{1}H-NMR (300 MHz, d_6-DMSO) δ 7.87-7.96 (m, 1H), 7.80 (d, *J* = 8.1 Hz, 1H), 7.53 (d, *J* = 8.5 Hz, 1H), 7.43 (td, *J* = 7.7, 1.3 Hz, 1H), 7.26-7.34 (m, 1H), 6.87 (d, *J* = 2.4 Hz, 1H), 6.64 (dd, *J* = 8.5, 2.4 Hz, 1H), 6.18 (s, 2H); MS (ESI) $C_{13}H_{10}ClN_2S_2$ $[MH]^+$ *m/z* expected = 293.0, observed = 293.0; HPLC-1 = 98%.

.....

47: 4-(Benzo[*d*]thiazol-2-ylthio)aniline. 2-Chlorobenzothiazole (2.00 g, 11.8 mmol), 4-aminothiophenol (1.70 g, 13.6 mmol), and potassium carbonate (3.24 g, 23.4 mmol) were stirred together in EtOH (15 mL) for 18 h. The reaction was then diluted with water and the precipitate was filtered, rinsed with water, and collected. Flash chromatographic purification (hexanes:EtOAc gradient) afforded **47** as an off-white solid (2.71 g, 89% yield). ^{1}H-NMR (300 MHz, d_6-DMSO) δ 7.85-7.91 (m, 1H), 7.78 (d, *J* = 7.7 Hz, 1H), 7.37-7.45 (m, 3H), 7.25-7.34 (m, 1H), 6.66-6.73 (m, 2H), 5.84 (s, 1H); MS (ESI) $C_{13}H_{11}N_2S_2$ $[MH]^+$ *m/z* expected = 259.0, observed = 259.0; HPLC-1 = >99%.

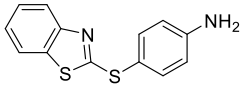

.....

48: 3,5-Dibromo-2-methoxybenzoic acid. Iodomethane (6.30 mL, 101 mmol), 3,5-dibromosalicylic acid (10.0 g, 33.7 mmol), and K_2CO_3 (14.0 g, 101 mmol) were stirred at R.T. overnight, then at 80°C for 4 h. The reaction was diluted into water and extracted into DCM. The organics were dried over Na_2SO_4, filtered, and concentrated. The intermediate ester was then stirred overnight with $LiOH•H_2O$ (5.70 g, 136 mmol) in a 3:1:1 mixture of THF:MeOH:H_2O (35 mL). The

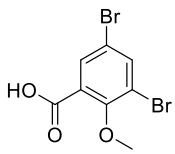

reaction was diluted with water and acidified with HCl. The precipitate was filtered, washed with water, and dried to afford **48** as a white solid (9.85 g, 94% yield). ^{1}H-NMR (300 MHz, d_6-DMSO) δ 13.56 (br s, 1H), 8.09 (d, J = 2.5 Hz, 1H), 7.83 (d, J = 2.5 Hz, 1H), 3.81 (s, 3H); MS (ESI) $C_8H_5Br_2O_3$ $[M-H]^-$ *m/z* expected = 308.9, observed = 309.1; HPLC-1 = >99%.

.....

49: 5-Bromo-2-methoxybenzoic acid. 5-Bromosalicylic acid (10.0 g, 46.1 mmol), iodomethane (8.60 mL, 138 mmol), and K_2CO_3 (19.0 g, 137 mmol) were stirred at R.T. overnight, then at 80°C for 4 h. The reaction was diluted into water and the precipitate was filtered, rinsed with water, and dried. The intermediate ester was then stirred overnight with LiOH•H_2O (7.70 g, 184 mmol) in a 3:1:1 mixture of THF:MeOH:H_2O (45 mL). The reaction was diluted with water and acidified with HCl. The precipitate was filtered, washed with water, and dried to afford **49** as a white solid (8.70 g, 82% yield). ^{1}H-NMR (300 MHz, d_6-DMSO) δ 12.98 (br s, 1H), 7.72 (d, J = 2.6 Hz, 1H), 7.66 (dd, J = 8.8, 2.6 Hz, 1H), 7.10 (d, J = 8.9 Hz, 1H), 3.81 (s, 3H); MS (ESI) $C_8H_6BrO_3$ $[M-H]^-$ *m/z* expected = 229.0, observed = 229.0; HPLC-1 = 98%.

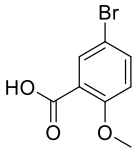

.....

GroEL and GroES Protein Expression and Purification

E. coli GroEL was expressed from a trc-promoted and Amp(+) resistance marker plasmid in DH5α *E. coli* cells. *E. coli* GroES was expressed from a T7-promoted and Amp(+) resistance marker plasmid in *E. coli* BL21 (DE3) cells. Transformed colonies were plated onto Ampicillin treated LB agar and incubated for 24 h at 37°C. Cells were grown at 37°C in Ampicillin treated LB medium until an OD_{600} of 0.5 was reached, then were induced with 0.5 mM IPTG and continued to grow for 2-3 h at 37°C. The cultures were centrifuged at 14,000 rpm, and the cell pellets re-suspended in Buffer A (50 mM

sodium acetate, pH 4.5, and 0.5 mM EDTA), supplemented with EDTA-free complete protease inhibitor cocktail (Roche), 100 µg/ml lysozyme, 10 µL (1000 u/ml) DNAase, and lysed by sonication. Clarified cell lysates were loaded on a cation exchange column (SP Sepharose fast flow resin, GE) and eluted with linear NaCl gradient with Buffer B (sodium acetate, pH 4.5, 0.5 mM EDTA, and 1 M NaCl). Fractions containing protein on the absorption spectrum were then quantified on an SDS PAGE gel, collected, and spin concentrated using 10 kD filter canonicals. Once concentrated to ~25µM, proteins were dialyzed in size-exclusion buffer (50 mM Tris-HCl, pH 7.4, and 300 mM NaCl) with 10 kDa SnakeSkin™ dialysis tubing (Thermo Scientific) for at least 12 hours. Proteins were then further purified using a Superdex 200 (HiLoad 26/600, GE) size-exclusion column with size-exclusion buffer, and eluted off into fractions with filtered H_2O. Fractions were then quantified by molecular weight using SDS PAGE, then spin concentrated (~150µM GroES, ~30µM GroEL). The concentration of protein was determined by Coomassie Protein Assay Kit (Thermo Scientific).

Human HSP60 and HSP10 Protein Expression and Purification

Human HSP60 purification:

Human mitochondrial HSP60 (mtHSP60) was expressed from a *T7*-promoted plasmid with an AMP and Chloramphenicol resistance marker in Rosetta™ 2 (DE3) pLysS *E. coli* using a previously reported plasmid (Abdeen 2016). For human HSP60 purification, pET21-*mtHSP60* with *N*-terminal octa-Histidine tag was transformed into Rosetta™ 2 (DE3) pLysS *E. coli* cells for over-expression. Cells were grown at 37°C in LB / Ampicillin / Chloramphenicol medium until an OD_{600} of 0.5 was reached at 37°C, then induced with 0.5 mM IPTG and continued to grow for 2-3 h at 25°C. After centrifuging at 14,000 rpm, the cell pellet was suspended in a 50 mL lysis buffer composed of 100 mM Tris-HCl (pH 7.7), 10 mM $MgSO_4$, 1 mM β-ME, 5% glycerol, 0.1% Triton X-100, 1500 Units DNase, and 100 µl of 50 mg/ml lysozyme. Cells were

homogenized by passing through a microfluidizer using a buffer containing 10 mM Tris-HCl (pH 7.7), 5% glycerol, and 0.1% Triton X-100.

*1st Nickel column purification and proteolytic removal of His-tag***:**

Cell lysate was supplemented with 10 mM imidazole, passed through a 0.2 µm filter (Millipore), and loaded onto a nickel-agarose resin column that was equilibrated with 20 mM Tris-HCl (pH 7.7), 5% glycerol, 200 mM NaCl, and 10 mM imidazole. Bound mtHSP60 was eluted with 500 mM Imidazole. Fractions that were enriched with the His-tagged mtHSP60 were collected, concentrated, dialyzed in 10 kDa SnakeSkin™ dialysis tubing (Thermo Scientific) at room temperature for 2 hours in 4 L of 20 mM Tris-HCl (pH 7.7), 200 mM NaCl, and 5% glycerol to remove imidazole. Proteolytic removal of the His-tag was next performed by addition of His-tagged TEV protease to the purified His-tagged mtHSP60 at a 1:10 (w:w) ratio, while dialyzing over night at 4°C in buffer containing 20 mM Tris-HCl (pH 7.7), 200 mM NaCl, and 5% glycerol.

2nd Nickel column purification:

The protein sample was loaded onto a second nickel-agarose resin column that was equilibrated with 20 mM Tris-HCl (pH 7.7), 5% glycerol, 10 mM NaCl, and 10 mM imidazole. The unbound fractions enriched with His-tag cleaved mtHSP60 were collected by raising Imidazole concentration. In this column, processed mtHSP60 can be separated from undigested His-tagged mtHSP60 as well as the His-tagged TEV protease. Anion-exchange purification was then performed on the same day.

Anion-exchange purification of processed mtHSP60:

Protein sample was loaded onto an anion-exchange column (SP Sepharose fast flow resin, GE) that was equilibrated with 20 mM Tris-HCl (pH 7.7) and 5% glycerol. Bound proteins were eluted from the column with a linear gradient of 100-400 mM NaCl. Fractions enriched with mtHSP60 were collected, concentrated and dialyzed in storage buffer (20 mM Tris-HCl (pH 7.7), 300 mM NaCl, 5% glycerol, and 10 mM $MgCl_2$) using

10 kDa SnakeSkin™ dialysis tubing (Thermo Scientific).Protein concentration was determined using a Coomassie Protein Assay Kit (Thermo Scientific). Protein can be stored at 4°C in storage buffer for two weeks (freeze-thaw storage is not recommended).

Human HSP10 purification:

For human HSP10 purification, pET30-*HSP10* with a Kan and Chloramphenicol resistance marker was transformed into Rosetta™ 2 (DE3) *E. coli* cells for over-expression. Cells were grown at 37°C in LB / Kanamycin / Chloramphenicol medium until an OD_{600} of 0.5 was reached, then induced with 0.5 mM IPTG and continued to grow for 2-3 h at 37°C. The culture was centrifuged at 14,000 rpm, and the cell pellet was re-suspended in Buffer A (50 mM sodium acetate (pH 4.5) and 0.5 mM EDTA) supplemented with EDTA-free complete protease inhibitor cocktail (Roche), 100 µg/ml lysozyme, 10 µL (1000 u/ml) DNAase, and lysed by sonication. Clarified cell lysate was loaded on a cation-exchange column (SP Sepharose fast flow resin, GE) and eluted with a linear NaCl gradient of Buffer A to Buffer B (sodium acetate (pH 4.5), 0.5 mM EDTA, and 1 M NaCl). Fractions containing HSP10 were concentrated, dialyzed with storage buffer (50 mM Tris-HCl (pH 7.4) and 300 mM NaCl) using 10 kDa SnakeSkin™ dialysis tubing (Thermo Scientific), and re-purified using a Superdex 200 column size-exclusion column (HiLoad 26/600, GE) and eluting with storage buffer. Protein concentration was determined using a Coomassie Protein Assay Kit (Thermo Scientific). Protein was stored at 4°C in 50 mM Tris-HCl (pH 7.4), 300 mM NaCl, and 1 mM DTT.

Denatured Malate Dehydrogenase Refolding Assay

Reagent preparation:

For these assays, four primary reagent stocks were prepared: **1)** GroEL/ESdMDH or HSP60/10-dMDH binary complex stock; **2)** ATP initiation stock; **3)** EDTA quench stock; **4)** MDH enzymatic assay stock. Denatured MDH (dMDH) was prepared by 2-fold dilution of MDH (5 mg/ml, soluble pig heart MDH from Roche, product

#10127248001) with denaturant buffer (7 M guanidine-HCl, 200 mM Tris (pH 7.4), and 50 mM DTT). MDH was completely denatured by mixing with denaturant buffer then incubating at room temperature for 40 min. The binary complex solutions were prepared by adding the dMDH stock to a solution containing GroEL (or HSP60) and GroES (or HSP10) in folding buffer (50 mM Tris-HCl (pH 7.4), 50 mM KCl, 10 mM $MgCl_2$, and 1 mM DTT). The binary complex stocks were prepared prior to use and had final protein concentrations of 83.3 nM GroEL (MW 800 kDa) or HSP60 (MW 400 kDa), 100 nM GroES or HSP10 (MW 70 kDa), and 20 nM dMDH. For the ATP initiation stock, solid ATP was diluted into folding buffer to a final concentration of 2.5 mM. Quench solution contained 600 mM EDTA (pH 8.0). The MDH enzymatic assay stock consisted of 20 mM sodium mesoxalate and 2.4 mM NADH in reaction buffer (50 mM Tris-HCl (pH 7.4), 50 mM KCl, and 1 mM DTT).

Assay Protocol:

First, 30 µL aliquots of the GroEL/ES-dMDH or HSP60/10-dMDH binary complex stocks were pipetted into clear, flat-bottom, 384-well polystyrene plates. Next, 0.5 µL of the compound stocks (10 mM to 4.6 µM, 3-fold dilutions in DMSO) were added by pin-transfer (V&P Scientific). The chaperonin-mediated refolding cycles were initiated by addition of 20 µL of ATP stock (reagent concentrations during refolding cycle: 50 nM GroEL or HSP60, 60 nM GroES or HSP10, 12 nM dMDH, 1 mM ATP, and compounds of 100 µM to 46 nM, 3-fold dilution series). After incubation for 45 minutes at 37°C (time of quenching found from kinetics assay ran prior – see note below), the assays were quenched by addition of 10 µL of the EDTA stock. Enzymatic activity of the refolded MDH was initiated by addition of 20 µL MDH enzymatic assay stock and followed by measuring the NADH absorbance in each well at 340 nm using a Molecular Devices SpectraMax Plus384 microplate reader (NADH absorbs at 340 nm, while NAD^+ does not). A_{340} measurements were recorded at 0.5 minutes (start point) and at successive

time points until the amount of NADH consumed reached ~90% in the non-inhibited, DMSO control wells (end point, generally between 30-60 minutes). The differences between the start and end point A_{340} values were used to calculate the % inhibition of the GroEL/ES or HSP60/10 machinery by the compounds. IC_{50} values for the test compounds were obtained by plotting the % inhibition results in GraphPad Prism 6 and analyzing by non-linear regression using the log(inhibitor) vs. response (variable slope) equation. Results presented represent the averages of IC_{50} values obtained from at least triplicate experiments.

Note: Time of quenching with EDTA was found from kinetics testing of purified protein where quenching took place over a time course of 60 min to know if the protein was functional, the time it took for the chaperonin system to have just completed refolding of ~90% dMDH (quench time point during the assays).

Denatured Rhodanese Refolding Assay

Reagent preparation:

For this assay, five primary reagent stocks were prepared: **1)** GroEL/ES-dRho binary complex stock; **2)** ATP initiation stock; **3)** thiocyanate enzymatic assay stock; **4)** formaldehyde quench stock; **5)** ferric nitrate reporter stock. Denatured Rhodanese (dRho) was prepared by 3-fold dilution of Rhodanese (Roche product #R1756, diluted to 10 mg/mL with H_2O) with denaturant buffer (12 M urea, 50 mM Tris-HCl (pH 7.4), and 10 mM DTT) and incubated at room temperature for 30 min. The binary complex solution was prepared by slowly adding the dRho stock to a stirring stock of concentrated GroEL in modified folding buffer (50 mM Tris-HCl (pH 7.4), 50 mM KCl, 10 mM $MgCl_2$, 5 mM $Na_2S_2O_3$, and 1 mM DTT). The solution was centrifuged at 16,000 x g for 5 minutes, and the supernatant was collected and added to a solution of GroES in modified folding buffer to give final protein concentrations of 100 nM GroEL, 120 nM GroES, and 80 nM dRho. The binary complex stock was prepared immediately prior to use. For the ATP

initiation stock, solid ATP was diluted into modified folding buffer to a final concentration of 2.0 mM. The thiocyanate enzymatic assay stock was prepared to contain 70 mM KH_2PO_4, 80 mM KCN, and 80 mM $Na_2S_2O_3$ in water. The formaldehyde quench solution contained 30% formaldehyde in water. The ferric nitrate reporter stock contained 8.5% w/v $Fe(NO_3)_3$ and 11.3% v/v HNO_3 in water.

Assay Protocol:

First, 10 µL aliquots of the GroEL/ES-dRho complex stock were dispensed into clear, flat-bottom, 384-well polystyrene plates. Next, 0.5 µL of the compound stocks (10 mM to 4.6 µM, 3-fold dilutions in DMSO) were added by pin-transfer. The chaperonin-mediated refolding cycle was initiated by addition of 10 µL of ATP stock (reagent concentrations during refolding cycle: 50 nM GroEL, 60 nM GroES, 40 nM dRho, 1 mM ATP, and compounds of 250 µM to 114 nM, 3-fold dilution series). After incubating for 60 minutes at 37°C for the refolding cycle, 30 µL of the thiocyanate enzymatic assay stock was added to initiate the enzymatic reporter reaction of the refolded rhodanese. After incubating for 60 min at R.T., the reporter reaction was quenched by adding 10 µL of the formaldehyde quench stock, and then 40 µL of the ferric nitrate reporter stock was added to quantify the amount of thiocyanate produced, which is proportional to the amount of dRho refolded by GroEL/ES. After incubating at R.T. for 15 min, the absorbance by $Fe(SCN)_3$ was measured at 460 nm using a Molecular Devices SpectraMax Plus384 microplate reader. A second set of baseline control plates were prepared analogously, but without binary solution, to correct for possible interference from compound absorbance or turbidity. IC_{50} values for the test compounds were obtained by plotting the A_{460} results in GraphPad Prism 6 and analyzing by non-linear regression using the log(inhibitor) vs. response (variable slope) equation. Results presented represent the averages of IC_{50} values obtained from at least 4 replicates of experiments.

Native Malate Dehydrogenase and Native Rhodanese Activity Counter-screens

Reagent Preparations & Assay Protocol:

Reagents were identical to those used in the GroEL/ES-dMDH and GroEL/ES-dRho refolding assays described above; however, the assay protocols differed in the sequence of compound addition to the wells. For the native MDH counter-screen, compounds were pin-transferred after the EDTA quenching step, but prior to the addition of the enzymatic reporter reagents. For the native rhodanese counter-screen, compounds were added immediately prior to addition of the enzymatic reporter reagents. Thus, the refolding reactions could proceed in the absence of test compounds (providing maximal MDH and Rho refolding), but the enzymatic activity of the refolded reporter enzymes (MDH and Rho) was monitored in the presence of test compounds. The inhibitor concentration ranges were 83.3 µM to 38 nM (3-fold dilutions) for the MDH enzymatic reporter reaction, and 100 µM to 46 nM (3-fold dilutions) for the Rho enzymatic reporter reaction. Results presented represent the averages of IC_{50} values obtained from at least 4 replicates of experiments.

Bacterial Proliferation Assays

Stock cell cultures used and storage:

All evaluated bacterial cultures are listed below with manufacturer name(s) and lot #s: Enterococcus faecium cells-(Orla-Jensen) Schleifer and Kilpper-Balz strain NCTC 7171 (ATCC 19434). Staphylococcus aureus cells -Rosenbranch strain Seattle 1945 (ATCC 25923). Methicillin-resistant S. aureus (MRSA)-Rosenbach strain HPV107 (ATCC BAA-44). Klebsiella Pneumonia cells- (Schroeter) Trevisan strain NCTC 9633 (ATCC 13883). Acinetobacter baumanii cells- Bouvet and Grimont strain 2208 (ATCC 19606). Pseudomonas aeruginosa cells- (Schroeter) Migula strain NCTC 10332 (ATCC 10145). Enterobacter cloacae cells- E. cloacae, subsp. cloacae (Jordan) Hormaeche

and Edwards strain CDC 442-68 (ATCC 13047). All bacterial cell stocks were stored at -80°C.

General Assay Protocol:

Stock bacterial cultures were streaked onto BHI (Brain-heart infusion media, Becton, Dickinson, and Company) agar plates and grown overnight at 37°C. Fresh aliquots of broth were inoculated with single bacterial colonies and the cultures were grown overnight at 37°C with shaking (240 rpm) in BHI media supplemented with $MgCl_2$ and $CaCl_2$ to a final concentration of 2.5(Mg) and 25(Ca)mg/mL. The following morning, the overnight cultures were sub-cultured (1:5 dilution) into fresh aliquots of media and grown at 37°C for 1-2 hours with shaking. After 2 h, cultures were diluted into fresh media to achieve final OD_{600} readings of 0.017. Aliquots of these diluted cultures (30 µL) were added to clear, flat-bottom, 384-well polystyrene plates that were stamped with 0.5 µL of test compounds in 20 µL media. The inhibitor concentration range during the proliferation assay was 100 µM to 46 nM (3-fold dilution series). Plates were sealed with "Breathe Easy" oxygen permeable membranes (Diversified Biotech) and left to incubate at 37°C without shaking (stagnant assay). OD_{600} readings were taken at either 6-8 h (*S. aureus, Klebsiella, E. cloacae, P. aeruginosa,* and MRSA) or 24 h *(E. faecium* and *A. baumanii).* A second set of baseline control plates were prepared analogously, but without any bacteria added, to correct for possible compound absorbance and/or precipitation. Plates were then read at 600 nm using a Molecular Devices SpectraMax Plus384 microplate reader. EC_{50} values for the test compounds were obtained by plotting the OD_{600} results in GraphPad Prism 6 and analyzing by non-linear regression using the log(inhibitor) vs. response (variable slope) equation. Results presented represent the averages of EC_{50} values obtained from at least 4 replicates of experiments.

Human Cell Cytotoxicity Assay Using HEK 293 and THLE-3 Cell Lines

HEK 293 kidney cells (ATCC #CRL-1573) were maintained in MEM medium (Corning Cellgro, 10-009 CV) supplemented with 10% FBS (Sigma, F2242). THLE-3 liver cells (ATCC #CRL-11233) were maintained in Clonetics BEBM medium (Lonza, CC-3171) supplemented with the BEGM bullet kit (Lonza, CC-3170) and 10% FBS. All assays were carried out in clear, flat-bottom, 384-well polystyrene plates (BRAND cell culture grade plates, 781980). Briefly, cells at 80% confluence were harvested and diluted in growth medium, then 50 µL of the HEK 293 cells (15,000 cells/well) or THLE-3 cells (5,000 cells/well) were plated and incubated at 37°C with 5% CO_2 for 24 h. Compound stocks (1 µL of 10 mM to 4.6 µM, 3-fold dilutions in DMSO) were added by pin-transfer and the plates were incubated for an additional 48 h at 37°C with 5% CO_2. Alamar Blue reporter reagents were then added to a final concentration of 10% (6 µL in 60 µL of treated cells). The plates were incubated for 24 h, then sample fluorescence (535 nm excitation, 590 nm emission) was read using a Molecular Devices FlexStation II plate reader. Cell viability was calculated as per vendor instructions. CC_{50} values for the test compounds were obtained by plotting the % Alamar Blue reduction results in GraphPad Prism 6 and analyzing by non-linear regression using the log(inhibitor) vs. response (variable slope) equation. Results presented represent the averages of CC_{50} values obtained from at least 4 replicates of experiments.

MRSA Gain-of-Resistance Assay

To identify potential resistance toward the parent scaffold (**1**) and analog **11**, a liquid culture serial passage assay for a period of 12 consecutive days was carried out alongside control compounds vancomycin and "**28R**" with Methicillin-resistant *Staphylococcus aureus* (MRSA ATCC BAA-44), as described elsewhere (Kim 2014). In brief, MRSA (ATCC BAA-44) bacteria were streaked onto a Tryptic Soy Broth (TSB) agar plate and grown overnight at 37°C. A fresh aliquot of TSB was inoculated with a

single bacterial colony and the cultures were grown overnight at 37°C with shaking (250 rpm). The overnight culture was then sub-cultured (1:5 dilution) into a fresh aliquot of media and grown at 37°C for 1 h with shaking, then diluted into fresh media to achieve a final OD_{600} reading of 0.01. Aliquots of the diluted culture (200 µL) were dispensed into 96 well plates along with addition of 2 µL test compounds in DMSO. The inhibitor concentration range during the resistance assay was 100 µM to 48.8 nM (2-fold dilution series). Plates were sealed with "Breathe Easy" oxygen permeable membranes (Diversified Biotech) and left to incubate at 37°C without shaking (stagnant assay). OD_{600} readings were taken at the 24 h time point to monitor for bacterial growth. A second set of baseline control plates were prepared analogously, but without any bacteria added, to correct for possible compound absorbance and/or precipitation, as well as plate and media baseline effects. For inoculations on subsequent days, bacteria from the wells with the highest drug concentration, where the OD_{600} was >0.2, were diluted with fresh media to OD_{600} of 0.01 and dispensed into a new 96-well plate. Test compounds were added, and the bacteria propagated again as described above. This procedure was repeated each day for a total of 12 days to observe whether EC_{50} values would increase, indicating that bacteria were generating resistance to the test compound. EC_{50} values for the test compounds were obtained by plotting the OD_{600} results in GraphPad Prism 6 and analyzing by non-linear regression using the log(inhibitor) vs. response (variable slope) equation. Results presented represent the averages of EC_{50} values obtained from at least 4 replicates of experiments.

***S. aureus* Biofilm Prevention Assay**

The biofilm prevention assay was carried out with *S. aureus* Rosenbach (ATCC 25923) using a quantitative crystal violet-based adherence assay on 96-well plates as described previously (Kwasny 2010). *S. aureus* (ATCC 25923) bacteria were streaked onto a Tryptic Soy Broth (TSB) agar plate and grown overnight at 37°C. A fresh aliquot

of TSB media was inoculated with a single bacterial colony and the cultures were grown overnight at 37°C with shaking (250 rpm). The overnight culture was then sub-cultured (1:5 dilution) into a fresh aliquot of TSB media supplemented to a final conc. of 0.5% glucose and grown at 37°C for 1 h with shaking, then diluted into fresh TSB media supplemented with 0.5% glucose to achieve a final OD_{600} reading of 0.01. Aliquots of the diluted culture (100 µL) were dispensed to 96 well polystyrene plates along with addition of 1 µL test compounds in DMSO. The inhibitor concentration range during the assay was 100 µM to 46 nM (3-fold dilution series). A second set of baseline control plates were prepared analogously, but without any bacteria added, to correct for possible compound absorbance and/or precipitation. Plates were sealed with "Breathe Easy" oxygen permeable membranes (Diversified Biotech) and left to incubate at 37°C without shaking (stagnant assay) until the biofilm was formed. After 24 h, the planktonic cultures were removed and the plates were washed gently 2-3 times with 200 µl of water. Next the plates were air dried and the adherent biofilms were stained with 150 µL of 2.3% crystal violet (2.3 % crystal violet in 20% Ethanol, Sigma Aldrich #HT90132) for 15 minutes at room temperature. The unbound crystal violet stain was removed, then plates were gently washed again with running water and air dried for 10 min. Quantitative assessment of biofilm formation was obtained by adding 100 µL of developer solution (4:1:5 mixture of MeOH:AcOH:H_2O) per well. Plates were then read at 595 nm using a Molecular Devices SpectraMax Plus384 microplate reader. EC_{50} values for the test compounds were obtained by plotting the Absorbance 595 nm results in GraphPad Prism 6 and analyzing by non-linear regression using the log(inhibitor) vs. response (variable slope) equation. Results presented represent the averages of EC_{50} values obtained from at least 4 replicates of experiments.

S. aureus Biofilm Penetration and Bactericidal Activity Assay

The biofilm penetration and bactericidal activity assay was carried out with *S. aureus* Rosenbach (ATCC 25923) as described previously (Kwasny 2010). *S. aureus* (ATCC 25923) bacgeria were streaked onto a Tryptic Soy Broth (TSB) agar plate and grown overnight at 37°C. A fresh aliquot of TSB media was inoculated with a single bacterial colony and the cultures were grown overnight at 37°C with shaking (250 rpm). The overnight culture was then sub-cultured (1:5 dilution) into a fresh aliquot of TSB media supplemented with 0.5% glucose and grown at 37°C for 1 h with shaking, then diluted into fresh TSB media supplemented with 0.5% glucose to achieve a final OD_{600} reading of 0.01. Aliquots of the diluted culture (100 µL) were dispensed to 96 well polystyrene plates without any compounds added. A second set of baseline control plates were prepared analogously, but without any bacteria added, to correct for possible compound absorbance and/or precipitation. Plates were sealed with "Breathe Easy" oxygen permeable membranes (Diversified Biotech) and left to incubate at 37°C without shaking (stagnant assay) until biofilm was formed. After 24 h, the planktonic cultures were removed and the plates were washed gently 3 times with 200 µL of sterile phosphate buffered saline (PBS). Then aliquots (100 µL) of fresh TSB media were dispensed to the plates along with addition of 1 µL of test compounds in DMSO. The inhibitor concentration range during the assay was 100 µM to 46 nM (3-fold dilution series). The plates were sealed with "Breathe Easy" membrane and incubated at 37°C without shaking to allow compounds to penetrate and kill bacteria in the biofilms. After 24 h, the cultures were removed and plates were washed again gently 3 times with 200 µL of sterile PBS. The remaining bacteria in the biofilms were allowed to recover by adding 100 µL of fresh TSB media per well and incubating for 24 hours at 37°C. At the end of this final incubation, bacterial growth was monitored by measuring the OD_{600} using a Molecular Devices SpectraMax Plus384 microplate reader. EC_{50} values for the

test compounds were obtained by plotting the OD_{600} results in GraphPad Prism 6 and analyzing by non-linear regression using the log(inhibitor) vs. response (variable slope) equation. Results presented represent the averages of EC_{50} values obtained from at least 4 replicates of experiments.

Calculating IC_{50}, EC_{50}, and CC_{50} Values

Average IC_{50}, EC_{50}, and CC_{50} values were calculated from individual dose-response curves in replicate assays as follows: 1) IC_{50} values obtained from each dose-response curve (plotted in GraphPad Prism 6) were log-transformed and the average log(I/E/CC_{50}) values and standard deviations (SD) calculated; 2) Outlier log(I/EC/C_{50}) values were identified using the ROUT method in GraphPad Prism 6 (Q of 10%); and 3) Average IC_{50}, EC_{50}, and CC_{50} values were back-calculated from the average log(I/E/CC_{50}) values.

APPENDIX - Tables of Log(IC_{50}), Log(EC_{50}), and Log(CC_{50}) Results

Table 7. Log(IC_{50}) results and standard deviations for compounds tested in the GroEL/ES-mediated dMDH and dRho folding assays, and the native MDH and Rho reporter counter-screens.

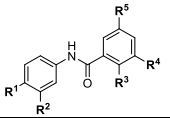

Compound Substituents & Substructures					Compound # / Name	Biochemical Assay IC_{50} (μM)			
						Native Rho Reporter	Native MDH Reporter	GroEL/ES-dRho Refolding	GroEL/ES-dMDH Refolding
R^1	R^2	R^3	R^4	R^5	Closantel	>2	0.75 ± 0.17	0.19 ± 0.10	0.33 ± 0.18
					Rafoxanide	>2	1.1 ± 0.1	0.34 ± 0.11	0.44 ± 0.09
	Cl	OH	Br	Br	**1**	>2	0.93 ± 0.21	0.19 ± 0.08	0.29 ± 0.24
	Cl	OH	Br	H	**2**	>2	>1.8	0.58 ± 0.15	0.98 ± 0.23
	Cl	OH	H	Br	**3**	>2	>1.8	1.0 ± 0.4	1.6 ± 0.4
	Cl	OH	H	H	**4**	>2	>1.8	1.8 ± 0.3	1.6 ± 0.3
	H	OH	Br	Br	**5**	>2	0.92 ± 0.21	0.12 ± 0.37	0.43 ± 0.19
	H	OH	Br	H	**6**	>2	>1.8	1.1 ± 0.1	1.5 ± 0.2
	H	OH	H	Br	**7**	>2	>1.8	1.5 ± 0.1	1.6 ± 0.3
	H	OH	H	H	**8**	>2	>1.8	1.9 ± 0.2	1.6 ± 0.3
H	Cl	OH	Br	Br	**9**	>2	1.4 ± 0.2	1.7 ± 0.1	1.4 ± 0.2
H	Cl	OH	Br	H	**10**	>2	>1.8	>2.4	>2
H	Cl	OH	H	Br	**11**	>2	>1.8	>2.4	>2
H	Cl	OH	H	H	**12**	>2	>1.8	>2.4	>2
H	H	OH	Br	Br	**13**	>2	1.7 ± 0.2	>2.4	1.8 ± 0.1
H	H	OH	Br	H	**14**	>2	>1.8	>2.4	>2
H	H	OH	H	Br	**15**	>2	>1.8	>2.4	>2
H	H	OH	H	H	**16**	>2	>1.8	>2.4	>2
	Cl	H	Br	Br	**17**	>2	>1.8	>2.4	>2
	Cl	H	Br (H)	H (Br)	**18**	>2	>1.8	>2.4	>2
	Cl	H	H	H	**19**	>2	>1.8	>2.4	>2
	H	H	Br	Br	**20**	>2	>1.8	>2.4	>2
	H	H	Br (H)	H (Br)	**21**	>2	>1.8	>2.4	>2
	H	H	H	H	**22**	>2	>1.8	>2.4	>2
H	Cl	H	Br	Br	**23**	>2	>1.8	>2.4	>2
H	Cl	H	Br (H)	H (Br)	**24**	>2	>1.8	>2.4	>2
H	Cl	H	H	H	**25**	>2	>1.8	>2.4	>2
H	H	H	Br	Br	**26**	>2	>1.8	>2.4	>2
H	H	H	Br (H)	H (Br)	**27**	>2	>1.8	>2.4	>2
H	H	H	H	H	**28**	>2	>1.8	>2.4	>2
	Cl	OCH_3	Br	Br	**29**	>2	>1.8	>2.4	>2
	Cl	OCH_3	Br	H	**30**	>2	>1.8	>2.4	>2
	Cl	OCH_3	H	Br	**31**	>2	>1.8	>2.4	>2
	Cl	OCH_3	H	H	**32**	>2	>1.8	>2.4	>2
	H	OCH_3	Br	Br	**33**	>2	>1.8	>2.4	>2
	H	OCH_3	Br	H	**34**	>2	>1.8	>2.4	>2
	H	OCH_3	H	Br	**35**	>2	>1.8	>2.4	>2
	H	OCH_3	H	H	**36**	>2	>1.8	>2.4	>2
H	Cl	OCH_3	Br	Br	**37**	>2	>1.8	>2.4	>2
H	Cl	OCH_3	Br	H	**38**	>2	>1.8	>2.4	>2
H	Cl	OCH_3	H	Br	**39**	>2	>1.8	>2.4	>2
H	Cl	OCH_3	H	H	**40**	>2	>1.8	>2.4	>2
H	H	OCH_3	Br	Br	**41**	>2	>1.8	>2.4	>2
H	H	OCH_3	Br	H	**42**	>2	>1.8	>2.4	>2
H	H	OCH_3	H	Br	**43**	>2	>1.8	>2.4	>2
H	H	OCH_3	H	H	**44**	>2	>1.8	>2.4	>2

Table 8. Log(EC_{50}) results and standard deviations for compounds tested in the bacterial proliferation assays.

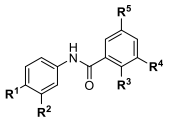						Bacterial Proliferation EC_{50} /µM						
					Compound # / Name	*E. faecium*	*S. aureus*		*K. pneumoniae*	*A. baumanii*	*P. aeruginosa*	*E. cloacae*
							Sensitive	*Resistant*				
Compound Substituents & Substructures					Closantel	0.09 ± 0.40	-0.33 ± 0.09	-0.37 ± 0.13	>2	>2	>2	>2
R^1	R^2	R^3	R^4	R^5	Rafoxanide	-0.003 ± 0.491	-0.49 ± 0.13	-0.53 ± 0.60	>2	1.5 ± 0.4	>2	1.6 ± 0.3
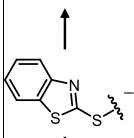	Cl	OH	Br	Br	**1**	-0.29 ± 0.38	-0.44 ± 0.18	-0.34 ± 0.27	>2	1.8 ± 0.2	>2	>2
	Cl	OH	Br	H	**2**	1.4 ± 0.4	-0.35 ± 0.29	-0.26 ± 0.27	>2	0.46 ± 0.12	>2	>2
	Cl	OH	H	Br	**3**	1.2 ± 0.2	-0.93 ± 0.24	-0.09 ± 0.40	>2	>2	>2	>2
	Cl	OH	H	H	**4**	1.8 ± 0.5	-0.51 ± 0.31	-0.38 ± 0.30	>2	>2	>2	>2
	H	OH	Br	Br	**5**	-0.05 ± 0.77	-0.36 ± 0.17	-0.31 ± 0.08	>2	>2	>2	>2
	H	OH	Br	H	**6**	0.92 ± 1.06	-0.12 ± 0.18	-0.03 ± 0.22	>2	1.1 ± 0.2	>2	>2
	H	OH	H	Br	**7**	1.3 ± 0.3	-0.92 ± 0.19	-0.90 ± 0.28	>2	>2	>2	>2
	H	OH	H	H	**8**	1.8 ± 0.2	-0.69 ± 0.08	-0.47 ± 0.29	>2	>2	>2	>2
H	Cl	OH	Br	Br	**9**	1.2 ± 0.7	-0.18 ± 0.16	0.01 ± 0.24	2.0 ± 0.1	1.7 ± 0.1	>2	1.9 ± 0.2
H	Cl	OH	Br	H	**10**	>2	0.12 ± 0.03	0.15 ± 0.05	>2	>2	>2	>2
H	Cl	OH	H	Br	**11**	>2	-0.34 ± 0.02	-0.36 ± 0.02	>2	>2	>2	>2
H	Cl	OH	H	H	**12**	>2	0.49 ± 0.06	0.61 ± 0.07	>2	>2	>2	>2
H	H	OH	Br	Br	**13**	>2	0.09 ± 0.10	0.24 ± 0.11	>2	>2	>2	>2
H	H	OH	Br	H	**14**	>2	0.81 ± 0.05	0.94 ± 0.04	>2	>2	>2	>2
H	H	OH	H	Br	**15**	>2	0.44 ± 0.05	0.60 ± 0.12	1.9 ± 0.2	>2	>2	>2
H	H	OH	H	H	**16**	>2	1.4 ± 0.1	1.7 ± 0.10	>2	>2	>2	>2
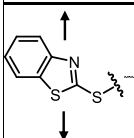	Cl	H	Br	Br	**17**	>2	>2	>2	>2	>2	>2	>2
	Cl	H	Br (H)	H (Br)	**18**	>2	>2	>2	>2	>2	>2	>2
	Cl	H	H	H	**19**	>2	1.6 ± 0.2	>2	>2	>2	>2	>2
	H	H	Br	Br	**20**	>2	>2	>2	>2	>2	>2	>2
	H	H	Br (H)	H (Br)	**21**	>2	>2	>2	>2	>2	>2	>2
	H	H	H	H	**22**	>2	>2	>2	>2	>2	>2	>2
H	Cl	H	Br	Br	**23**	>2	1.1 ± 0.1	1.1 ± 0.1	>2	>2	>2	>2
H	Cl	H	Br (H)	H (Br)	**24**	>2	1.7 ± 0.1	1.8 ± 0.1	>2	>2	>2	>2
H	Cl	H	H	H	**25**	>2	>2	>2	>2	>2	>2	>2
H	H	H	Br	Br	**26**	>2	>2	>2	>2	>2	>2	>2
H	H	H	Br (H)	H (Br)	**27**	>2	>2	>2	>2	>2	>2	>2
H	H	H	H	H	**28**	>2	>2	>2	>2	>2	>2	>2
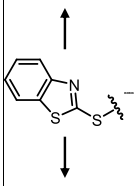	Cl	OCH_3	Br	Br	**29**	>2	>2	>2	>2	>2	>2	>2
	Cl	OCH_3	Br	H	**30**	>2	>2	>2	>2	>2	>2	>2
	Cl	OCH_3	H	Br	**31**	>2	>2	>2	>2	>2	>2	>2
	Cl	OCH_3	H	H	**32**	>2	>2	>2	>2	>2	>2	>2
	H	OCH_3	Br	Br	**33**	>2	>2	>2	>2	>2	>2	>2
	H	OCH_3	Br	H	**34**	>2	>2	>2	>2	>2	>2	>2
	H	OCH_3	H	Br	**35**	>2	>2	>2	>2	>2	>2	>2
	H	OCH_3	H	H	**36**	>2	>2	>2	>2	>2	>2	>2
H	Cl	OCH_3	Br	Br	**37**	>2	1.7 ± 0.2	>2	>2	>2	>2	>2
H	Cl	OCH_3	Br	H	**38**	>2	>2	>2	>2	>2	>2	>2
H	Cl	OCH_3	H	Br	**39**	>2	>2	>2	>2	>2	>2	>2
H	Cl	OCH_3	H	H	**40**	>2	>2	>2	>2	>2	>2	>2
H	H	OCH_3	Br	Br	**41**	>2	>2	>2	>2	>2	>2	>2
H	H	OCH_3	Br	H	**42**	>2	>2	>2	>2	>2	>2	>2
H	H	OCH_3	H	Br	**43**	>2	>2	>2	>2	>2	>2	>2
H	H	OCH_3	H	H	**44**	>2	>2	>2	>2	>2	>2	>2

Table 9. Log(IC_{50}) and Log(CC_{50}) results and standard deviations for compounds tested in the human HSP60/10-dMDH folding assay and the THLE3 and HEK 293 cytotoxicity assays.

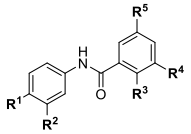						Biochemical Assay IC_{50} (μM)	Cell Viability CC_{50} (μM)	
					Compound # / Name	HSP60/10-dMDH Refolding	THLE3 (Liver)	HEK 293 (Kidney)
Compound Substituents & Substructures					Closantel	0.17 ± 0.12	1.6 ± 0.2	1.8 ± 0.1
R^1	R^2	R^3	R^4	R^5	Rafoxanide	0.19 ± 0.06	1.4 ± 0.1	>2
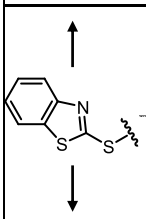	Cl	OH	Br	Br	**1**	0.60 ± 0.38	1.2 ± 0.3	1.9 ± 0.2
	Cl	OH	Br	H	**2**	0.73 ± 0.09	1.3 ± 0.2	1.8 ± 0.3
	Cl	OH	H	Br	**3**	>2	1.1 ± 0.2	1.6 ± 0.2
	Cl	OH	H	H	**4**	>2	1.5 ± 0.10	1.8 ± 0.2
	H	OH	Br	Br	**5**	0.52 ± 0.05	1.3 ± 0.2	1.8 ± 0.2
	H	OH	Br	H	**6**	1.4 ± 0.4	1.6 ± 0.2	1.9 ± 0.2
	H	OH	H	Br	**7**	>2	0.99 ± 0.07	1.2 ± 0.2
	H	OH	H	H	**8**	>2	1.4 ± 0.1	1.8 ± 0.2
H	Cl	OH	Br	Br	**9**	1.4 ± 0.2	1.0 ± 0.2	1.1 ± 0.2
H	Cl	OH	Br	H	**10**	>2	1.2 ± 0.1	1.2 ± 0.2
H	Cl	OH	H	Br	**11**	>2	0.4 ± 0.1	0.4 ± 0.1
H	Cl	OH	H	H	**12**	>2	1.2 ± 0.2	1.1 ± 0.1
H	H	OH	Br	Br	**13**	1.8 ± 0.2	1.4 ± 0.1	1.4 ± 0.1
H	H	OH	Br	H	**14**	>2	1.8 ± 0.1	1.8 ± 0.1
H	H	OH	H	Br	**15**	>2	1.2 ± 0.1	1.2 ± 0.1
H	H	OH	H	H	**16**	>2	1.9 ± 0.1	1.9 ± 0.1
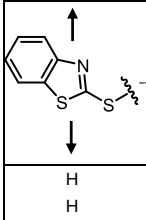	Cl	H	Br	Br	**17**	>2	>2	>2
	Cl	H	Br (H)	H (Br)	**18**	>2	1.9 ± 0.1	>2
	Cl	H	H	H	**19**	>2	1.9 ± 0.1	2.0 ± 0.1
	H	H	Br	Br	**20**	>2	>2	>2
	H	H	Br (H)	H (Br)	**21**	>2	1.9 ± 0.2	1.9 ± 0.1
	H	H	H	H	**22**	>2	>2	>2
H	Cl	H	Br	Br	**23**	>2	1.7 ± 0.1	1.7 ± 0.1
H	Cl	H	Br (H)	H (Br)	**24**	>2	1.7 ± 0.1	1.7 ± 0.1
H	Cl	H	H	H	**25**	>2	>2	>2
H	H	H	Br	Br	**26**	>2	>2	>2
H	H	H	Br (H)	H (Br)	**27**	>2	>2	>2
H	H	H	H	H	**28**	>2	>2	>2
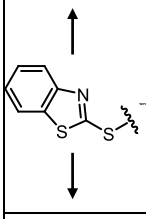	Cl	OCH_3	Br	Br	**29**	>2	>2	>2
	Cl	OCH_3	Br	H	**30**	>2	>2	>2
	Cl	OCH_3	H	Br	**31**	>2	>2	>2
	Cl	OCH_3	H	H	**32**	>2	>2	>2
	H	OCH_3	Br	Br	**33**	>2	>2	>2
	H	OCH_3	Br	H	**34**	>2	>2	>2
	H	OCH_3	H	Br	**35**	>2	>2	>2
	H	OCH_3	H	H	**36**	>2	>2	>2
H	Cl	OCH_3	Br	Br	**37**	>2	>2	>2
H	Cl	OCH_3	Br	H	**38**	>2	>2	>2
H	Cl	OCH_3	H	Br	**39**	>2	2.0 ± 0.16	>2
H	Cl	OCH_3	H	H	**40**	>2	>2	>2
H	H	OCH_3	Br	Br	**41**	>2	>2	>2
H	H	OCH_3	Br	H	**42**	>2	>2	>2
H	H	OCH_3	H	Br	**43**	>2	>2	>2
H	H	OCH_3	H	H	**44**	>2	>2	>2

REFERENCES

Abdeen, S., Salim, N., Mammadova, N., Summers, C. M., Frankson, R., Ambrose, A. J., Anderson, G. G., Schultz, P. G., Horwich, A. L., Chapman, E., and Johnson, S. M. (2016) GroEL/ES inhibitors as potential antibiotics. *Bioorg Med Chem Lett* **26**, 3127-3134

Armstrong, G. L., Conn, L. A., and Pinner, R. W. (1999) Trends in infectious disease mortality in the United States during the 20th century. *Jama-J Am Med Assoc* **281**, 61-66

Baig, U. I., Bhadbhade, B. J., Mariyam, D., and Watve, M. G. (2014) Protein aggregation in E. coli : short term and long term effects of nutrient density. *PLoS One* **9**, e107445

Bao, Y. P., Cook, L. J., O'Donovan, D., Uyama, E., and Rubinsztein, D. C. (2002) Mammalian, yeast, bacterial, and chemical chaperones reduce aggregate formation and death in a cell model of oculopharyngeal muscular dystrophy. J Biol Chem 277, 12263-12269

Bjarnsholt, T. (2013) The role of bacterial biofilms in chronic infections. APMIS Suppl, 1-51

Boucher, H. W., Talbot, G. H., Bradley, J. S., Edwards, J. E., Gilbert, D., Rice, L. B., Scheld, M., Spellberg, B., and Bartlett, J. (2009) Bad bugs, no drugs: no ESKAPE! An update from the Infectious Diseases Society of America. *Clin Infect Dis* **48**, 1-12

Brotz-Oesterhelt, H., Beyer, D., Kroll, H. P., Endermann, R., Ladel, C., Schroeder, W., Hinzen, B., Raddatz, S., Paulsen, H., Henninger, K., Bandow, J. E., Sahl, H. G., and Labischinski, H. (2005) Dysregulation of bacterial proteolytic machinery by a new class of antibiotics. *Nat Med* **11**, 1082-1087

Brown, A. G., Butterworth, D., Cole, M., Hanscomb, G., Hood, J. D., Reading, C., and Rolinson, G. N. (1976) Naturally-occurring beta-lactamase inhibitors with antibacterial activity. *J Antibiot (Tokyo)* **29**, 668-669

Carmichael, J., Chatellier, J., Woolfson, A., Milstein, C., Fersht, A. R., and Rubinsztein, D. C. (2000) Bacterial and yeast chaperones reduce both aggregate formation and cell death in mammalian cell models of Huntington's disease. Proc Natl Acad Sci U S A 97, 9701-9705

CDC. (2013) Antibiotic Resistance Threats in the United States Centers for Disease Control and Prevention

Chapman, E., Farr, G. W., Usaite, R., Furtak, K., Fenton, W. A., Chaudhuri, T. K., Hondorp, E. R., Matthews, R. G., Wolf, S. G., Yates, J. R., Pypaert, M., and Horwich, A. L. (2006) Global aggregation of newly translated proteins in an Escherichia coli strain deficient of the chaperonin GroEL. *Proc Natl Acad Sci U S A* **103**, 15800-15805

Cheng, M. Y., Hartl, F. U., Martin, J., Pollock, R. A., Kalousek, F., Neupert, W., Hallberg, E. M., Hallberg, R. L., and Horwich, A. L. (1989) Mitochondrial heat-shock protein hsp60 is essential for assembly of proteins imported into yeast mitochondria. *Nature* **337**, 620-625

Chiappori, F., Fumian, M., Milanesi, L., and Merelli, I. (2015) DnaK as Antibiotic Target: Hot Spot Residues Analysis for Differential Inhibition of the Bacterial Protein in Comparison with the Human HSP70. PLoS One 10, e0124563

Dalbey, R. E., Wang, P., and van Dijl, J. M. (2012) Membrane proteases in the bacterial protein secretion and quality control pathway. *Microbiol Mol Biol Rev* **76**, 311-330

Davies, J., and Davies, D. (2010) Origins and evolution of antibiotic resistance. *Microbiol Mol Biol Rev* **74**, 417-433

de Groot, N. S., and Ventura, S. (2010) Protein aggregation profile of the bacterial cytosol. *PLoS One* **5**, e9383

Eaves, D. J., Randall, L., Gray, D. T., Buckley, A., Woodward, M. J., White, A. P., and Piddock, L. J. (2004) Prevalence of mutations within the quinolone resistance-determining region of gyrA, gyrB, parC, and parE and association with antibiotic resistance in quinolone-resistant Salmonella enterica. *Antimicrob Agents Chemother* **48**, 4012-4015

Enright, M. C. (2003) The evolution of a resistant pathogen--the case of MRSA. *Curr Opin Pharmacol* **3**, 474-479

Giedraitiene, A., Vitkauskiene, A., Naginiene, R., and Pavilonis, A. (2011) Antibiotic resistance mechanisms of clinically important bacteria. *Medicina (Kaunas)* **47**, 137-146

Gonzalez-Zorn, B., and Courvalin, P. (2003) VanA-mediated high level glycopeptide resistance in MRSA. *Lancet Infect Dis* **3**, 67-68

Hancock, R. E. (2005) Mechanisms of action of newer antibiotics for Gram-positive pathogens. *Lancet Infect Dis* **5**, 209-218

Hartl, F. U., Bracher, A., and Hayer-Hartl, M. (2011) Molecular chaperones in protein folding and proteostasis. *Nature* **475**, 324-332

Hiramatsu, K., Hanaki, H., Ino, T., Yabuta, K., Oguri, T., and Tenover, F. C. (1997) Methicillin-resistant Staphylococcus aureus clinical strain with reduced vancomycin susceptibility. *J Antimicrob Chemother* **40**, 135-136

Horwich, A. L., Fenton, W. A., Chapman, E., and Farr, G. W. (2007) Two families of chaperonin: physiology and mechanism. *Annu Rev Cell Dev Biol* **23**, 115-145

Intelligence, B. H. (2017) The Health of America Report: Antibiotic Prescription Fill Rates Declining in the U.S., 27

Jacob, A. E., and Hobbs, S. J. (1974) Conjugal transfer of plasmid-borne multiple antibiotic resistance in Streptococcus faecalis var. zymogenes. *J Bacteriol* **117**, 360-372

Johnson, S. M., Sharif, O., Mak, P. A., Wang, H. T., Engels, I. H., Brinker, A., Schultz, P. G., Horwich, A. L., and Chapman, E. (2014) A biochemical screen for GroEL/GroES inhibitors. *Bioorg Med Chem Lett* **24**, 786-789

Kim, S., Lieberman, T. D., and Kishony, R. (2014) Alternating antibiotic treatments constrain evolutionary paths to multidrug resistance. *Proc Natl Acad Sci U S A* **111**, 14494-14499

Kroemer, G., and Reed, J. C. (2000) Mitochondrial control of cell death. *Nat Med* **6**, 513-519

Kumar, C. M., Mande, S. C., and Mahajan, G. (2015) Multiple chaperonins in bacteria--novel functions and non-canonical behaviors. *Cell Stress Chaperones* **20**, 555-574

Kwasny, S. M., and Opperman, T. J. (2010) Static biofilm cultures of Gram-positive pathogens grown in a microtiter format used for anti-biofilm drug discovery. *Curr Protoc Pharmacol* **Chapter 13**, Unit 13A 18

Lewis, K. (2013) Platforms for antibiotic discovery. *Nat Rev Drug Discov* **12**, 371-387

Lowy, F. D. (2003) Antimicrobial resistance: the example of Staphylococcus aureus. *J Clin Invest* **111**, 1265-1273

Maisonneuve, E., Ezraty, B., and Dukan, S. (2008) Protein aggregates: an aging factor involved in cell death. *J Bacteriol* **190**, 6070-6075

Musk, D. J., Jr., and Hergenrother, P. J. (2006) Chemical countermeasures for the control of bacterial biofilms: effective compounds and promising targets. *Curr Med Chem* **13**, 2163-2177

Nakae, T. (1986) Outer-membrane permeability of bacteria. *Crit Rev Microbiol* **13**, 1-62

Nathan, C. (2004) Antibiotics at the crossroads *Nature* **431**, 3

Navarre, W. W., and Schneewind, O. (1999) Surface proteins of gram-positive bacteria and mechanisms of their targeting to the cell wall envelope. *Microbiol Mol Biol Rev* **63**, 174-229

Nikaido, H. (1996) Multidrug efflux pumps of gram-negative bacteria. *J Bacteriol* **178**, 5853-5859

Park, H. K., Lee, J. E., Lim, J., Jo, D. E., Park, S. A., Suh, P. G., and Kang, B. H. (2014) Combination treatment with doxorubicin and gamitrinib synergistically augments anticancer activity through enhanced activation of Bim. *BMC Cancer* **14**, 431

Pence, M. A., Haste, N. M., Meharena, H. S., Olson, J., Gallo, R. L., Nizet, V., and Kristian, S. A. (2015) Beta-Lactamase Repressor BlaI Modulates Staphylococcus

aureus Cathelicidin Antimicrobial Peptide Resistance and Virulence. *PLoS One* **10**, e0136605

Piper, P. W., and Millson, S. H. (2012) Spotlight on the microbes that produce heat shock protein 90-targeting antibiotics. Open Biol 2, 120138

Salton, M. R. J., and Kim, K. S. (1996) Structure. in *Medical Microbiology* (Baron, S. ed.), 4th Ed., Galveston (TX). Pp

Singh, R., Ray, P., Das, A., and Sharma, M. (2010) Penetration of antibiotics through Staphylococcus aureus and Staphylococcus epidermidis biofilms. *J Antimicrob Chemother* **65**, 1955-1958

Stefani, M., and Dobson, C. M. (2003) Protein aggregation and aggregate toxicity: new insights into protein folding, misfolding diseases and biological evolution. J Mol Med (Berl) 81, 678-699

Stewart, P. S., and Costerton, J. W. (2001) Antibiotic resistance of bacteria in biofilms. *Lancet* **358**, 135-138

Stromberg, B. E., Schlotthauer, J. C., and Conboy, G. A. (1984) The efficacy of closantel against Fascioloides magna in sheep. *J Parasitol* **70**, 446-447

Talon, D. (1999) The role of the hospital environment in the epidemiology of multi-resistant bacteria. *J Hosp Infect* **43**, 13-17

Wang, Q., Buckle, A. M., and Fersht, A. R. (2000) From minichaperone to GroEL 1: information on GroEL-polypeptide interactions from crystal packing of minichaperones. *J Mol Biol* **304**, 873-881

Whitesell, L., and Lindquist, S. L. (2005) HSP90 and the chaperoning of cancer. *Nat Rev Cancer* **5**, 761-772

Wright, G. D., and Sutherland, A. D. (2007) New strategies for combating multidrug-resistant bacteria. *Trends Mol Med* **13**, 260-267

Yarlagadda, V., Manjunath, G. B., Sarkar, P., Akkapeddi, P., Paramanandham, K., Shome, B. R., Ravikumar, R., and Haldar, J. (2016) Glycopeptide Antibiotic To Overcome the Intrinsic Resistance of Gram-Negative Bacteria. *ACS Infect Dis* **2**, 132-139

CURRICULUM VITAE

Trent A. Kunkle

Education

Northern Illinois University-Dekalb, IL August 2012-Spring 2016

Bachelor of Science in Chemistry (Biochemistry Emphasis)

GPA: 3.42

Indiana University-Indianapolis, IN August 2016-July 2018

Master of Science in Biochemistry

Research Experience

Undergraduate Research Assistant (Dr. James Horn Lab) –

Northern Illinois University *August 2015-May 2016*

Involved researcher in the lab of Dr. James Horn, learning concepts of small molecule-protein interactions and how new therapeutics can be evaluated for binding and inhibiting enzymatic activity.

Project focused on identifying compounds that inhibit activity with IspD and IspE protein(s) in parasites.

Disruption of protein activity ultimately was hypothesized to decrease proliferation through the disturbance of the cholesterol synthesis for the cellular membrane.

Utilization of techniques such as differential scanning fluorimetry, isothermal titration calorimetry, and circular dichroism were necessary in quantifying structural characteristics of investigated proteins in native and molecule-bound form.

Work-up towards experimental analysis of proteins required techniques regarding full protein purification protocols in high performance liquid chromatography (HPLC), utilizing anion exchange, size exclusion, and IMAC nickel columns.

At the end of the spring semester, presented data and discussed conclusions to audience of peers and mentors of the department.

Graduate Research (Dr. Steven Johnson L -

Indiana University School of Medicine *November 2016-February 2018*

Thesis-Antibiotic Discovery Targeting Bacterial GroEL/GroES Chaperonin Systems

Graduate work explored dynamics of the GroEL/ES chaperonin system that mediates protein folding for therapeutic development.

Goal was to inhibit growth of resistant ESKAPE pathogens, using protein folding disruption was the primary aim of project.

Experiments centered around interpretation of structural activity relationships in derivatives of compound parent scaffolds to evaluate crucial substituents that may attribute toward disruption of protein folding mechanism and cause antibacterial activity.

Techniques utilized bacterial culturing, proliferation/growth assays, high throughput assay analysis, and enzymatic activity were utilized for the bulk of work.

Full purification protocols of native and mutant strains of chaperone proteins were transformed and purified using fast-protein liquid chromatography (FPLC) with anion-exchange and size exclusion columns, which was optimized then taught to new graduate students in late 2017.

Results have indicated a subset of structures that specifically target chaperone proteins, disrupting protein folding leading to cidal effects within invasive microbials.

Additional studies have taken these compounds in consideration for anti-cancerous properties from the presence of overexpressing chaperones in immortalized cell lines

Results and conclusions will be made public late spring in two papers.

Related Coursework

Biochemistry
Molecular Biology
Cell Biology
Organic Chemistry I and II
Inorganic Chemistry
Analytical Chemistry I and II
Cancer Signaling
Physiology
Structural Biology
Chemical Biology

Programs/Interfaces Used

Microsoft Excel
Microsoft Powerpoint
GraphPad Prism 6
ChromLab
SoftMaxPro
ChemOffice
BIOVIA Discovery Studio
Pymol
COOT
Chimera
CCP4

Laboratory Skills

Protein purification protocols via HPLC and FPLC

Includes anion-exchange, size exclusion, and nickel column(s)

Differential Scanning Fluorimetry (DSF)

Circular Dichroism (CD)

Cell based assays (Prokaryotic (BSL1-2) and Eukaryotic (immortalized human cell lines))

Biochemical Assays determining inhibitory response to molecule treatment

Following Equipment Utilized:

SpectraMax Plate Reader
NGC Fast Protein Liquid Chromatography Instrument
Fluorescence plate reader
CD Spectrometer
PCR Thermal Cycler
Laminar Flow biohoo

Leadership Experience

President- Phi Kappa Theta Fraternal organization August 2014-May2015

Led organization of 90+ members including weekly meetings, managing committee leaders, and communicating with university leadership.

Associate member Educator-Phi Kappa

Theta Fraternal organization August 2015-May 2016

Wrote eight-week new member process of organization which highlighted leadership workshops, resume building workshops, and dialogue from distinguished alumni.

Conducted grade checkups and persisted with financial obligations to more than 35 young men which ultimately yielded 100% full payment and full re-enrollment for the proceeding semester for all new members.

Inspyrewear Initiative Coordinator November 2014-February 2015

Organized t-shirt fundraiser on central campus of which every shirt profit in turn was donated to Stop Hunger Now to supply six meals for malnourished children in third world countries.

Made over $1800 in sales which in turn packed and shipped more than 300 meals worldwide.

Honors

Recipient of the Northern Illinois University Emerging Leader Award

Scholarship recipient for Northern Illinois May 2013

University Out of State Scholarship August 2012